

Abstract

Parasitic helminth infections of livestock are a threat to the health and production of livestock, crops and to human health. One third of the world's animal population was affected in 2015 by helminth infestations causing severe morbidity. The shortfall of new drugs against nematode parasites and the resistance hazard represents an urgent need for the development of novel anti-parasitic drugs with effective delivery to the target site. It is hypothesised that the toxic efficacy and selectivity of anthelmintic drugs can be improved using prodrug forms that possess intracellular drug targeting moieties that can circumvent resistance mechanisms.

A series of novel targeted anthelmintic candidate drugs have been synthesized, based on a colchicine (Col) core; code-named: AM1 (Col-prolinol), AM3 (Col-4-hydroxypiperidine), AM4 (Col-(*R*)-3-pyrrolidinol), AM5 (Col-Boc-aminopyrrolidine) and AM6 (Col-aminopyrrolidine), these compounds are broadly tubulin targeting amino-colchicine derivatives. Amino-colchicines were then conjugated with a lipophilic, cationic targeting moiety TPP (triphenylphosphonium) ion that has potential to bypass resistance and achieve selectivity by direct and fast accumulation in the matrix of mitochondria. Novel prodrugs AM2 (Col-prolinol-TPP), AM7 (Col-aminopyrrolidine-TPP), AM8 (Col-4-hydroxypiperidine-TPP), AM9 (Col-(*R*)-3-pyrrolidinol-TPP) are ester-linked triphenylphosphonium butanoyl (TPP) conjugates of amino-colchicines AM1, AM6, AM3 and AM4 respectively that are designed to not only pass through cell membranes and localise in the mitochondria but also facilitate drug cellular uptake by avoiding p-glycoprotein-type mediated efflux mechanisms. All novel compounds have been characterised by high resolution mass spectrometry and ¹H and ¹³C NMR spectroscopy. Preliminary biological evaluation of AM1 and AM2 was carried out by treatment of the *C. elegans* non-parasite model organism. Results demonstrated that AM2 (100µM) showed significant toxicity against *C. elegans* at an incubation time of 22h. Physicochemical properties of these novel agents has been described in terms of distribution coefficient log D values, that showed they are lipophilic in nature and should have the ability to cross lipid bilayers and mitochondrial membrane. Preliminary molecular docking studies also demonstrated binding affinity of AM6 (Col-aminopyrrolidine) with tubulin. These novel prodrugs have the potential to be developed as effective anthelmintic agents in the treatment of parasitic helminth disease.

Declaration

It is hereby declared that this thesis and the research work upon which it is based were conducted by the author, Aiman Rehan

Aiman Rehan

Acknowledgements

I am thankful and indebted to the Almighty ALLAH who made me able to fulfil the daunting task which without Him was impossible to come to such a point where I am now. I started very humbly, and He took it to the acme. I am thankful to all my supervisors; Dr. David Mincher, Dr. Agnes Turnbull and Dr. Lorna Proudfoot my for all their support, aspiring guidance, pearls of knowledge, sharing expertise, valuable guidance and encouragement throughout the project. I am grateful to all for their illuminating comments on different issues related to project and those comments led me towards my target. The beauty if in this thesis, is due to my supervisors' hard work which is reflected in me and mistakes are all mine. Thanks, are also due to Dr. Eva Malone for being an independent panel chair and reviewing my performance during my journey. Also, I would like to thank the EPSRC National Mass Spectrometry Facility, University of Swansea and NMR-facility at Heriot-Watt University (Dr Alan Boyd). I also like to thank all my colleagues and friends in past and present; Eytayo Oluwadare, Sunil Mathur, Omar Muhammad, Yao Ding, Debbie McFarlan and Olga Biskou. I am also thankful to all the technicians who helped me in labs.

I would also like to thank and express the hand who not only nurtured but also prayed untiringly, selflessly, dedicatedly and made a strong, hardworking person out of a raw material which I was; these are my parents. I am thankful to Rehan, my mentor, friend, alter ego and a lovely husband without which I can't even think of going out of my house, gave me courage, boosted my morale, shared my responsibilities and proved a true out of this world husband. I dedicate this piece of research to Rehan. I am also thankful to little Zeemal & Haneen who suffered most in this period and always there for me to cheer me up no matter how tired I was.

Table of Contents

List of Figures.....	ix
List of Tables.....	xiii
List of Appendices.....	xiv
Abbreviations	xv
Aim and Hypothesis	xvii
Chapter 1	1
1.0 Background & Introduction:.....	1
1.1 Helminths	1
1.1.1 Categorisation of helminths	1
1.1.2 Anatomical features of Helminths	2
1.1.3 Parasitic Helminths a threat to humans, livestock & crops	3
1.1.4 Gastro-intestinal Nematodes	4
1.1.5 Life cycle of Strongylida nematodes	5
1.2 Introduction to Anthelmintic drugs:.....	7
1.2.1 Classification of Anthelmintic Drugs	8
1.2.2 Limitations of Anthelmintic or Nematicide or Dewormer	10
1.3 Microtubules (MT)	12
1.3.1 Microtubules Organisation	12
1.4 – Microtubules as target molecules in antiparasitic treatments:.....	14
1.4.1 Microtubule Targeting Strategies.....	14
1.4.2 Targeted delivery of tubulin binders.....	15
1.4.3 Binding sites of tubulin binders	15
1.4.4 Tubulin Binding Agents (TBA's).....	16
1.4.5 Novel Example of Tubulin Binders.....	18
1.5 Resistance:	19
1.5.1 Mechanism of Drug Resistance.....	21

1.6	Targeted Delivery by prodrug strategy:	24
1.6.1	Mitochondria, “a promising target” in chemotherapy.....	25
	Mitochondria targeting approaches	26
1.6.2	26
1.7	Introduction of Lipophilic cation: Triphenylphosphonium compound (TPP):	26
1.7.1	Mitochondrial membrane potential.....	27
1.7.2	Hydrophobicity of TPP Drug complex.....	28
1.7.3	TPP application as a “magic bullet” in targeted drug delivery	28
	<i>Caenorhabditis elegans</i> as a Model Organism.....	30
1.8	30
1.8.1	Properties of <i>C. elegans</i> as a model experimental system.....	30
1.8.2	Self-Fertilisation:.....	32
1.8.3	Non-Animal Model & 3R's:.....	32
1.8.4	Comparison of <i>C. elegans</i> with other vertebrate models:	32
1.8.5	Homology with humans:	32
2	Results & Discussion	34
2.1	Design strategy for novel amino-colchicines:	34
2.2	Prodrug design strategy for novel amino-colchicines in conjugation with TPP	37
	2.2.1 Overview of the project.....	38
2.3	Rationale design of TPP-linked amino-colchicine Prodrugs:.....	39
	Synthesis Strategy:	43
2.4	43
2.4.1	Synthesis of Colchicine-Prolinol (AM1).....	43
2.4.2	Synthesis of Colchicine-Prolinol-TPP (AM2):.....	47
2.4.3	Synthesis of Colchicine-4-hydroxypiperidine (AM3):	50
2.4.4	Synthesis of Colchicine-(R)-3-Pyrrolidinol (AM4):.....	54

2.4.5	Synthesis of Colchicine-(R)-3-(Boc-aminopyrrolidine) (AM5)	58
2.4.6	Synthesis of Colchicine-(R)-3-(aminopyrrolidine)-TFA (AM6):.....	61
2.4.7	Synthesis of Colchicine-(R)-3-aminopyrrolidine-TPP (AM7):.....	65
2.4.8	Synthesis of Colchicine-4-hydroxypiperidine-TPP (AM8)	68
2.4.9	Synthesis of Colchicine-(R)-3-Pyrrolidinol)-TPP (AM9)	73
2.5	Distribution Coefficient Studies:	77
2.5.1	Determination of distribution coefficient (Log D) method:	78
2.6	Effect of Novel targeted anthelmintic prodrugs on <i>C. elegans</i> :	81
2.6.1	<i>C. elegans</i> viability assay	81
2.7	Molecular Docking:.....	86
2.8	Conclusion & Future work:	90
3	Chapter.....	92
3.0	Experimental	92
3.1	Analytical Methods	92
3.1.1	Thin layer chromatography	92
3.1.2	Column chromatography	92
3.1.3	Mass spectrometry	92
3.1.4	Proton and carbon nuclear magnetic resonance (¹ H and ¹³ C nmr).....	93
3.1.5	Chemical reagents.....	93
3.2	Synthesis of colchicine-based small molecule compounds (AM series):.....	93
3.2.1	Synthesis of Colchicine-Prolinol {N-[10-(2-Hydroxymethyl-pyrrolidin-1-yl)-1,2,3-trimethoxy-9-oxo-5,6,7,9-tetrahydro-benzo[α]heptalene-7-yl]-acetamide} (AM1).....	93
3.2.2	Synthesis of Colchicine-Prolinol-TPP {4-[1-(7-Acetylamino-1,2,3-trimethoxy-9-oxo-5,6,7,9-tetrahydro-benzo[α]heptalene-10-yl)-pyrrolidin-2-ylmethoxycarbonyl]-butyl}-triphenyl-phosphonium; bromide} (AM2):	94

3.2.3	Synthesis of Colchicine-4-hydroxypiperidine {(S)-N-(10-(4-hydroxypiperidin-1-yl)-1,2,3-trimethoxy-9-oxo-5,6,7,9-tetrahydrobenzo[α]heptalene-7-yl)acetamide} (AM3)	95
3.2.4	Synthesis of Colchicine-(R)-3-Pyrrolidinol {1-(7-Acetylamino-1,2,3-trimethoxy-9-oxo-5,6,7,9-tetrahydro-benzo[α]heptalen-10-yl)-pyrrolidin-3-yl-ammonium;trifluoro-acetate} (AM4):	96
3.2.5	Synthesis of Colchicine-(R)-3-(Boc-amino) Pyrrolidine {1-(7-Acetylamino-1,2,3-trimethoxy-9-oxo-5,6,7,9-tetrahydro-benzo[α]heptalene-10-yl)-pyrrolidin-3-yl]-carbamic acid ter-butyl ester} (AM5):	97
3.2.6	Synthesis of AM6 (Col-(R)-3-(amino) Pyrrolidine-TFA) {1-(7-Acetylamino-1,2,3-trimethoxy-9-oxo-5,6,7,9-tetrahydro-benzo[α]heptalene-10-yl)-pyrrolidin-3-yl-ammonium; trifluoro-acetate} (AM6)	98
3.2.7	Synthesis of AM7 (Col-(R)-3-(aminopyrrolidine-TPP) {(5-(((R)-1-((S)-7-acetamido-1,2,3-trimethoxy-9-oxo-5,6,7,9-tetrahydrobenzo[α]heptalene-10-yl)pyrrolidine-3-yl)amino)-5-oxopentyl)triphenylphosphonium; bromide (AM7): .	99
3.2.8	Synthesis of Colchicine-4-hydroxypiperidine-TPP {4-[1-(7-Acetylamino-1,2,3-trimethoxy-9-oxo-5,6,7,9-tetrahydro-benzo[α]heptalene-10-yl)-piperidin-4-yloxy-carbonyl]-butyl}-triphenyl-phosphonium; bromide} (AM8)	100
3.2.9	Synthesis of Colchicine-(R)-3-Pyrrolidinol-TPP {4-[1-(7-Acetylamino-1,2,3-trimethoxy-9-oxo-5,6,7,9-tetrahydro-benzo[α]heptalene-10-yl)-pyrrolidin-3-yloxy-carbonyl]-butyl}-trphenyl-phosphonium; bromide} (AM9).....	101
3.3	Distribution coefficient measurement	102
3.3.1	Preparation of saturated solutions	102
3.3.2	Preparation of calibration curves	102
3.3.3	Distribution coefficient methods.....	103
3.4	Compound Lethality Treatments on <i>C. elegans</i> worms.....	104
3.4.1	Materials and Methods	104
3.4.2	Toxic assessment of AM series as novel anthelmintic agents	104
3.4.3	Anthelmintic worm viability assay	105
4	Chapter	106

Structure Library	106
4.1	106
4.1.1 Structure of AM1	106
4.1.2 Structure of AM2	106
4.1.3 Structure of AM3:	107
4.1.4 Structure of AM4	107
4.1.5 Structure of AM5	108
4.1.6 Structure of AM6	108
4.1.7 Structure of AM7:	109
4.1.8 Structure of AM8:	109
4.1.9 Structure of AM9	110
4.1.10 Structure of TPP (Triphenylphosphonium):	110
4.1.11 Structure of Colchicine (Col)	111
4.1.12 Structure of Prolinol (Pro)	111
4.1.13 Structure of 4-hydroxypiperidine	111
4.1.14 Structure of <i>R</i> -3-pyrrolidinol	112
4.1.15 Structure of (<i>R</i>)-3-Boc-aminpyrrolidine:	112
References	1
Appendices	18

List of Figures

Figure 1. 1 Shows % of diagnosable submission of cattle and sheep in the Vet. Hospital of Scotland with PGE (parasitic gastroenteritis) yearly (Wilson et al., 2008).	5
Figure 1. 2 Shows life cycle of gastrointestinal nematodes of order strongylida in small ruminants (Peebles, 2007).	6
Figure 1. 3 The chemical structure of piperazine.	8
Figure 1. 4 Chemical structure of benzimidazole.	9
Figure 1. 5 Chemical structure of levamisole (LEV).	9
Figure 1. 6 Organisation of MT in a eukaryotic cell, showing tubulin dimers, protofilaments and catastrophe switch (Akhmanova & Steinmetz, 2015).	13
Figure 1. 7 Chemical structure of colchicine showing three rings: A (6 membered ring), B (7-membered ring) and C (7-membered ring).	17
Figure 1. 8 Chemical structure of Bal27862, showing benzimidazole (BZ) part, Aniline and cyanoethyl.	18
Figure 1. 9 Decreased uptake of drug by the cell due to mutation, so no drug at the target site, and uptake of drug molecule by p-gp receptors results in increased efflux or removal of the drug from the cell.	22
Figure 1. 10 Conversion of phenytoin prodrug (insoluble) into active parent drug (soluble) under physiological conditions.	25
Figure 1. 11 Chemical structure of TPP (4-carboxybutyl) triphenylphosphonium).	26
Figure 1. 12 TPP-betulin prodrug complex (showing ester bond) and its non-prodrug form betulin.	29
Figure 1. 13 Life cycle of <i>C. elegans</i> at 25 °C (Donald L Riddle, 1997).	31
Figure 2. 1 General design strategy of amino-colchicine derivatives with amino-alcohol. Where R ¹ can be H or 5 membered (prolinol and (<i>R</i>)-3-pyrrolidinol) or 6 membered (4-hydroxypiperidine) alcohols.	35
Figure 2. 2 Structures of selected colchicine derivatives with amino-alcohols AM1 (colchicine-prolinol) AM3 (colchicine-4-hydroxy piperidine) and AM4 (colchicine-(<i>R</i>)-3-pyrrolidinol).	35

Figure 2. 3 General design strategy of amino-colchicine derivatives with diamine. Where R ¹ is H or part of carbocyclic ring R is part of carbocyclic ring, exemplified by 3-aminopyrrolidine in which R ² is Boc at the exocyclic amino group.	36
Figure 2. 4 Structures of AM5 (Colchicine-(<i>R</i>)-3-(Bocaminopyrrolidine) and AM6 (Col-(<i>R</i>)-3-aminopyrrolidine-TFA).	36
Figure 2. 5 TPP-linked colchicine derivatives; AM2 (Colchicine-Prolinol-TPP), AM8 (Colchicine-4-hydroxypiperidine-TPP) and AM9 (Colchicine-(<i>R</i>)-3-pyrrolidinol-TPP).	37
Figure 2. 6 TPP-linked colchicine derivative with diamine AM7 Col-(<i>R</i>)-3-aminopyrrolidine-TPP.	38
Figure 2. 7 Colchicine with all the rings and showing position C-10 for modification.	40
Figure 2. 8 A Prodrug activation concept of TPP-linked colchicine derivatives (the AM series), as potential anthelmintic agents, showing cleavage by an esterase between TPP and the amino-alcohol.	42
Figure 2. 9 Synthesis of Col-prolinol (AM1) from Colchicine.	43
Figure 2. 10 ESI (+) Mass spectrum of AM1 (Col-prolinol).	44
Figure 2. 11 Comparison of the observed data with the theoretical isotope model for AM1.	44
Figure 2. 12 ¹ H NMR assignments (ppm values) and atomic numbering.	45
Figure 2. 13 ¹³ C NMR signals with assignments (ppm values) and atomic numbering.	46
Figure 2. 14 Synthesis of Col-prolinol-TPP (AM2) from Col-Pro (AM1).	47
Figure 2. 15 ESI (+) Mass spectrum of AM1 (Col-prolinol)	48
Figure 2. 16 Comparison of the observed data with the theoretical isotope model of AM2.	48
Figure 2. 17 ¹ H NMR signals and assignments (ppm values) and atomic numbering.	49
Figure 2. 18 Synthesis of Colchicine-4-hydroxypiperidine (AM3) from Colchicine. ..	50
Figure 2. 19 ESI (+) Mass spectrum of AM3 (Col--4-hydroxypiperidine).	51
Figure 2. 20 Comparison of the observed data with the theoretical isotope model of AM3.	51
Figure 2. 21 ¹ H NMR signals and assignments (ppm values) and atomic numbering.	52

Figure 2. 22	¹³ C NMR with assignments (ppm values) and atomic numbering.....	53
Figure 2. 23	Synthesis of Colchicine-(R)-3-Pyrrolidinol (AM4) from colchicine.....	54
Figure 2. 24	ESI (+) Mass spectrum of AM4 (Col-(R)-3-Pyrrolidinol).....	55
Figure 2. 25	Comparison of the observed data with the theoretical isotope model of AM4.....	56
Figure 2. 26	¹ H NMR assignments (ppm values) and atomic numbering.	56
Figure 2. 27	¹³ C NMR with assignments (ppm values) and atomic numbering.....	57
Figure 2. 28	Synthesis of Colchicine-(R)-3-(Boc-aminopyrrolidine) (AM5) from colchicine.	58
Figure 2. 29	¹ H NMR assignments (ppm values) and atomic numbering for AM5...	59
Figure 2. 30	¹³ C NMR with assignments (ppm values) and atomic numbering for AM5.	60
Figure 2. 31	Synthesis of Colchicine-(R)-3-(aminopyrrolidine)-TFA (AM6) from AM5 (Colchicine-(R)-3-(Boc-aminopyrrolidine) (removal of Boc group).....	61
Figure 2. 32	ESI (+) Mass spectrum of AM6 (Col-(R)-3-aminopyrrolidine-TFA).	62
Figure 2. 33	Comparison of the observed data with the theoretical isotope model of AM6.....	63
Figure 2.34.	¹ H NMR assignments (ppm values) and atomic numbering for AM6...	63
Figure 2. 35	¹³ C NMR with assignments (ppm values) and atomic numbering for AM6.	64
Figure 2. 36	Synthesis of Col-(R)-3-aminopyrrolidine-TPP (AM7) from AM6 (Col-(R)-3-aminopyrrolidine-TFA) (Addition of TPP).	65
Figure 2. 37	ESI (+) Mass spectrum of AM7 (Col-(R)-3-aminopyrrolidine-TPP).	67
Figure 2. 38	Comparison of the observed data with the theoretical isotope model for AM7.....	67
Figure 2. 39	Synthesis of AM8 (Colchicine-4-hydroxypiperidine-TPP) from AM3 (Colchicine-4-hydroxypiperidine) (Addition of TPP).....	68
Figure 2. 40	ESI (+) Mass spectrum of AM8 (Col--4-hydroxypiperidine-TPP).	70
Figure 2. 41	Comparison of the observed data with the theoretical isotope model of AM8.....	70
Figure 2. 42	¹ H NMR assignments (ppm values) and atomic numbering for AM8...	71
Figure 2. 43	¹³ C NMR with assignments (ppm values) and atomic numbering for AM8.	72

Figure 2. 44 Synthesis of Colchicine-(<i>R</i>)-3-Pyrrolidinol)-TPP (AM9) from AM4 (Colchicine-(<i>R</i>)-3-Pyrrolidinol)	73
Figure 2. 45 ESI (+) Mass spectrum of AM9 (Col-(<i>R</i>)-3-Pyrrolidinol-TPP).	74
Figure 2. 46 Comparison of the observed data with the theoretical isotope model of AM9.....	75
Figure 2. 47 ¹ H NMR assignments (ppm values) and atomic numbering for AM9... 75	
Figure 2. 48 % survival of <i>C. elegans</i> for AM1 and AM2 at different concentrations (0.1 μM, 1 μM, 10 μM and 100 μM in the presence of negative controls (<i>S. medium</i> control and DMSO control) at 22h. % survival of <i>C.elegans</i> was calculated by considering number of live worms and divided by sum of live and dead worms multiplied by 100 to get % of survival. The experiment was repeated in triplicates with n=3.....	82
Figure 2. 49 The comparison between effects AM1 and TPP-conjugate AM2 on worm's viability in terms of motility at 2 h and 24 h exposure, with both negative controls; <i>s. medium</i> and DMSO. Motility was measured by total number of turns per individual worm per minute (Adopted from the results provided by Dr. Lorna Proudfoot).	83
Figure 2. 50 The comparison between effects AM6 and TPP-conjugate AM7 on worm viability in terms of motility at 2 h, 24 h and 48 h exposure, with both negative controls; <i>s. medium</i> and DMSO. Motility was measured by total number of turns per individual worm per minute, data shown in mean of number of turns per minute. Experiment was performed in duplicate with n=4. (Adopted from the results provided by Dr. Lorna Proudfoot).	84
Figure 2. 51 CN2 (N-deacetyl-N-(2-mercaptoacetyl)-colchicine in complex with X-ray crystal structure of bovine α, β-tubulin in the colchicine binding pocket. Crystal structure obtained from the protein database in the pdb form.	87
Figure 2. 52 Binding model of compound AM1 (Col-Pro) (a potential tubulin modulator), in the colchicine binding pocket; top ranked pose.	88

List of Tables

Table 1. 1. Showing important helminths, their transmission routes and mode of entry (Castro, 1996).	2
Table 1. 2. List of registered drugs for the treatment of parasitic worms' infections in human (Greenberg, 2005; Pharmaceutical Journal, 2019).....	7
Table 1. 3 List of some recommended drugs against haemonchosis in sheep (Kaplan, 2004; Kaplan, 2014).	11
Table 1. 4. Some examples of drugs to which resistant strains of <i>Haemonchous contortus</i> were reported in different countries (Getachew <i>et al.</i> , 2007).	20
Table 2. 1 Log D values for aminocolchicine derivatives (Appendix A.2.1-Appendix A.2.6).....	79
Table 2. 2 Log D values for TPP-conjugated aminocolchicine (Appendix A.2.2-Appendix A.2.9).....	80
Table 2. 3 Binding energies of AM1, AM3, AM4, AM6 and CN2 (the reference compound).	89

List of Appendices

Appendix A:.....	18
Appendix B:.....	23

Abbreviations

AV	Avermectin
CoL	Colchicine
CBS	Colchicine binding site
CBSI	Colchicine binding site inhibitors
DIPEA	N,N'-Diisopropylethylamine
DMF	N,N'-Dimethylformamide
DMSO	Dimethyl sulfoxide
ESI(+) or (-)	Electrospray ionisation/positive or negative mode
Eq	Molar equivalents
g	Grams
h	Hour(s)
HOBt	Hydroxybenzotriazole
LEV	Levamisole
M	Molar
Mg	Milligram(s)
Min	Minutes
Mmol	Millimole(s)
MS	Mass spectrum
MTT	3-(4,5-dimethylthiazol-2-yl)-2,5-diphenyltetrazolium bromide
MT	Microtubule
MTA	Microtubule targeting agents
NMR	Nuclear magnetic resonance
Pro	Prolinol

PyBop	Benzotriazol-1-yl-oxytripyrrolidinophosphonium hexafluorophosphate
rt	Room temperature
R_f	Retention factor
TFA	Trifluoroacetic acid
TLC	Thin layer chromatography

Aim and Hypothesis

Aim

The principal aim of this project is to design & develop novel targeted anthelmintic amino-colchicine prodrugs that can deliver the active drug inside mitochondria (target site), by the use of lipophilic, cationic drug delivery vehicle; TPP (Triphenyl phosphonium cation) to achieve selectivity and toxic efficacy of these agents. These “smarter” prodrugs may be able to circumvent developing resistance and reduce general toxicity.

Hypothesis

It was hypothesised that by the help of TPP, triphenyl phosphonium which is a lipophilic, delocalised cationic carrier molecule, drugs can be directed to the target sites (mitochondria) by potentially bypassing the resistance mechanisms and in doing so it will achieve maximum efficacy and decreased general toxicity to the host.

Drug molecules conjugated to TPP with a specific linkage (such as an ester or amide linkage) designed to be cleaved by esterase or peptidase in the host to release active drugs at the site of action. The negative membrane potential of cell and mitochondrial membrane can be exploited to direct TPP (cationic drug carrier) towards matrix of mitochondria.

Chapter 1

1.0 Background & Introduction:

1.1 Helminths

Helminth is a Greek word meaning “worm”, helminths infested humans, animals, and crops before our earliest written history. Thousands of years ago eggs of intestinal helminths were found in mummified human faeces (Lindquist and Cross, 2017).

The course of the modern twentieth century world was altered markedly by the same kind of helminths. In China, during the cold war, schistosomes that were known as “the blood fluke that saved Formosa” sickened troops of Mao causing acute schistosomiasis (Kreston, 2014). A study tells that helminths infect approximately one third of the world’s population (Besier *et al.*, 2016; Hotez *et al.*, 2006) and can have a significant effect on disease in farm animals (Roeber *et al.*, 2013).

1.1.1 Categorisation of helminths

Helminths include invertebrates and are categorised on the basis of their general and external shape, the organs of host they reside in, egg morphology and larval or adult stages. There are two forms of helminths namely; bisexual and hermaphroditic.

There are two main phyla of helminths:

- 1) The nematodes (known as round worms): this phylum includes major intestinal worms also called soil-transmitted worms and the filarial worms that cause filariasis (Hotez *et al.*, 2006).
- 2) The Platyhelminths (known as flat worms): this phylum includes the flukes (also called as trematodes), such as Schistosomes and the tapeworms (also known as cestodes) such as the pork tapeworm that causes cysticercosis (**Table 1.1**) (Hotez *et al.*, 2008).

Table 1. 1. Showing important helminths, their transmission routes and mode of entry (Castro, 1996).

Parasite	Transmission	Entry route
Roundworm		
<i>Enterobius vermicularis</i> (pin worm)	Eggs, direct faecal contamination	Mouth
<i>Trichuris trichiura</i> (whip worm)	Eggs matured in soil	Mouth
<i>Ascaris lumbricoides</i>	Eggs matured in soil	Mouth
<i>Necator americanus</i>	Larvae matured in soil	Skin
Tapeworms		
<i>Taenia solium</i> (pork tapeworm)	Larvae in infected pork	Mouth
<i>Taenia saginata</i> (beef tapeworm)	Larvae in infected beef	Mouth
<i>Echinococcus granulosus</i>	Eggs in dog faeces	Mouth
Blood flukes		
<i>Schistosoma species</i>	Larvae swimming in water	or mucosa
Liver fluke		
<i>Clonorchis sinensis</i>	Larvae in marine plants or mouth	Mouth
Lung fluke		
<i>Paragonimus westermani</i>	Larvae in infected crustaceans	Mouth
Intestinal fluke		
<i>Fasciolopsis buski</i>	Larvae in marine plants or fish	Mouth

1.1.2 Anatomical features of Helminths

Nematodes and platyhelminths share the same anatomical features that are necessary for inhabiting the host. The outer layer of helminths is called the tegument in platyhelminths or the cuticle in nematodes (Richardson and Smail, 1998). Flukes or trematodes are leaf shaped worms, they are mostly hermaphrodites (genderless that means having sex organs of both sexes in the same individual hence both self and cross fertilisation occur) with the exception of blood flukes, *Schistosoma species* (that have both male and female separate sexes but live in pair as male and female schistosomes or fluke) (Halton, 2004). Tapeworms or cestodes are hermaphrodites. Adults reside in the intestinal lumen of host whereas larval forms live in extra-intestinal

tissues of the host. They have segmented bodies and are elongated in shape (Castro, 1996; O'Connell and Nutman, 2016).

Roundworms or Nematodes are bisexual worms that are cylindrical in shape. Both adults and larval forms reside in intestinal and extra-intestinal tissues of host (Gasser *et al.*, 2016).

1.1.3 Parasitic Helminths a threat to humans, livestock & crops

Norman Stoll (1947), made a worldwide estimation about the number of people infected with parasites in his research entitled "the wormy world" (Stoll, 1999). According to a recent estimation approximately one-third of the almost three billion people of Asia, Africa, America and others are infected with some kind of parasite (Horton, 2003). Diseases caused by helminths are the most neglected tropical diseases (NTDs) in the list of the top seventeen neglected diseases issued by WHO (McCarty *et al.*, 2014). All of these diseases are linked with poverty levels in that region. According to one study, more than one billion people are suffering from one of the NTD (Kyelem *et al.*, 2011).

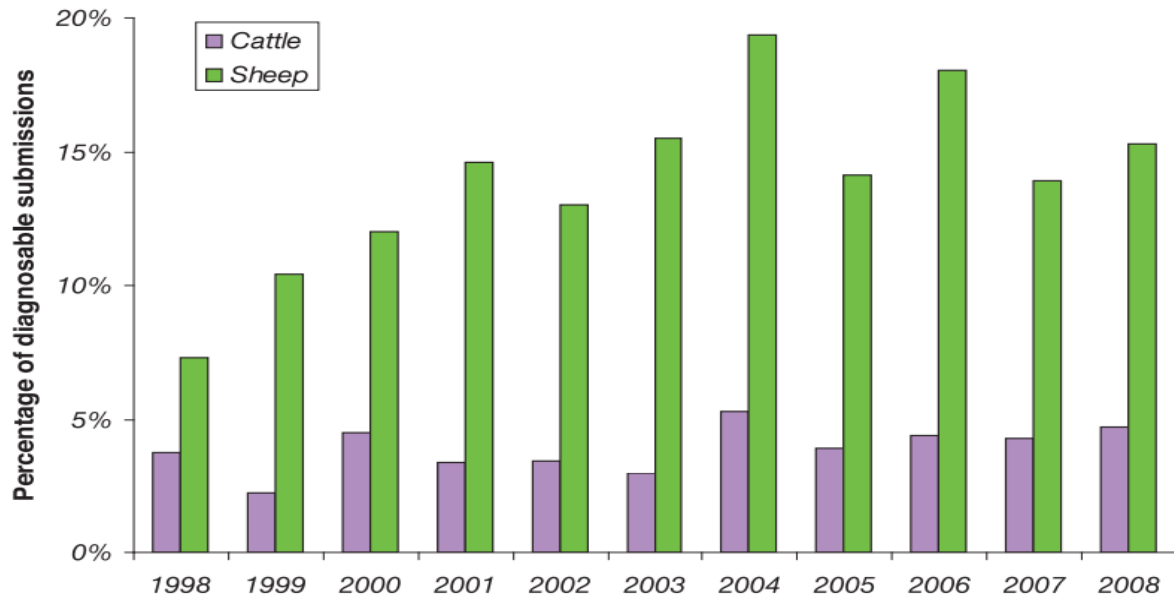
The most prevailing diseases in NTDs are the ones caused by helminths. Parasitic helminths often have long life and their reproductive rate is very high. This would mean that treatment employed to control the helminth infection can only be effective if they have the ability to produce long term sustainable effects (Tchuem Tchuente, 2011). Every year, due to parasitic diseases in sheep and cattle, there are estimated financial losses of 1 billion dollars in Australia (Roeber *et al.*, 2013). In UK, nematodes; *Haemonchus contortus*, *Teladorsagia circumcincta* and trematode *Fasciola hepatica* are economically the most important helminths that cause infections in sheep, goats and cattle (Papadopoulos *et al.*, 2012). *Fasciola hepatica*, a liver fluke, infects 300 million cattle and 250 million sheep throughout the world and costs financial losses of 3 billion US dollars a year. In some parts of the UK, 1 in 3 cattle and 1 in 5 sheep are infected with liver fluke (Fairweather and Fairweather, 2005). Helminths infections of livestock cause serious economic losses worldwide specifically parasite nematodes are a threat to human health, productivity and health of livestock and crops (Hotez *et al.*, 2008).

Amongst helminth infection, gastrointestinal infections such as: ascariasis, strongyloidiasis, fascioliasis and trichuriasis are of primary importance and affect more than one billion human population (McCarty *et al.*, 2014). In 2010, a study was conducted on the prevalence of helminths infection, demonstrating that 807-1221 million people affected by *Ascaris lumbricoids*, *Trichuris trichiura* infected 604-795 million people population and hookworm infected 576-740 million population of humans. An annual loss of 118 billion dollars has been estimated which is a result of compromised crop population due to nematode infestation (Howard J Atkinson *et al.*, 2012).

According to Nicol *et al.*, 2011 the production losses in crops are more than 14.6% in developing countries because most of developing or under developed countries are in tropical and sub-tropical regions where helminths infections are most prevalent. This is due to climate factors i.e. warm and humid environment that is in favour of helminths growth and survival, so more helminths mean more damage to the crops and less production.

1.1.4 Gastro-intestinal Nematodes

Among all helminths gastrointestinal nematodes are the major worm infections that affect both small and large ruminants, for example; sheep, goats, and cows in the whole world (Roeber *et al.*, 2013). The main gastrointestinal nematodes belong to order Strongylida family trichostrongylidae (Papadopoulos *et al.*, 2012). The most economically important nematode in order strongylida includes *Haemonchous contortus* and *Teladorsagia circumcincta* (Gasser *et al.*, 2016). PGE (parasitic gastroenteritis) (**Figure 1.1**) is the most prevailing gastro-intestinal disease in Scotland caused by *T.circumcincta* (a nematode) damaging livestock production efficiency (Wilson *et al.*, 2008).



Yearly increase in PGE infection in cattle & sheep

Figure 1. 1 Shows % of diagnosable submission of cattle and sheep in the Vet. Hospital of Scotland with PGE (parasitic gastroenteritis) yearly (Wilson *et al.*, 2008).

1.1.5 Life cycle of Strongylida nematodes

In the order strongylida, adults are dimorphic and reside in the digestive tract, where females lay eggs in large numbers. Those eggs are expelled from the body of the host through faeces (Gasser *et al.*, 2016).

Eggs are 70-150 μm in diameter and take 1-2 days for hatching. After hatching, larvae feed on bacteria and finally develop into 3rd stage ensheathed larvae (L3s) in the soil. The sheath represents a cuticular layer that protects L3s from harsh environment. Animals are infected when they ingest L3s stage of larvae, when L3s pass through the stomach of a ruminant, they lose their protective sheath and undergo a tissue phase before their transition to L4 stage or pre-adult stage (Levine, 1980) (**Figure 1.2**).

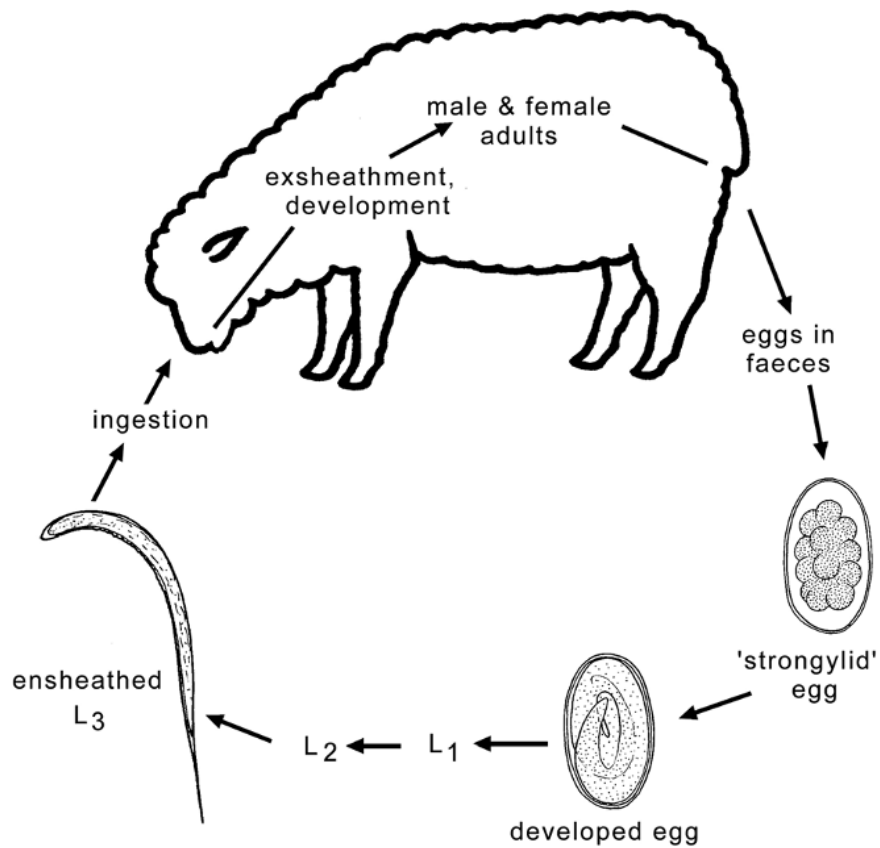


Figure 1. 2 Shows life cycle of gastrointestinal nematodes of order strongylida in small ruminants (Peebles, 2007).

At the end of the grazing season when conditions became unfavourable the larvae go through a phase of halted development called “hypobiosis”. This is common in *H. contortus* and *T. circumcincta*.

1.2 Introduction to Anthelmintic drugs:

Anthelmintic, nematicide or wormer (also known as dewormer or drench), is a chemical or drug that is used to treat infectious diseases caused by parasitic helminths including round worms (nematode) and flatworms (trematodes and cestodes) (**Table 1.2**).

Table 1. 2. List of registered drugs for the treatment of parasitic worms' infections in human (Greenberg, 2005; Pharmaceutical Journal, 2019).

Schistosomiasis (blood fluke)	Intestinal round worms
Oxamnaquine	Piperazine
Praziquantel	Benzimidazoles
	Morantel
	Pyrantel
Cestodiasis (tape worm)	Levamisole (LEV)
Albendazole	Avermectins (AM) and milbemycins
Niclosamide	Tribendimidine
Benzimidazoles (BZ)	
Praziquantel	
Fasciolasis (liver fluke)	Filariasis (tissue round worms)
Triclabendazole	Diethylcarbamazine
	Albendazole
	Ivermectin

1.2.1 Classification of Anthelmintic Drugs

Classification of these agents are based on similarities in chemical structure and mechanism of their actions.

1.2.1.1 Piperazine

Piperazine was used for the first time in 1950 as an anthelmintic drug and is still being used as active component of many remedies used for the thread worm infection in children and available as over the counter (OTC) drug. Piperazine was first studied on nematode *Ascaris suum*, where it produces flaccid (a reversible paralysis of belly muscles) by acting on GABA receptors as a GABA mimetic agent (Fennell *et al.*, 2008). R. J. Martin, 1997, investigated the mechanism of action of piperazine in *Caenorhabditis elegans* (*C. elegans*) and its activity was compared between wild and mutant gene (*unc-49*). They showed piperazine has the same inhibitory effect on both wild and mutant gene not only in a *C. elegans* developing assay but also in intact animals containing both genes (**Table 1.2**) (**Figure 1.3**).

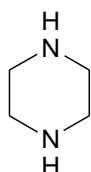


Figure 1.3 The chemical structure of piperazine.

1.2.1.2 Benzimidazoles (BZ)

Benzimidazoles (BZ) are broad spectrum anthelmintic drugs. Thiabendazole and Albendazole are the primary drugs in this class (**Table 1.2**). Thiabendazole was the first member of this class and was discovered in 1961 and several benzimidazoles (BZ) were discovered after that. A massive literature demonstrated that their efficacy is because of their selective binding with β -tubulin and as a result they interfere and

jeopardise microtubule cytoskeleton formation (**Figure 1.4**) (De Nollin and Borgers, 1975; Lacey, 1988).

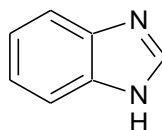


Figure 1. 4 Chemical structure of benzimidazole.

1.2.1.3 Imidazothiazoles and tetrahydropyrimidines

The most widely used imidazothiazole is levamisole (LEV) (**Figure 1.5**) and tetrahydro pyrimidines pyrantel and morantel are in widespread use. These compounds are very active against nematodes but happen to have no effect on trematodes and cestodes whatsoever. Levamisole is derived from the compound tetramisole which is a racemic mixture of D and L isoforms, whereas levamisole is purely an L-isomer. Pyrantel and morantel are from the class tetrahydro pyrimidines and have a similar structure. They both are very effective anthelmintic drugs (Hausen *et al.*, 2011; Scorza *et al.*, 2006). Both agents act as agonists of nicotinic receptors and cause paralytic spasticity on helminths' muscle wall by activating excitatory acetylcholine nicotinic receptors (nACRs) (Scorza *et al.*, 2006).

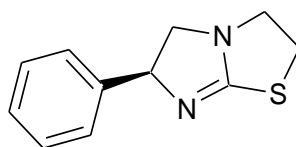


Figure 1. 5 Chemical structure of levamisole (LEV).

Levamisole also causes spastic paralysis in *Caenorhabditis elegans* specifically in egg laying worms. It is even more potent as compared to acetylcholine itself and exerts its activity at lower μM concentration than acetylcholine (Ruiz-Lancheros *et al.*, 2011). According to Martin *et al.*, (2015), EC_{50} value of levamisole is $9 \mu\text{M}$ in spastic paralysis.

1.2.1.4 Macrocyclic lactones: ivermectin (ivermectin)

In 1980, Merck introduced ivermectin for the first time. Ivermectin is a semi-synthetic derivative of avermectin (AM) (a macrocyclic lactone) which is formed as a fermentation product of the microbe *Streptomyces avermitilis* (Howard, 2011). Ivermectin induces a very intense and prolonged paralysis effect on pharyngeal and body wall musculature (Römbke *et al.*, 2010). It interacts with acetylcholine gated chloride channels, acetylcholine receptors and glycine receptors. Most importantly it has high affinity for glutamated chloride channels that defines its anthelmintic activity in nematodes (Guggisberg *et al.*, 2014; Pemberton *et al.*, 2001).

1.2.2 Limitations of Anthelmintic or Nematicide or Dewormer

Efficacy of anthelmintic drugs is in danger considering their long-term usage, incorrect handling of these agents and under dosage. All these factors can influence on their efficiencies and play a significant role in emergence of resistance against these agents (Nielsen *et al.*, 2014). Another factor that can contribute to their limitation, is unavailability of these drugs in the affected area, because of economic reasons or dearth in veterinary facilities. Especially in most part of tropical regions animal dies due to haemonchosis either acute or chronic and loose massive body weight that can be another constraint in the poor performance of ruminants in meat production (Getachew *et al.*, 2007).

Table 1. 3 List of some recommended drugs against haemonchosis in sheep (Kaplan, 2004; Kaplan, 2014).

Chemical group	Anthelmintic	Prescribed dose
Imidazothiazoles	Levamisole (LEV)	7.5 mg/kg
Benzimidazoles (BZ)	Albendazole	5 mg/kg
	Fenbendazole	5 mg/kg
	Oxfendazole	5 mg/kg
Macrocyclic lactones (avermectins)	Ivermectin	0.2 mg35/kg
	Moxidectin	0.2 mg/kg
Salicylanilides	Closantel	10 mg/kg

The mainstream anthelmintics are limited in their action between nematodes, cestodes and trematodes such as, praziquantel (**Table 1.2**), an anti-parasitic drug used for cestodes and trematodes infections in human, is completely useless against nematodes. Benzimidazole (BZ) is the only class of anthelmintics that possess cross-phyla efficacy but has shown more activity against nematodes than other phyla (**Table 1.3**) (Campbell, 1990). Moreover, for the crop protection from helminth infestation, use of nematicide or dewormer should take into consideration the stability of agent, leaching in the soil and ecotoxicity (environmental toxicity) (Prichard *et al.*, 2012). Ivermectin has been the most successful anthelmintic both in tropical diseases and veterinary medicine and a saviour drug in most parts of Africa where its consumption has changed the lives of populations that were previously confounded by Onchocerciasis (a tropical ailment), commonly called river blindness. However, resistance was developing against this drug according to the published researches (Diawara *et al.*, 2009; Kim *et al.*, 2015).

1.3 Microtubules (MT)

In the 19th Century Flemming explained that there are two components in a eukaryotic cell that undergo mitosis and those are: chromo elements or chromosomes and thin filaments called microtubules (MT) (Tansatit *et al.*, 2006). It is known by the analysis of different mutation in the microtubules cytoskeleton that a slight change can lead to functional deformity in the cell and organism itself (Janke, 2014).

1.3.1 Microtubules Organisation

Microtubules (MT) are a set of 25nm wide tubes that are hollow from inside. These tubes are made by sidelong interplay of 13 protofilaments and each protofilament in turn composed of heterodimers of α and β tubulin which interact head to tail to form these protofilaments. Alpha (α) and beta (β) tubulin are two closely related isoforms that bind GTP. This molecular organisation describes the polarity of microtubules. At one end only α -tubulin exposes and is also called the minus end, and on the other end only β -tubulin exposes called the “plus end” (**Figure 1.6**) (Akhmanova and Steinmetz, 2015; Curcio and Bradke, 2015).

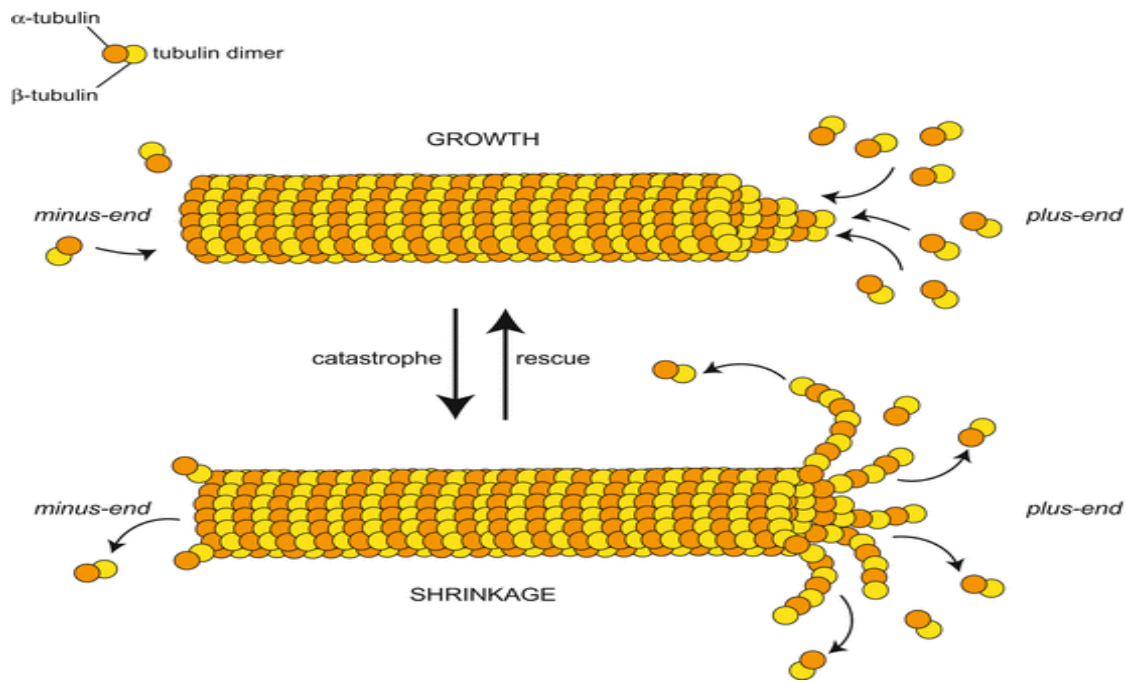


Figure 1. 6 Organisation of MT in a eukaryotic cell, showing tubulin dimers, protofilaments and catastrophe switch (Akhmanova and Steinmetz, 2015).

MTs can grow and shrink in the presence of GTP and it can go between these two phases by catastrophe switch (Gardner *et al.*, 2013; Lacey, 1988). Microtubule catastrophe is an event that manifest itself by a sudden switch between a growing stage and a rapidly shortening stage of microtubule in which MT growth interrupted by occasional switching to rapid shrinkage (or “MT catastrophe”) and then switching back from shrinkage to growth (“called rescue”) (**Figure 1.6**). The reason behind this catastrophe is either a single random event that happen due to sudden loss of MT protecting end or may consist of multi-process event (Gardner *et al.*, 2013). Mitchison and Kirschner, (1984) first described this microtubule (MT) instability in 1984. They demonstrated that all these events happen at the plus end (positive end) and that the negative or minus end is more stable (Horio *et al.*, 2014). Microtubules are essential for cell division which is key for life if anything happened with assembly and disassembly of microtubules that can be lethal, or it can produce cells with a wrong number of chromosomes. The condition with abnormal number of chromosomes (either gain or lose) is called aneuploidy and is a main cause of miscarriages, congenital defects and may also lead to cancer (Lüders, 2016).

1.4 – Microtubules as target molecules in antiparasitic treatments

Microtubules are the promising biological target for many small molecules because of its dynamic role in cytoskeletal organisation and cell functions. An important class of anthelmintic agents called benzimidazoles (BZ) (1.2.1.2) (**Figure 1.4**) binds with one of protein subunit of microtubule called β -tubulin causing unfolding of the protein leading to abnormal conformation that further inhibit polymerization of α - and β -tubulin subunits to form microtubules, this results in a lethal effect in rapidly dividing cells of helminth. BZ bind with 25-400 folds greater inhibition constant with nematode tubulin as compared to mammal's tubulin (Maddison *et al.*, 2008).

Colchicine which is a spindle poison and used as a main drug component in this research shares the same binding site as with the benzimidazoles (an anthelmintic drug), it shows a strong binding affinity with tubulin and binds at the interface of α and β tubulin by forming a colchicine-tubulin complex that depolymerises microtubule organisation (discussed in detail under 1.4.4.2.1).

1.4.1 Microtubule Targeting Strategies

Microtubules have highly dynamic properties that are mandatory for the spindle assembly function. But at the same time, they can also make mitotic cells very sensitive and a potential target for the chemotherapeutic agents or factors that can change their properties. Microtubule targeting agents (MTA) or tubulin binding agents (TBA) can alter dynamics of MT so it made tubulin a very important target in cancer therapy and they were used as pioneer chemotherapeutic agents in cancer therapy. There are several TBA exist that are extracted from wide range of species such as plants, sponges and bacteria. Tubulin binders or inhibitors are also knowns as “spindle poisons” or anti-mitotic compounds, because they halt mitosis by inhibiting spindle formation or cause disruption in spindle assembly (Jordan and Wilson, 2004). All these microtubule targeting agents work on one of these principles i.e. they either promote microtubule stabilisation or they mimic destabilisation of microtubules. The predominant idea behind employment of MTA as anti-cancer agents came from their

ability to interfere with mitotic cell division that occurs in cancer cells all the time. (Parker *et al.*, 2014). However, there is still the need of discovering novel ways to target microtubules or tubulin that can outweigh the ability of cancer cell to become resistant towards therapeutic effects of drugs.

1.4.2 Targeted delivery of tubulin binders

Tubulin binders have no selectivity for the dividing cells so can lead to off-target effects and general toxicity (Parker *et al.*, 2014). For achieving maximum efficiency and to overcome the problem of toxicity, Elena *et al.*, (2013), designed library of tubulin binders that are modified and synthesised in conjugation with fluorescent probe to achieve imaging of tubulin molecule. They demonstrated that modification in existing tubulin binders by conjugation, these compounds can modulate microtubule dynamics or its function. They used thio-colchicine, cephalomannine and paclitaxel as tubulin binders and employed FITC (fluorescein isothiocyanate) for the conjugation purpose to make a fluorescent probe for MT imaging (Riva *et al.*, 2013). Passarella *et al.*, (2009), proposed that histone deacetylase (HDAC) inhibitors are potential anti-cancer agents because of their ability to inhibit cell proliferation and induction of apoptosis. These agents enhance the acetylation of histone so as a result they reverse the epigenetic changes occurs in cancerous tissue. Also, these inhibitors modulate acetylation of non-histone proteins such as alpha-tubulin. On the basis of this finding they proposed by combining both tubulin binder and HDAC inhibitors there will be a synergistic effect. This hypothesis was also demonstrated by Itoh, *et al.*, (2007), where they employed thiocolchicine and paclitaxel with HDAC inhibitor and the final product showed synergism.

1.4.3 Binding sites of tubulin binders

Tubulin binders bind at various binding sites on tubulin. Some tubulin poisons bind at beta-tubulin, some bind at alpha-tubulin and some bind at the interface of alpha and

beta dimers. Beta tubulin has 3 conventional binding pockets, these include colchicine-binding sites, taxol or paclitaxel binding site and vinca-alkaloid binding site.

1.4.4 Tubulin Binding Agents (TBA's)

Tubulin binders divided into 2 classes depending on their effect on microtubule dynamics.

1.4.4.1 Microtubule Stabilising Agents

Taxol (paclitaxel), docetaxel and taxanes are in this category. These are natural agents and obtained from the bark of *Taxus brevifolia*. Taxanes use against solid tumours for example breast, prostate, lungs and ovarian cancers. They bind to beta-tubulin and stabilise MT. Microtubule targeting agent epothilone B analog ixabepilone (product of myxobacterium sporangium cellulosum was approved by FDA for advanced breast cancer. It binds on into the taxol binding site and stabilise MT assembly in a similar way as paclitaxel (Rodriguez-Garcia *et al.*, 2017).

1.4.4.2 Microtubule destabilising agents

This category includes Vinca alkaloids that are extracted from *Catharanthus roseus*, it includes compounds like; vincristine, vinblastine, vindesine, vinorelbine and vinflunine. They are active against a variety of solid tumors and lymphatic cancers. (Waight *et al.*, 2016). The second most important class of destabilisers include agents that bind on the colchicine binding site of beta-tubulin.

1.4.4.2.1 Colchicine:

Colchicine is the primary drug in this class. It is one of the oldest prescribed drugs that has been and still being used in the treatment of gout and FMF (familial Mediterranean fever as an anti-inflammatory agent (Cocco *et al.*, 2010; Zhang *et al.*, 2015) (**Figure 1.7**).

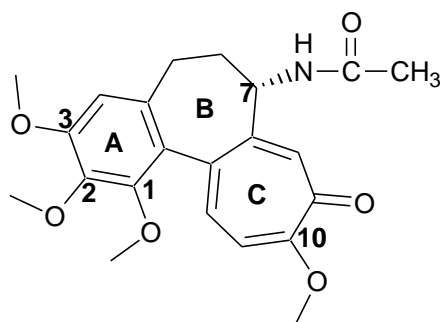


Figure 1.7 Chemical structure of colchicine showing three rings: A (6 membered ring), B (7-membered ring) and C (7-membered ring).

FDA in 2009 has approved colchicine as a medication for gout and FMF (Yang, 2010). Colchicine is obtained from a natural source, “*Colchicum autumnale*” (Colchicaceae), the meadow saffron, and other species called “*Gloriosa superba*”. Colchicine is a spindle poison that binds to tubulin with strong affinity at the interface of alpha & beta tubulin and forms a tubulin-colchicine complex, depolymerises the microtubule by acting as a disrupting agent and mediate mitotic arrest and cell death (Bhattacharya *et al.*, 2016; Nepali *et al.*, 2016). Abnormal increase in mitosis rate is one of the most significant and well-studied feature of cancer cells. This feature makes them so vulnerable against microtubule targeting agents (MTA’s), because microtubule (MT) is part of cytoskeletal and establishes the dynamics of spindle apparatus moreover comprises the main elements of mitosis cell division. Any agent that destabilises the MT will eventually halt the mitosis process.

Colchicine, that inhibits the MT polymerization, causes perturbation of both microtubule spindles and mitosis (Bhattacharya *et al.*, 2016; Rodriguez-Garcia *et al.*, 2017). The application of colchicine in cancer therapy is limited due to its cytotoxicity in the non-cancerous or normal cells of the body. Oral colchicine is safe when administered in safe proper clinical dose. A recent study demonstrated that colchicine can produce autophagy and premature senescence in human lung cancer cells when administered in safe clinical dose. Experiments showed that colchicine inhibited proliferation in A549 (human lung carcinoma cell line) in a concentration gradient manner. A 17% loss in viability of cancer cells was monitored when incubated for 96 h in a cell viability assay. Study further reported that colchicine produced ROS

(reactive oxygen species) that was responsible for induction of autophagy (Bhattachariya *et al.*, 2016).

1.4.5 Novel Example of Tubulin Binders

BAL27862 (**Figure 1.8**) is a very potent inhibitor of cancer cell growth and it promotes apoptosis in cancer cells. It showed potent activity in cancer cells that were resistant to conventional MTA's (microtubule targeting agents) taxanes and vinca alkaloids (Moudi *et al.*, 2013). Studies demonstrated that this new drug Bal27862 inhibits MT production by interfering with microtubules organisation and its dynamics within the cell (Bachmann *et al.*, 2015). A study by Andrea Porta (2014) demonstrated MOA of this novel drug. Study showed Bal27862 is a potent MTA that binds at the colchicine binding site (CBS) on tubulin molecule and exert significant effect on MT organisation in a cell (Prota *et al.*, 2014).

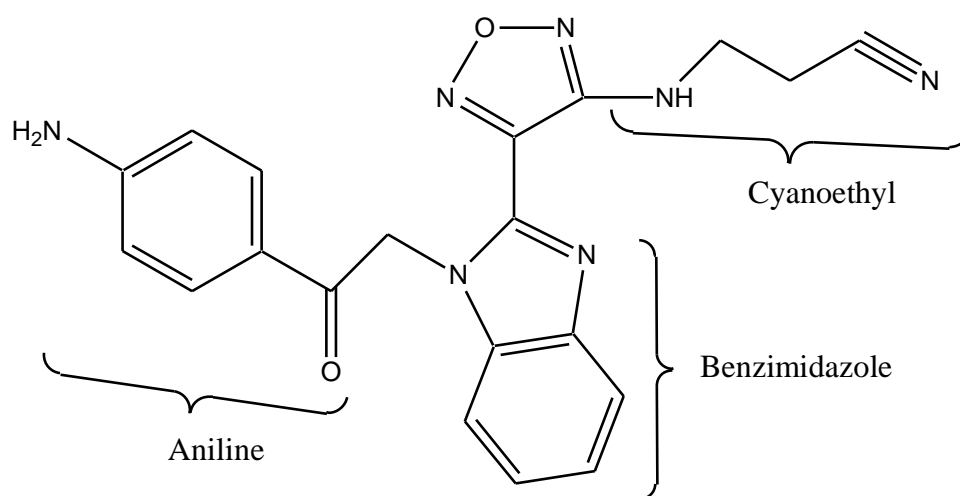


Figure 1. 8 Chemical structure of Bal27862, showing benzimidazole (BZ) part, Aniline and cyanoethyl.

1.5 Resistance

The biggest issue with the existing anti-parasitic drugs is emerging resistance against them (Lalchhandama and Lalchhandama, 2010; Ramos *et al.*, 2018). Resistance is the major problem when it comes to efficacy of anthelmintics and a hazard in sustainability of the UK's farming, animal welfare and agriculture income (Peebles, 2007) (**Table 1.4**).

Research showed that parasites are becoming resistant to antiparasitic drugs (Lalchhandama, 2010) and posing a great threat to global food security by affecting goat and sheep farms all across the globe (Brophy *et al.*, 2012; Ray M Kaplan, 2004). For example, *Haemonchus contortus*, which lives in the stomach of ruminants, has shown resistance against many anthelmintics available on the market, consequently causing great economic losses (Howard J Atkinson *et al.*, 2012). Nematodes that are resistant to the anthelmintic represent serious problems in small ruminants (sheep and cattle) due to their specialised stomach (Wolstenholme *et al.*, 2004). In Australia the profitability of the whole sheep industry has been threatened by severe prevailing resistance (Besier and Love, 2003) (**Table 1.4**). Epe and Kaminsky in 2013, discussed in detail the introduction, usage and limitation of 3 new anthelmintic agents namely; emodepside by the brand name profender, tablets for dogs and spot-on for cats, monepantel (zolvix for sheep), derquantel (for sheep) (Epe and Kaminsky, 2013) . Resistance has developed against all the major classes of broad spectrum anthelmintics such as benzimidazoles (BZ), avermectins (AM) (that includes ivermectin, moxidectin and doramectin), milbemycins, levamisole (LEV) and other nicotinic agonists. Moreover, anthelmintics of narrow-spectrum activity such as closantel also encounter resistance from nematodes (Fairweather and Fairweather, 2005).

Table 1. 4. Some examples of drugs to which resistant strains of *Haemonchous contortus* were reported in different countries (Getachew *et al.*, 2007).

Continent	Country	Anthelmintic
Africa	Ethiopia	Albendazole Tetramizole Ivermectin
	South Africa	Almost all groups
Europe	France	Benzimidazoles Levamisole
	Great Britain	Benzimidazoles
Asia	Malaysia	Benzimidazoles Levamisole Closantel Ivermectin
South America	Argentina	Benzimidazoles Levamisole Ivermectin
	Uruguay	Benzimidazoles Levamisole Ivermectin
Australia	Australia	Avermectin

In the past two decades, triclabendazole (TCBZ, a member of BZ) has been the primary choice to treat liver fluke infections in livestock because of its extraordinary activity against migrating stages of fluke (Fairweather and Fairweather, 2005) but resistance is developing. The first report of TCBZ resistance was in Australia, 1995. Later, it was reported in England, Ireland, Scotland, southwest Wales, the Netherlands and Spain. In 2003, in the UK, the season was reported as the worst especially in Scotland and northern England, due to dramatic renaissance of fasciolosis and a record number of cases affected from this infection. The reason was the change in climatic conditions and arrival of warm and wet weather. According to a survey, cattle (50%) and sheep (20%) livers were affected as a consequences of fluke infection (Abebe *et al.*, 2010).

A simultaneous failure of three classes of differently acting anthelmintic agents (ivermectin, oxfendazole and morantel) was reported first time in New Zealand in 1990, against nematodes that were derived from the goats, when these agents were administered to animals that belonged to different groups (Watson and Hosking, 1990).

1.5.1 Mechanism of Drug Resistance

Resistance against drugs can arise mostly in these possible ways.

1.5.1.1 Mutation in the target site:

Any change that occurs in the target molecules can affect the binding of drug to the target site because the drug moiety no longer recognises the target so no activity or effect of drug will initiate. For example, in case of some BZ, resistance arises because of mutations in β -tubulin isotype 1 and 2 (Demeler *et al.*, 2013).

In case of avermectins, it is the mutation of GluCl and/or GABA-R genes that are responsible for resistance. Levamisole resistant helminths showed changes in nicotinic acetylcholine receptors (Wolstenholme *et al.*, 2004).

1.5.1.2 Uptake of the drug:

Any change in distribution of a drug to the target site can lead to resistance such as difficulty of a drug molecule to reach its target or removal of drug from the target due to p-glycoprotein efflux pumps (**Figure 1.9**). P-glycoproteins are membrane bound proteins that are members of ABC or ATP binding cassettes commonly known as transporter proteins. In 1976, Juliana and Ling, identified these transporters first time in cancer cells causing MDR (multi-drug resistance) against chemotherapeutic anti-cancer agents. These proteins provide protection against external toxins found in food and environment (drugs) and in doing so they rescue cell and organelle from toxic effects of drugs. This resistance path presents a major problem in helminth's diseases

therapy by producing resistant worms and one of the main cause in failure of anthelmintic drugs (**Figure 1.9**) (Broeks *et al.*, 1995; Singh *et al.*, 2015).

For example, triclabendazole (TCBZ). Triclabendazole, a fasciolicide, is a very narrow spectrum BZ. Triclabendazole sulfoxide TCBZ.SO is an active form of TCBZ, it causes widespread shedding of tegument by blocking the tegumental secretions. In addition, it constrains mitotic cell division of spermatogenic cells which leads to microtubule disruption (Cancela *et al.*, 2010). Studies showed TCBZ resistance was not associated with mutations in the β -tubulin molecule of the fluke. In TCBZ-resistant flukes, considerably lower level of TCBZ and TCBZ.SO were detected than in TCBZ-susceptible flukes. This observation may suggest that P-glycoprotein-lined drug efflux pumps are associated with TCBZ resistance (Fairweather and Fairweather, 2005; Cancela *et al.*, 2010).

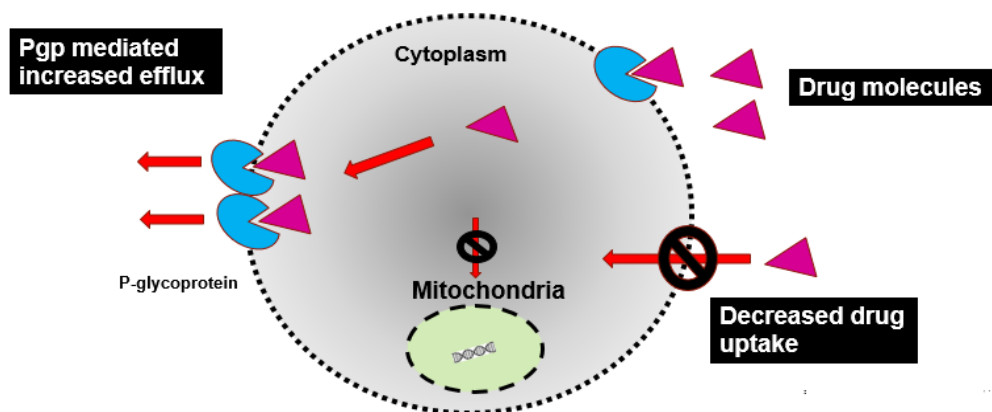


Figure 1. 9 Decreased uptake of drug by the cell due to mutation, so no drug at the target site, and uptake of drug molecule by p-gp receptors results in increased efflux or removal of the drug from the cell.

1.5.1.3 A metabolic change

A metabolic change that alters or prevents the drug activation or initiates its inactivation is also a cause of developing resistance (Zahreddine and Borden, 2013).

H. contortus has a great tendency to develop resistance to anthelmintic agents because of this drug resistance become a major complication which threatens farm

produce and welfare of the animals (Matoušková *et al.*, 2016; Raza *et al.*, 2016). One of the Pharmacokinetic-mediated mechanism that involved in decreased drug efficacy or inactivation is metabolic change or altered metabolism. In this way, the concentration of the active drug at the target site (within parasite cells) is decreased, a lesser number of drug molecules bind to target receptors hence reducing drug effect. This type of resistance is the outcome of over-expression and increased activity of xenobiotic-metabolizing enzymes. These are the protein that provide string defense against potential harmful effects of drugs. Several studies described an evidence of direct link between drug resistance in nematodes and the xenobiotic-metabolizing enzymes (Brophy *et al.*, 2012; Matoušková *et al.*, 2016).

It was evident in studies conducted on *Haemonchous contortous* that this nematode was able to metabolize albendazole (ABZ) and flubendazole (FLU) (Vokřál *et al.*, 2013).

1.5.1.4 Target Gene amplification

Drug resistance often leads to 'survival of the fittest' and reflect evolution, where a change in gene or gene expression is responsible for organism survival against a drug treatment. Gene amplification refers to increase in number of copies of a gene and this process is very common in cancer cells as well as in helminths. These amplified genes are responsible for helminth's survival against drug treatment. Amplification can occur in the target genes or any other gene. Any change in gene expression can lead to an amplification of target gene by increasing its production that means not enough drug molecules available at the target site leading to a massive decrease in drug efficacy. In ivermectin-resistant *H. contortus* or *T. circumcincta*, an increase of low-affinity L-glutamate-binding site was monitored that is a cause of resistance. Drug resistance against anti-parasitic drugs has been developed to a certain level where even Levamisol and BZ cannot be considered as highly effective anthelmintic drugs (Ray M. Kaplan, 2004; Scott *et al.*, 2013).

1.6 Targeted Delivery by prodrug strategy

The toxic efficacy and selectivity of anthelmintic can be improved by the use of prodrug forms that possess intracellular drug targeting moieties that may be able to circumvent P-gp type mediated resistance mechanism. The prodrug is a chemical entity (an inactive compound) that has no or less pharmacological activity against a specific target until after its metabolic transformation to an active or more active compound that has potential efficacy against that target. (Hamada, 2017).

Prodrug strategy is a practical way to improve availability of drug at the biological site. Prodrug approaches potentially can overcome all the barriers that decrease the drug's benefits and its availability, these include; water solubility, drug stability, side effect profile, duration of an effect, safety index and taste of the drugs (Hamada, 2017; Ortiz de Montellano, 2013). Some conventional drugs are prodrugs because they can only be activated after a metabolic reaction or any modification. Examples include; Levodopa which is a precursor of dopamine, norepinephrine and epinephrine (neurotransmitters) (Levy *et al.*, 2011). Numerous recent developments have occurred in designing prodrug strategies; these rely on possible modification for example amidation, benzylation, and esterification. One strategy in designing prodrugs involved the use of the drug or parent molecule with a hydroxyl group. One example of such a prodrug strategy is oseltamivir (an anti-inflammatory drug) which is an ester type prodrug (Cacciatore *et al.*, 2018; Zawilska *et al.*, 2013).

The other strategy of prodrug design is to modify the hydroxyl (OH) group found in many drug molecules by carriers, targeting groups or self-eliminating linkers. These molecules possess changeable moieties such as sugars, amino acids, phosphate and organic acids. These moieties can be attached to the parent drug by a covalent bond and can be converted back to the parent molecule by specific enzymes such as sugar digesting enzymes, alkaline phosphatases, peptidases and esterases (El-Kamel *et al.*, 2008; Hamada, 2016). Prodrugs that contain hydrophilic moieties such as; sugars, amino acids and phosphates are water soluble in nature, their bioavailability is often higher as compared to the sparingly soluble and less efficient parent drug molecules. Recently a series of novel prodrugs of the sparingly soluble drug phenytoin has been designed and synthesised based on an arginine-methyl ester decomposition reaction.

The prodrug form can easily be converted into the parent molecule (**Figure 1.10**) in suitable physiological conditions. The research proved that phenytoin prodrug showed most promising effects and hence was more soluble as compared to parent drugs (Hamada, 2016).

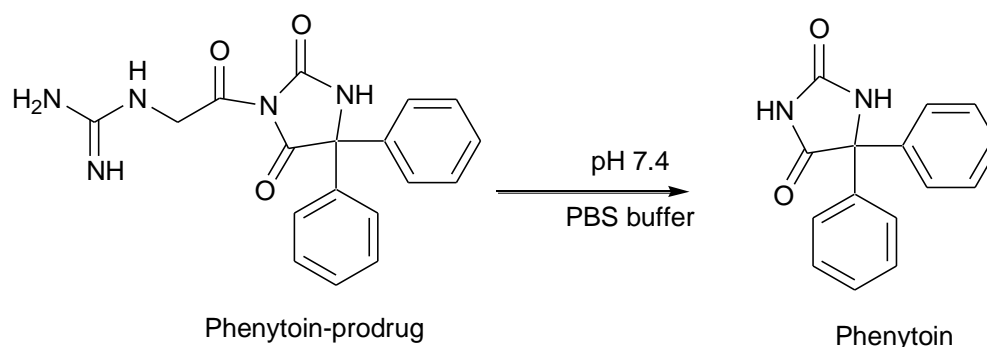


Figure 1. 10 Conversion of phenytoin prodrug (insoluble) into active parent drug (soluble) under physiological conditions.

1.6.1 Mitochondria, “a promising target” in chemotherapy

Mitochondria are considered a power house of a cell. They are a small organelle within a cell that generate cellular energy in the form of ATP (adenosine triphosphate) (Milane *et al.*, 2015). Apart from being a power generating house, mitochondria contribute to many functions of a cell that are important for survival and integrity of the cell (Zielonka *et al.*, 2017a). Any defect or dysfunctionality of mitochondria can lead to several neurological and CVS (cardiovascular system) diseases. Mitochondria are vulnerable to oxidative stress (damage) that can contribute towards dysfunctioning of mitochondria and ultimately apoptosis (Picard *et al.*, 2016; Vásquez-Trincado *et al.*, 2016). Some research in cancer therapy is focussed on selective targeting and accumulating MTAs (mitochondria targeting agents) in the matrix of mitochondria that in return interfere with proliferation process in cancer cells by generating ROS (reactive oxygen species) and induce apoptosis (Cheng *et al.*, 2015).

1.6.2 Mitochondria targeting approaches

A popular strategy over the past decade is to modify small drug molecule into a drug delivery vehicle to target mitochondria. This concept gained popularity because of effortless and easy synthesis process and maximum efficacy (Lu *et al.*, 2016).

There are two important mitochondrial targeting approaches: one includes conjugation of a therapeutic agent directly with a targeting moiety, for example, TPP conjugates with therapeutic drugs, and the second consists of inclusion of a nano-vehicle with a targeting agent.

1.7 Introduction of Lipophilic cation: Triphenylphosphonium compound (TPP)

TPP, triphenylphosphonium is a lipophilic, delocalised cationic carrier molecule that can be conjugated with different drug moieties by a specific linkage (such as an ester or amide linkage) that directs the drug to the target mitochondria site and potentially bypassing the resistance mechanisms and in doing so it will achieve maximum efficacy and decreased general toxicity to the host (Millard *et al.*, 2010) (**Figure 1.11**).

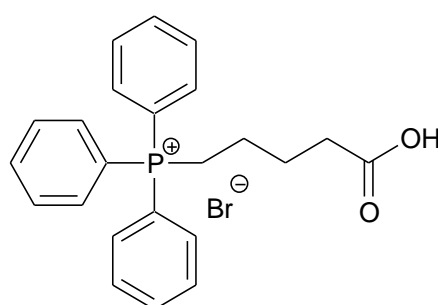


Figure 1.11 Chemical structure of TPP (4-carboxybutyl) triphenylphosphonium).

TPP and TPP-like cations were first used in the form of probes to better understand the mitochondrial membrane potential mechanism (Battogtokh *et al.*, 2018). They are also utilised to deliver small drug molecules, antioxidants, vitamins and

pharmacophore to target mitochondria. Examples of lipophilic cations include triphenylphosphonium ions, peptides and rhodamine, these positively charged molecules can be attached to a drug molecule to ensure their mitochondrial uptake (Hardy *et al.*, 2014).

1.7.1 Mitochondrial membrane potential

Membrane potential $\Delta\Psi$ is potential gradient that forces ions to move passively in one direction that means positively charged molecules are attracted towards the negative side of the membrane and vice versa. It represents an electrical potential difference between inside and outside of a physiological cell membrane. Mitochondrial membrane potential is one of the reasons behind selective uptake of lipophilic cations like TPP conjugated drugs by mitochondria. Drug moieties must cross both cell and mitochondrial membranes to reach the mitochondrial matrix. This step is easy for lipophilic cations such as TPP because the inner sides of the cell membrane and mitochondrial membrane are negative, that allows gradual accumulation of lipophilic cations first in the cytosol and then inside of the mitochondria. Membrane potential of plasma membrane is 30-60 mV (negative inside, positive outside) that causes 3-5 times increase in the penetration of cations in the cytosol as compared to extracellular environment. In addition, membrane potential of mitochondrial membrane is approximately 150-180 mV and that favours easy passage of lipophilic cations to the matrix of mitochondria (Román Luque-Ortega *et al.*, 2010; Zielonka *et al.*, 2017a).

It was stated that due to membrane potential of mitochondrial inner membrane (negative inside) drug molecules with the positive charged carriers penetrate through the mitochondrial membrane and gathers in the matrix. Targeting mitochondria using TPP molecule in the form of prodrug is not a new approach as plentiful literature already showed maximum efficacy of TPP containing drugs (Kezic *et al.*, 2016).

1.7.2 Hydrophobicity of TPP Drug complex

Membrane potential and charge on the molecule is not the only reason for attracting cationic compounds inside the mitochondria, but there is another significant feature that facilitates passage of lipophilic cations through the lipid bilayer membrane and that is hydrophobicity or lipophilicity of the compounds. High lipophilicity of a compound means increase uptake by mitochondria and vice versa (Ross *et al.*, 2005).

TPP was employed to functionalised conventional nanoparticles such as liposomes and dendritic polymers targeting mitochondria. These polymers showed great deal of specificity in targeting mitochondria in the presence of TPP, because of this they may be considered as second-generation drug delivery systems (DDS's). In vitro experiments proved that these TPP conjugated polymers showed promising results by not only successfully enter the cell membrane and accumulated inside the mitochondria, but also remained stable and intact during this process until they reach to the target site that is mitochondria (Paleos *et al.*, 2016).

A series of novel compounds have been synthesised that composed of mitochondrial targeting antioxidants in which TPP was linked to the antioxidant vitamin E by an alkyl linker. All the synthesised compounds were mitochondrial targeting vitamin E derivatives (mito-E analogues) and possessed varying degree of hydrophobicity depending on different linkers of different lengths. These analogues presented maximum degree of efficiency by accumulating in the matrix of mitochondria (Jameson *et al.*, 2015).

1.7.3 TPP application as a “magic bullet” in targeted drug delivery

TPP conjugated drug applications were initiated by Murphy and co-researchers (Coulter *et al.*, 2000; Murphy, 1997). TPP based drug conjugates have significant advantages over other targeted delivery vehicles that include: straightforward synthesis and purification, stability of TPP molecule in a living system, mixture of lipophilic and hydrophilic properties in a same conjugate and non-reactivity towards other components of cell (Zielonka *et al.*, 2017). A variety of researches have been conducted based on the direct conjugation of triphenylphosphonium cations with anti-

cancer drugs or antioxidants since 1995 when Murphy's group conducted a study based on mitochondria targeting conjugates with antioxidants (Burns *et al.*, 1995). It is now proved by studies that anticancer drugs or any antioxidant when conjugated directly with a MTA (mitochondrial targeting agent) is capable of increasing cytotoxicity and anti-oxidising property by localizing specifically to mitochondria in comparison with their parent drugs that has no targeting moiety attached (Battogtokh *et al.*, 2018). In a recent study TPP was linked to anti-cancer agents; betulin and betulinic acid to achieve specificity in targeting mitochondria of cancer cells. These agents were of limited use before due to some limitations such as poor bioavailability, poor water solubility and low intracellular acquisition. These problems were solved by the application of TPP-drug complex (**Figure 1.12**).

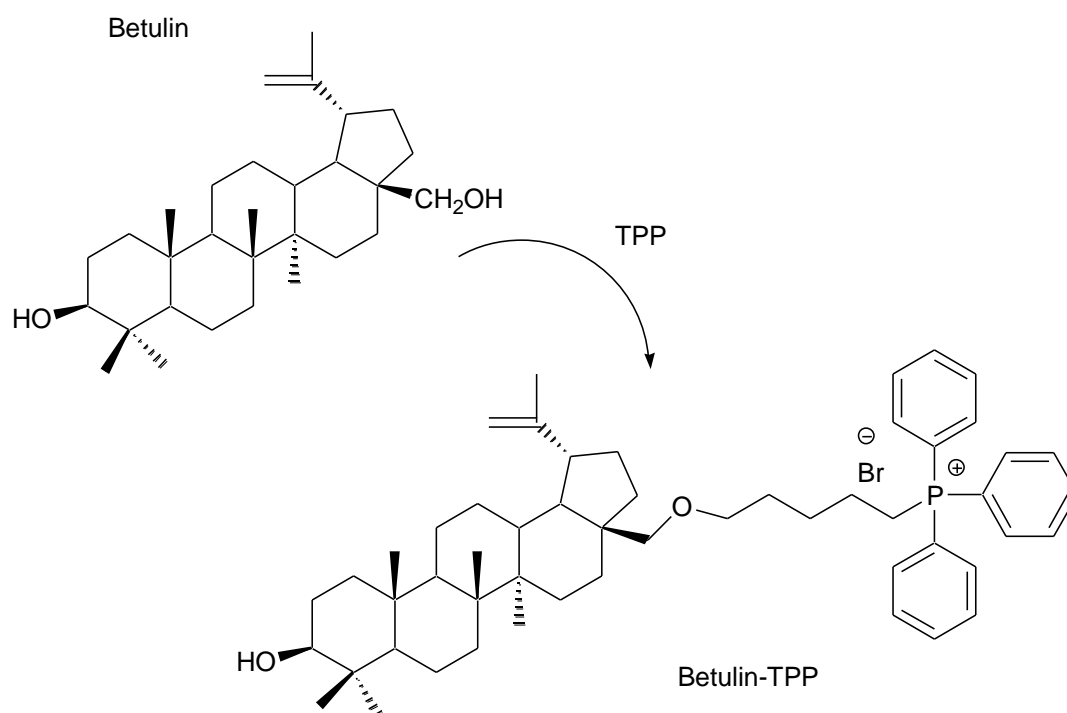


Figure 1.12 TPP-betulin prodrug complex (showing ester bond) and its non-prodrug form betulin.

Results from different assays showed that these targeted agents with attached TPP exhibited increased uptake, significant cytotoxicity and selectivity between cancer cells and normal cells as compared to non-conjugated parent drugs betulin and betulinic acid (Ye *et al.*, 2017).

Strobykina *et al.*, (2015), synthesised a series of novel anti-mitotic agents in which TPP moiety was used as a delivery vehicle to achieve selectivity in terms of accumulating in the matrix of mitochondria. The compounds comprised of diterpenoid

isosteviol attached with TPP cations. In an assay, isosteviol-TPP complex when tested on fertilised eggs, induced mitotic arrest by acting on mitochondrial DNA. TPP based targeting approach is considered as most promising when it comes to the selective targeting and cytotoxic efficiency in cancer therapy without producing off-target effects. Millard *et al.*, (2013), designed and synthesised a novel TPP derivative of nitrogen mustard chlorambucil called, Mito-chlor. Nitrogen mustard excessively used chemotherapeutic agent but was limited in efficacy and safety profile. By synthesising it as a TPP conjugate, it has overcome these limitations. Mito-chlor was able to localise on cancer cell mitochondria and produce apoptosis by arresting cell cycles in breast and pancreatic cancer cells as compared to parent drug molecule that was unable to show any toxicity.

1.8 *Caenorhabditis elegans* as a Model Organism

In 1963, Sydney Brenner proposed that the success of molecular biology is because of presence of extremely simple model system, such as a simple organism that can be controlled and handled even if it is in large numbers (Brenner, 1974). Brenner introduced *C. elegans* as a model system for conducting research in developmental biology (Kaletta and Hengartner, 2006a). After his introduction, this organism has been widely used as a research tool (Kenyon, 1988).

1.8.1 Properties of *C. elegans* as a model experimental system

Caenorhabditis elegans or *C. elegans* is a free living, non-parasitic roundworm or nematode naturally exist in soil of temperate climate (Culetto, 2000; Labouesse, 2003). *C. elegans* is an excellent model organism and favoured by the scientist because of its amazing properties such as, its small size (1 mm) that makes it easily maintained, transparency (transparent from outside that makes it easy to observe and manipulate) and it is very easy to work with in the laboratories. It can be easily cultivated and housed in large numbers such as 10,000 worms/petri dish (Buckingham *et al.*, 2014; Kaletta and Hengartner, 2006b; Kenyon, 1988). *C. elegans* can also be maintained in liquid culture. It can swim using an oscillating, stereotyped body motion that can be either indirect assay to monitor organism health or a direct representation of the

neuromuscular system. The swimming rate or thrashing (number of folds or bend per minute) can be measured manually (Buckingham *et al.*, 2014).

The life cycle of *C. elegans* is very short, it takes about 3 days from egg to egg, life span is about 2-3 weeks and this short life cycle facilitates biological research because of reduced experimental cycle (Kaufman and Miska, 2010).

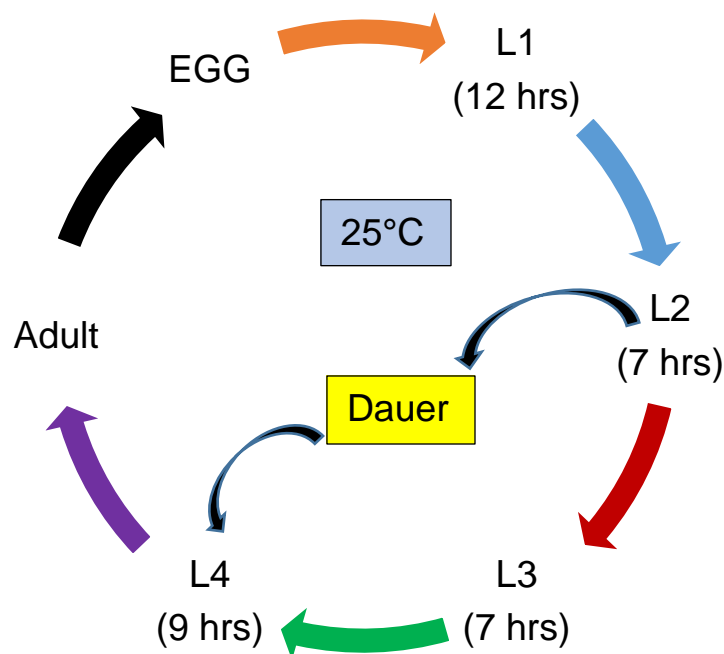


Figure 1. 13 Life cycle of *C. elegans* at 25 °C (Donald L Riddle, 1997).

Due to unfavourable conditions, that can be either change in environment or food deprivation, in the life cycle of *C. elegans* the L1 or L2 Larvae stage can convert into the Dauer stage, which is the most stable stage (**Figure 1.13**) (Cassada and Russell, 1975; Schindler *et al.*, 2014).

1.8.2 Self-Fertilisation

C.elegans has 6 pairs of chromosomes in which 5 pairs are autosomes and one pair of sex chromosomes. It has 2 sex types; males and hermaphrodites. The type of the sex depends on the 6th pair of sex chromosome, if it is XX it will be a hermaphrodite and if it is XO it will be a male. Hermaphrodites are the most common sex in nature and are capable of self-fertilisation. It can produce 300-350 offspring's in self-fertilisation. Self-fertilisation of hermaphrodite can be manipulated in the laboratories to generate progeny with specific genotype that can especially helpful in genetic research (Woods *et al.*, 2011).

1.8.3 Non-Animal Model & 3R's

C.elegans also complies with the "3 R's Principles" for animal experiments that are widely accepted ethical principles, which demonstrate as: 1) Reduction of the higher animal use, 2) Refinement of current techniques and 3) finally replacement of animals with alternative systems (De Boer *et al.*, 2015).

1.8.4 Comparison of *C. elegans* with other vertebrate models

Other vertebrate models such as zebrafish (*Danio rerio*) and mice are the most experimented models in laboratory because of their homology with human beings but their exploitation is much more complex, and they have longer life cycles (Hulme, 2011).

1.8.5 Homology with humans

In 1998, *C. elegans* was the first multicellular organism whose genome was fully sequenced. Its genome is approximately hundred million base pairs long, no doubt

that it is smaller than human genome but possess same number of genes (*C. elegans* 20,000 genes; humans 23,000). According to bioinformatics analysis 60-80% of homology exist between worm and human and that makes its application favourable to study human genetic disorders (Berezikov, 2004; Driscoll *et al.*, 1989).

This altogether makes its use as a model of parasitic nematodes in anthelmintic drug research extremely valuable (Bruinsma *et al.*, 2008).

Chapter 2

2 Results & Discussion

Resistance is the hallmark when it comes to the efficacy of anthelmintic agents and a major cause of their failure (Howard J. Atkinson *et al.*, 2012; Ray M Kaplan, 2004; Scott *et al.*, 2013). Selectivity and toxic efficacy can be improved by a prodrug design strategy by incorporation of a targeted moiety in the main drug design that target the anthelmintic agents to the target site i.e. helminths. This chapter presents the results and discussion of the design, synthesis and biological evaluation of novel potential anthelmintic prodrugs based on colchicine-derived compounds that were substituted with different amino alcohols (or diamines) to establish any structure-activity relationships within the closely structurally related series. In order to achieve selectivity and toxic efficacy, these novel agents are further conjugated with TPP, triphenylphosphonium cations, as a 'smart' carrier to produce highly efficient prodrugs that might function as Magic Bullets (Finichiu *et al.*, 2013).

TPP or triphenylphosphonium ions are one of the most studied and successfully used lipophilic cations can be easily accumulated into the matrix of mitochondria due to its highly delocalised positive charge and highly lipophilic or hydrophobic nature that would encourage easy passing from the lipid bilayer of not only a cell membrane but also from the mitochondrial membrane; in doing so, it could not only prevent the host from general toxicity by selective targeting to helminth's mitochondria but also has the potential to circumvent the acquired drug resistance (Finichiu *et al.*, 2013; Zielonka *et al.*, 2017).

2.1 Design strategy for novel amino-colchicines

In this project, these novel potential anthelmintic prodrugs are amino colchicine derivatives, further conjugated with TPP for the targeted drug delivery. The general design includes production (synthesis) of novel amino colchicine derivatives with aminoalcohols and diamines to provide the substrate for ester (in case of amino alcohol) and amide (in case of diamine) bond formation to afford the target

compounds. Colchicine was derivatised at carbon-10 with amino-alcohols to generate these novel amino-colchicine derivatives. The series (code-named AM) includes AM1 (colchicine-prolinol), AM3 (colchicine-4-hydroxypiperidine) and AM4 (colchicine-(*R*)-3-pyrrolidinol) (**Figures 2.1 & 2.2**).

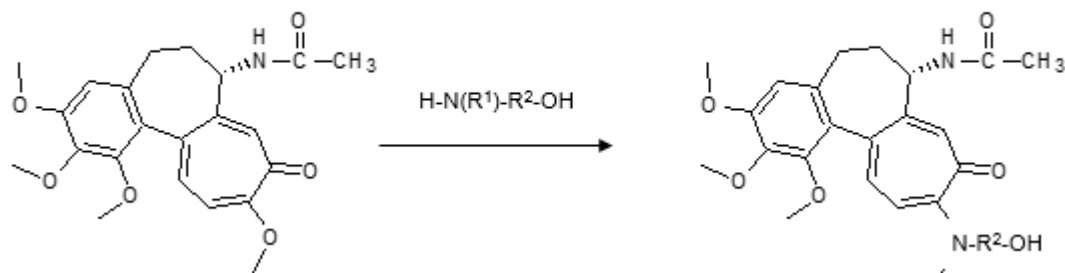


Figure 2.1 General design strategy of amino-colchicine derivatives with amino-alcohol. Where R¹ can be H or 5 membered (prolinol and (*R*)-3-pyrrolidinol) or 6 membered (4-hydroxypiperidine) alcohols.

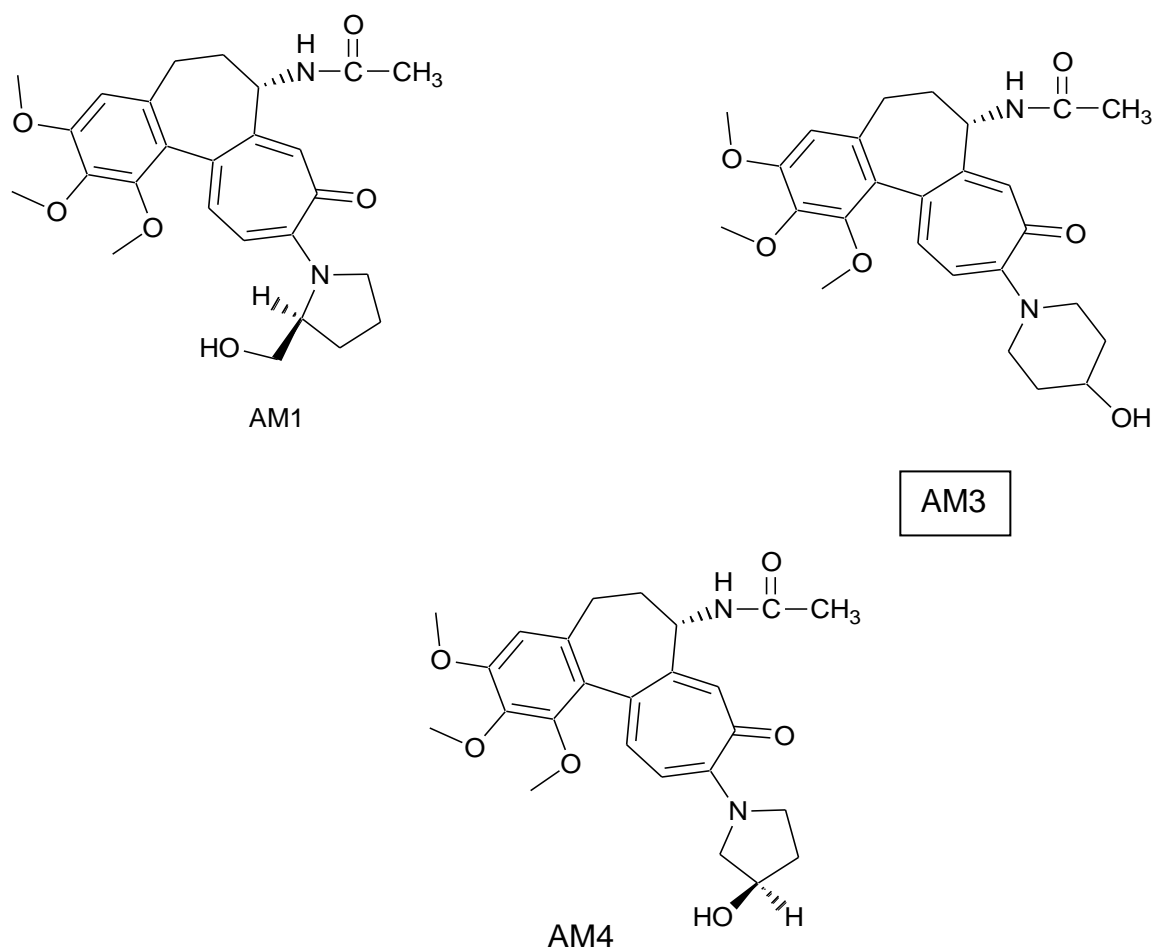


Figure 2.2 Structures of selected colchicine derivatives with amino-alcohols AM1 (colchicine-prolinol) AM3 (colchicine-4-hydroxy piperidine) and AM4 (colchicine-(*R*)-3-pyrrolidinol).

Another design strategy was used in which colchicine was derivatised with a diamine to produce AM5 (Colchicine-(*R*)-3-(Boc-aminopyrrolidine)) and AM6 (Col-(*R*)-3-aminopyrrolidine-TFA) (**Figures 2.3 & 2.4**).

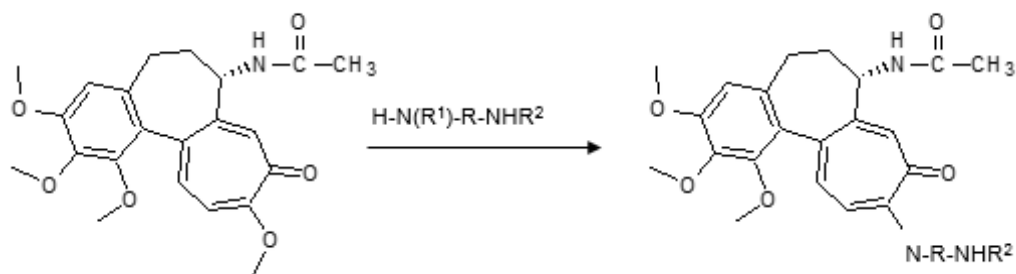


Figure 2.3 General design strategy of amino-colchicine derivatives with diamine. Where R¹ is H or part of carbocyclic ring R is part of carbocyclic ring, exemplified by 3-aminopyrrolidine in which R² is Boc at the exocyclic amino group.

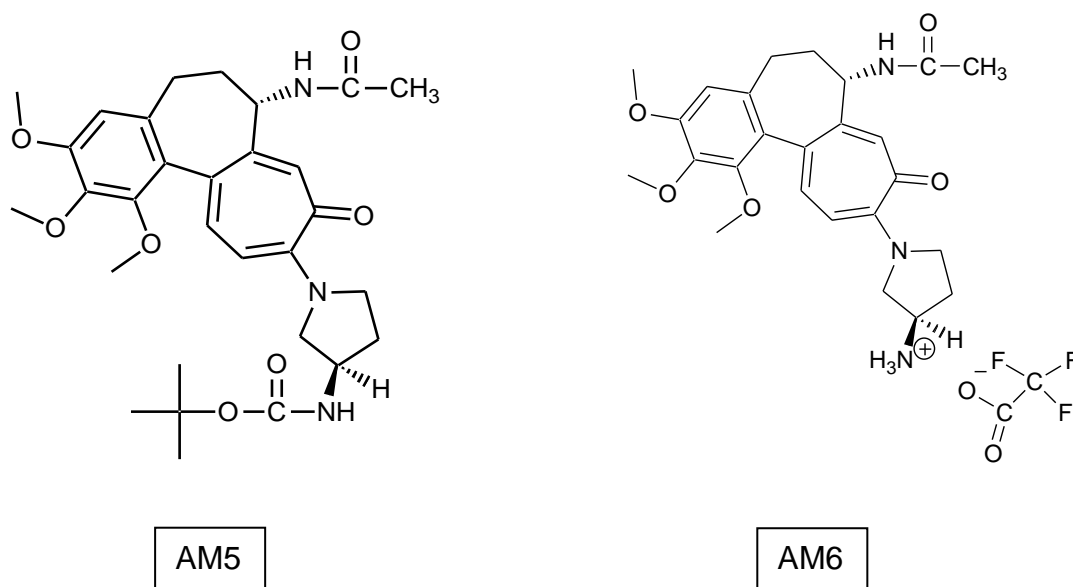


Figure 2.4 Structures of AM5 (Colchicine-(*R*)-3-(Bocaminopyrrolidine)) and AM6 (Col-(*R*)-3-aminopyrrolidine-TFA).

2.2 Prodrug design strategy for novel amino-colchicines in conjugation with TPP

These aminocolchicine derivatives were further conjugated with TPP in order to synthesise novel targeted prodrugs. The series includes AM2 (Colchicine-prolinol-TPP), AM7 Col-(*R*)-3-aminopyrrolidine-TPP). (Figure 2.6), AM8 (Colchicine-4-hydroxypiperidine-TPP) and AM9 (Colchicine-(*R*)-3-Pyrrolidinol-TPP). **Figure 2.5** shows the structures of these colchicine derivatives and their TPP linked conjugates.

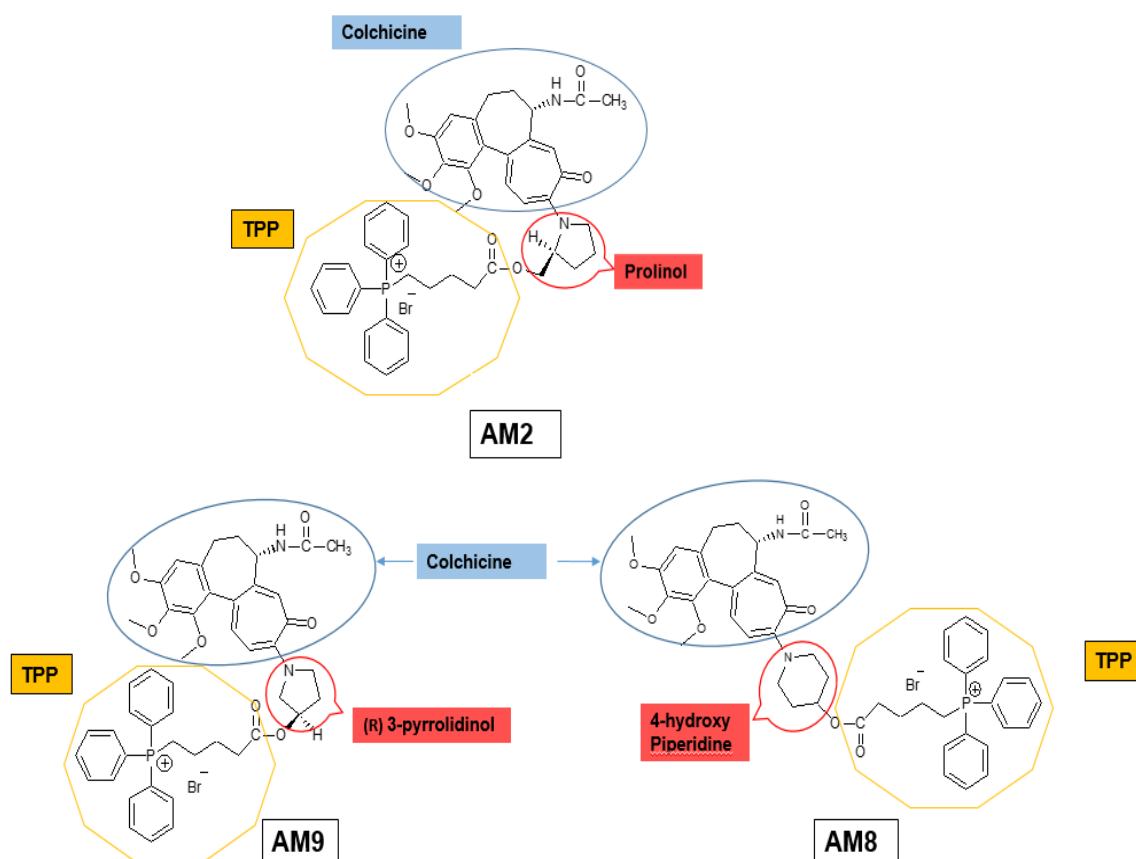


Figure 2. 5 TPP-linked colchicine derivatives; AM2 (Colchicine-Prolinol-TPP), AM8 (Colchicine-4-hydroxypiperidine-TPP) and AM9 (Colchicine-(*R*)-3-pyrrolidinol-TPP).

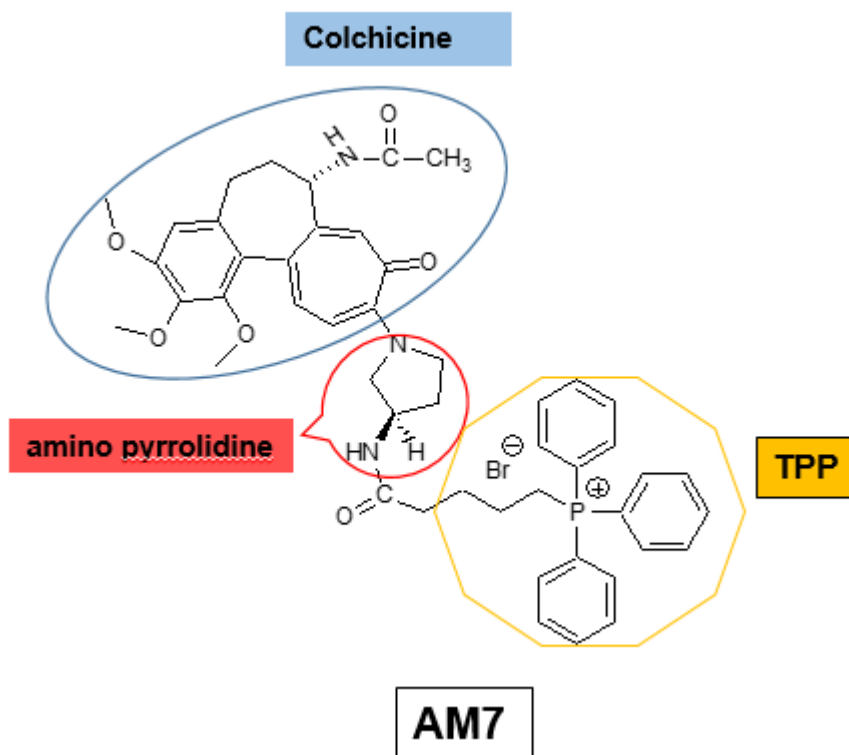


Figure 2. 6 TPP-linked colchicine derivative with diamine AM7 Col-(*R*)-3-aminopyrrolidine-TPP.

2.2.1 Overview of the project

The earlier parts are an outline of design strategy of AM series and the following section describe in detail the rational design, synthetic strategy (solution-based synthesis methods), purification processes, chemical characterisation (mass spectrometry, NMR spectroscopy) and biological evaluation. Biological evaluation includes *C. elegans* viability assay. The *C. elegans* worm was used as model organism for evaluating potential anthelmintic properties of these prodrugs, partition coefficient assay to determine the lipophilicity of these agents and molecular docking studies on AM1, AM6 and CN2 (Ravelli *et al.*, 2004).

2.3 Rationale design of TPP-linked amino-colchicine Prodrugs

This section describes the design of novel colchicine derivatives and their TPP-linked prodrugs. The TPP-linked prodrugs utilised a three components structure design that included a colchicine substituent with an amino alcohol (different in each drug, to act as a linker between colchicine & TPP, and to provide an ester substrate for the action of esterase) and with a diamine (to provide a substrate for amidase or peptidase in the system) and TPP, as a carrier for targeted mitochondrial drug delivery.

Colchicine, that is a known small molecule drug, currently being used as an anti-inflammatory agent in the treatment of gout or Mediterranean fever, is an alkaloidal drug obtained from the floral extract of *Colchicum autumnale*. Studies demonstrated that colchicine interferes with the microtubule assembly by binding with the protein tubulin that consequently leads to disruption of various functions associated with microtubules including cellular chemotaxis, mitosis and phagocytosis (Dalbeth *et al.*, 2014). Colchicine has a high binding affinity for tubulin (a basic unit of microtubules). It binds at the interface of α and β sub-units and forms a curved tubulin dimer due to steric interaction of colchicine and the tubulin. The derived curved dimer then further stops the polymerisation, depolymerises microtubules and inhibits the assembly of microtubules (Ravelli *et al.*, 2004).

There are three main rings of the colchicine structure, a six-membered benzene ring A, a heptane ring B, and another heptane ring C (the tropolone ring) (**Figure 2.7**). It has been known by SAR of colchicine from the literature, that A and C rings of colchicine are important structural features in relation to its high binding affinity for tubulin and intrinsic biological activity. Any changes in the A-ring can lead to loss of binding affinity to tubulin but modification can be made on ring B and at the C-7 and C-10 positions in the colchicine (Dong *et al.*, 2016; Fournier-Dit-Chabert *et al.*, 2012; Zhang *et al.*, 2015). In this study, modification was made to the C-ring of colchicine at the C-10 position by addition of amino-alcohols in the case of AM1, AM3, and AM4 and with a diamine in case of AM5 and AM6 (as shown in **Figure 2.5**).

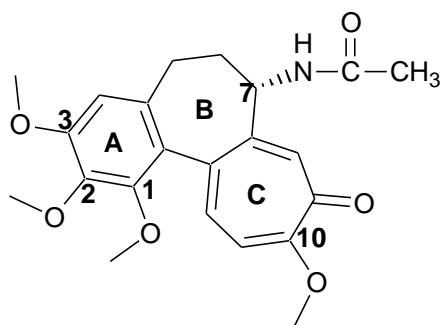


Figure 2. 7 Colchicine with all the rings and showing position C-10 for modification.

Although colchicine has no direct action on mitochondria, depolymerisation of microtubules affects mitochondrial biogenesis, this is because MT are a part of cytoskeletal and play a main role in spindle dynamics during anaphase of mitosis and inhibit formation of mitochondrial content (Karbowski *et al.*, 2006). Colchicine is not known as anthelmintic drug but it shares an important feature with a well-known class of anthelmintics, the benzimidazoles, that is they both bind at the same colchicine binding site on the tubulin molecule (Lu *et al.*, 2012). In part, motivation comes from the known antitubulin action of the benzimidazole class of anthelmintics and the need to develop more potent alternatives that bypass resistance. In preliminary work, hydroxyethylaminodeoxycolchicine has been shown to have significant toxic potency in the nonparasitic *C. elegans* model organism.

This was the main motivation behind developing the potential anthelmintic pro-drugs described in the current research. Research also revealed that selection of benzimidazoles over other anthelmintic is also encouraged due to the ability of host cells to undergo genetic transformation that would block the MT (microtubules) disruption caused by benzimidazoles or by drugs similar to benzimidazoles, as compared to worm cell (Aleyasin *et al.*, 2015).

Toxicity is the major challenge when it comes to the therapeutic efficacy of colchicine derivatives because of its low therapeutic index. This challenge can be addressed by designing its prodrug forms by an addition of targeted carrier molecule such as TPP and targeting drugs to the site of action (which is in this case the worm's mitochondria) that would not only reduce general toxicity to host but also circumvent the possible resistance mechanisms against typical anthelmintic drugs. An approach that would exploit the negative membrane potential of inner membrane of mitochondria and would

attract lipophilic cations, like TPP and draw them towards the matrix of mitochondria, is needed. TPP is one of the less toxic lipophilic carrier cations among other cations used for the same purpose such as rhodamine-123 and thiopyrylium AA1, to deliver drugs or to detect the localisation of drug molecule at the target site (*Modica-Napolitano et al.*, 1984). An early report (Levi-Schaffer *et al.*, 1984) showed that lipophilic, cationic phosphonium compounds had some significant toxicity towards adult *Schistosoma mansoni* worms and had been shown to act as inhibitors of acetylcholinesterase (AChE). In a study, phosphonium lipo-cationic derivatives of betulin and betulinic acid have shown potential as antiparasitic agents against *S. mansoni* (Spivak *et al.*, 2014).

Mitochondria which are a main target in this study, are the power generating organelles in a cell, apart from this main function they also produce ROS (reactive oxygen species). Production of ROS is a sign of oxidative stress and involves in the destruction of other biomolecules in a cell. Hence oxidative stress which is responsible for aging and cell death can originate from dysfunction of mitochondria (Balaban *et al.*, 2005). Payne and Chinnery, 2015 suggested that mutated mitochondrial DNA may produce metabolic abnormalities in mitochondria and is a main reason that implicate aging is mediated through apoptosis. Hence, considering the main role of mitochondria in cell death and cellular functions, the recent research selects mitochondria as a main target for TPP-linked colchicine derivatives in the therapy of helminth diseases.

Studies demonstrate that TPP conjugates are safer and less toxic to the mammalian cell as compared to parasitic helminth cell. This is because helminth's cell membrane is even more negative as compared to the host cell, this feature also encourages TPP-linked prodrugs to be more attracted towards the helminth cell and not to the host mammalian cell. This was proved by different studies where drug complexes were found to be accumulated in the helminth cell as compared to a host cell (Román Luque-Ortega *et al.*, 2010).

The novel anthelmintic amino-colchicine derivatives were designed in a prodrug form by conjugating with TPP (for targeted delivery of these agents) that will release active drugs as amino-colchicine in the mitochondrial matrix. TPP was attached with amino alcohol or a diamine with the formation of an ester bond (or in AM7 an amide bond) that would cleave in a biological system by an enzyme an esterase or amidase (for

AM7) to liberate the active drug amino-colchicine derivatives and TPP at the site of action (worm's mitochondria). **Figure 2.8** shows the prodrug activation concept.

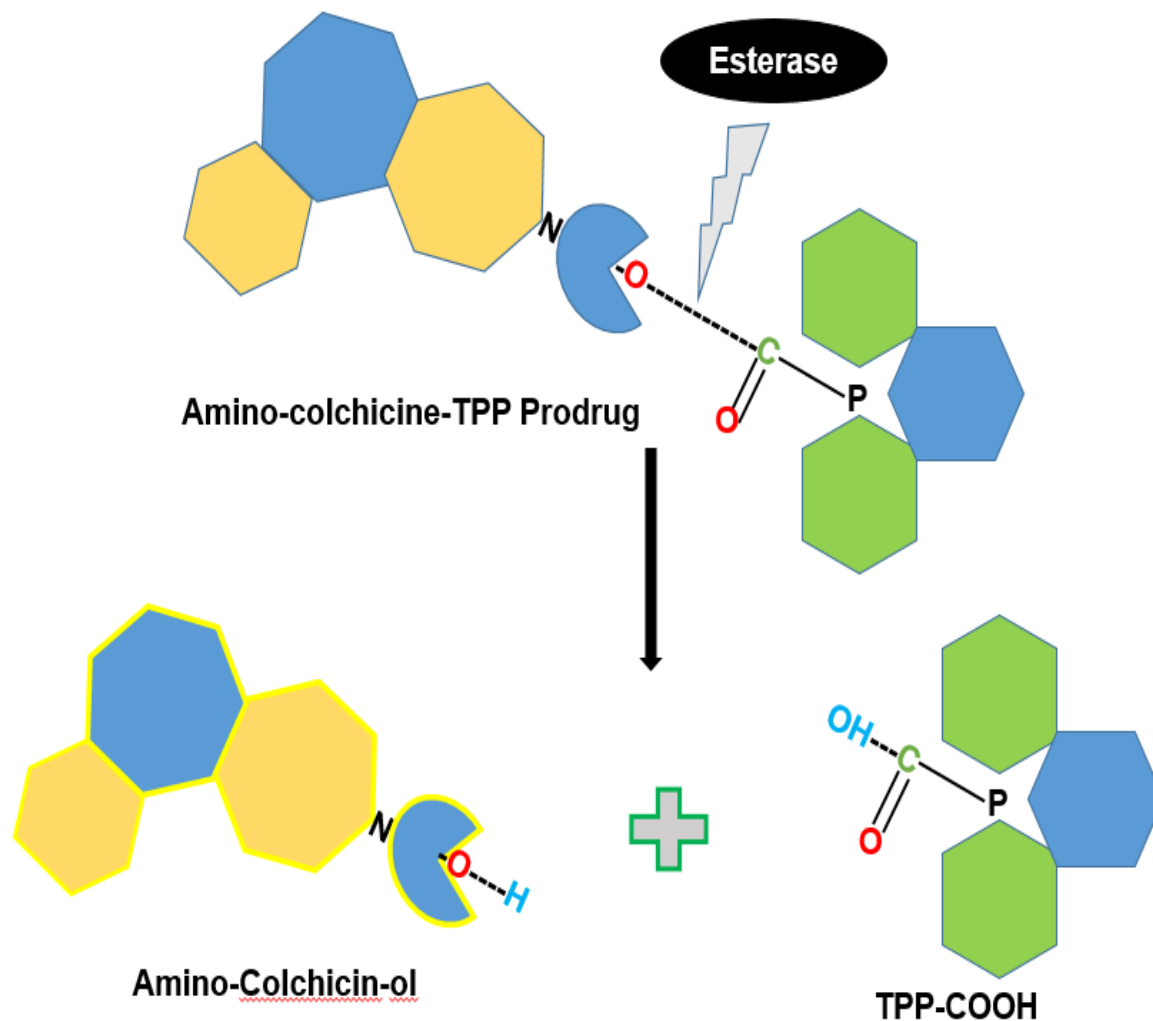
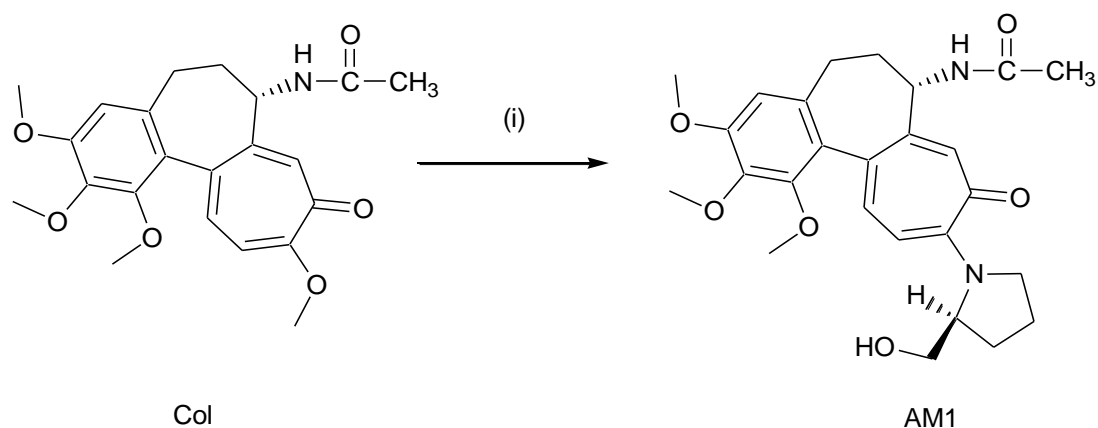


Figure 2. 8 A Prodrug activation concept of TPP-linked colchicine derivatives (the AM series), as potential anthelmintic agents, showing cleavage by an esterase between TPP and the amino-alcohol.

The objective behind the current study was to investigate the potential of novel colchicine based prodrugs as anthelmintic agents and in the longer term, to demonstrate the mechanism of action of the colchicine derivatives in depolymerisation of MT that would in turn disrupt the mitochondrion function and have the potential to lead to cell death and stress in parasitic helminth worms (Vinaud *et al.*, 2008).

2.4 Synthesis Strategy:

2.4.1 Synthesis of Colchicine-Prolinol (AM1)



Reagents and conditions: (i) Prolinol {(S)-pyrrolidin-2-yl methanol}, DMF, 20 °C, 24 h.

Figure 2.9 Synthesis of Col-prolinol (AM1) from Colchicine.

AM1 was synthesised by dissolving colchicine and prolinol in DMF, then the reaction mixture was stirred and kept for 24 h at room temperature (**Figure 2.9**). Solvent extraction was performed to remove excess amount of DMF with chloroform/water mixture and the progress of the reaction was monitored by TLC which showed completion of the reaction with the formation a new yellow spot in the product lane running higher than the starting material. Crude product (AM1) was purified by silica gel column chromatography, firstly, chloroform was used as a mobile phase to remove the high running impurities in the mixture and unreacted colchicine, then chloroform: methanol (9:1) and (4:1) and lastly methanol alone was used (in order of increasing polarity) to elute AM1. All the fractions containing pure AM1 (confirmed by TLC) were eluted, combined and filtered to remove silica, evaporated to reduce the volume, cooled over ice bath and finally diethyl ether was added into the mixture to get a yellow precipitate of Col-prolinol (AM1). The precipitate was filtered and dried to afford yellow solid AM1 in a good yield.

AM1 was characterised by its MS (ESI+) mass spectrum that showed a signal at m/z 469.23 Da ($M+H$)⁺ for the species $[C_{26}H_{32}N_2O_6]^+$ and its sodium adduct at m/z 491.21 ($M+Na$)⁺ and confirmed the molecular mass of 468.23 Da. (**Figures 2.10 and 2.11**)

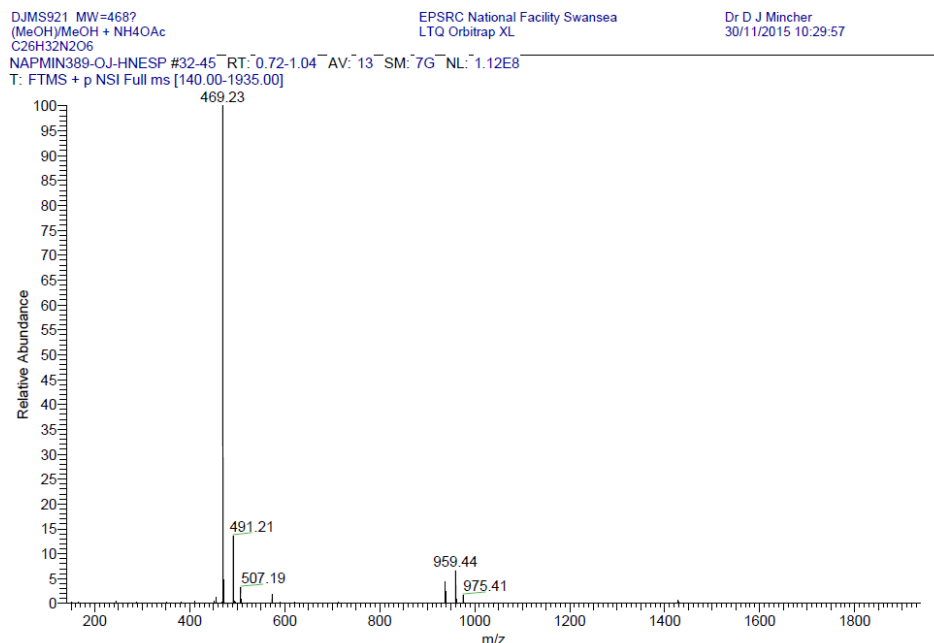


Figure 2. 10 ESI (+) Mass spectrum of AM1 (Col-prolinol).

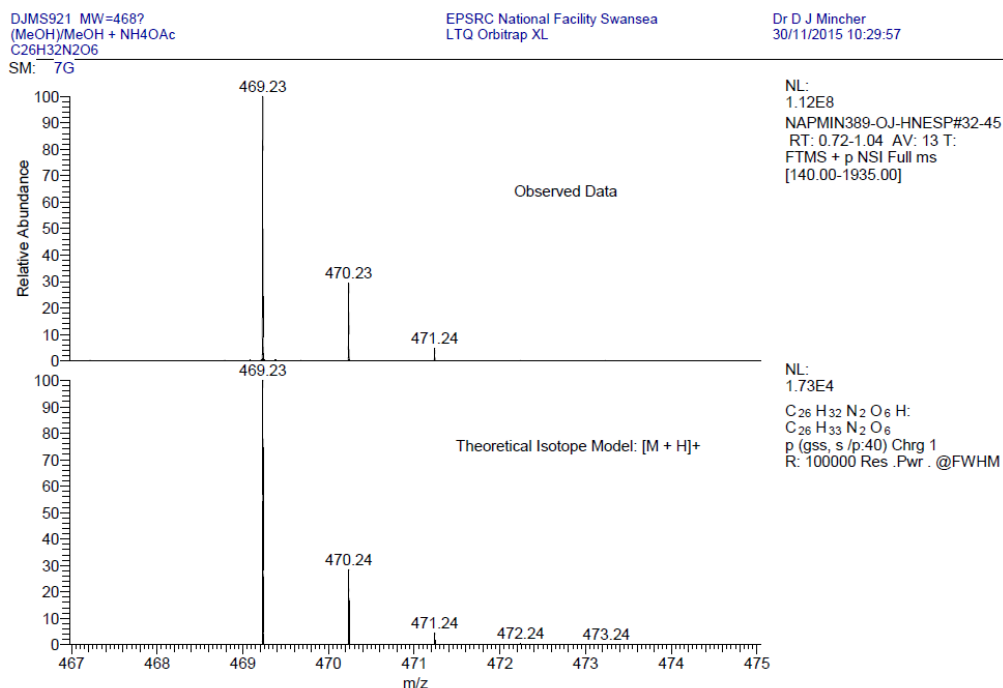


Figure 2. 11 Comparison of the observed data with the theoretical isotope model for AM1

The structure of the compound was also confirmed by its ^1H NMR spectrum. A three-proton multiplet at 1.69-1.90 ppm was assigned to a methylene group of $\text{N-CH}_2\text{-CH}_2$ and one of the CH protons of C6. The three-proton singlet was assigned to the methyl group of the acetamide substituent at 2.03 ppm. The three-proton multiplet at 2.38 ppm was assigned to the methylene CH_2 group of C5 and the CH proton of C6.

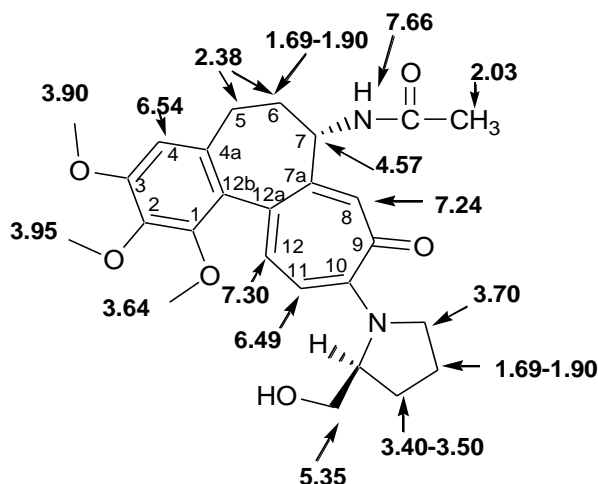


Figure 2.12 ^1H NMR assignments (ppm values) and atomic numbering.

A two-proton multiplet at 3.40-3.50 ppm was assigned to the methylene CH_2 of the prolinol ring ($\text{N-CH}_2\text{-CH}_2\text{-CH}_2$). A three-proton singlet at 3.64 ppm was assigned to the methoxy group of C1 (C1-OCH_3). Methylene protons (next to nitrogen, N-CH_2) were assigned to a two-proton multiplet at 3.70 ppm. A methoxy group protons at C3 were assigned to a three-proton singlet at 3.90 ppm. A three-proton, singlet at 3.95 ppm was assigned to the methoxy group of C2. A one-proton multiplet at 4.57 ppm was assigned to the methane of C7 (H-7). A one-proton doublet at 6.49 ppm, with $J=12$ Hz was assigned to the aromatic H-11 proton. A methine proton of C4 was assigned to a one-proton singlet found at 6.54 ppm. A methine proton of C8 was assigned to a one-proton multiplet found at 7.24 ppm. A one-proton, doublet with $J=12$ Hz, at 7.30 ppm was assigned to the aromatic methine proton of C12 (H-12). A doublet was assigned to a proton attached to nitrogen of acetamide found at 7.66 ppm that is coupled to H7 (**Figure 2.12**).

Additionally, the ^{13}C NMR spectrum showed signals from all the carbon atoms.

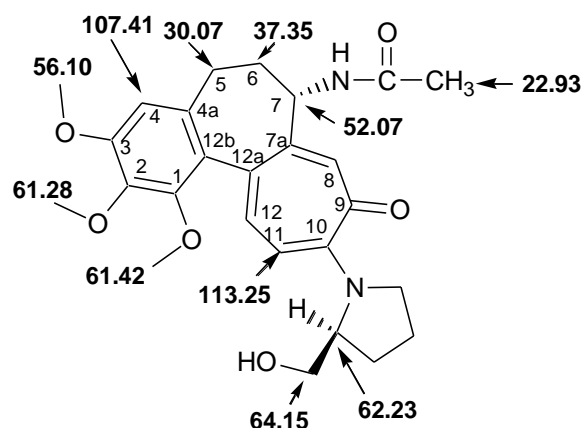
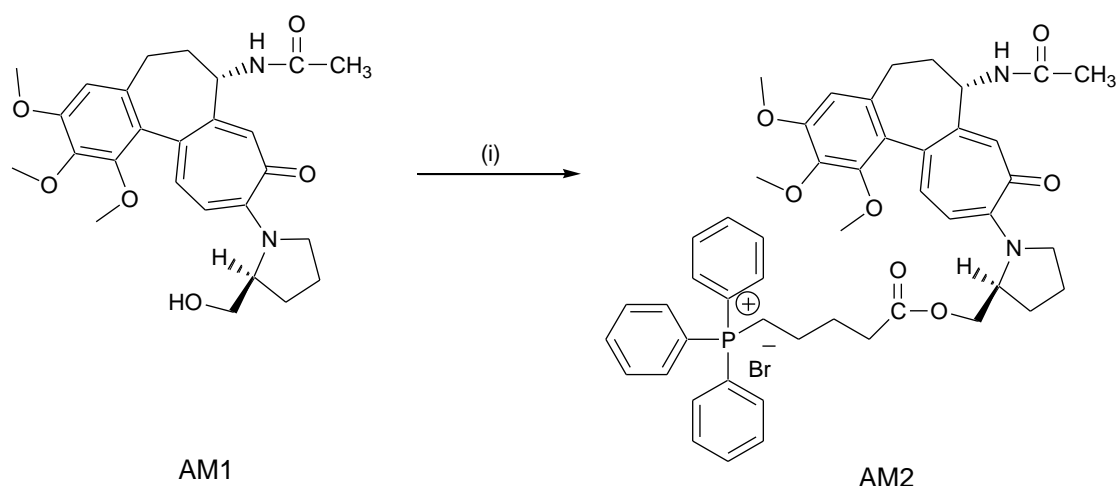


Figure 2. 13 ^{13}C NMR signals with assignments (ppm values) and atomic numbering

A DEPT experiment differentiated the methyl, methylene and methine carbons from the remaining quaternary carbon group signals. A negative signal at 22.46 ppm was assigned to a methylene carbon CH_2 . A positive signal at 22.93 ppm was assigned to the methoxy C14 carbon. A negative signal at 28.07 ppm was assigned to a further methylene CH_2 carbon. A methylene CH_2 negative signal was assigned to C5 carbon at 30.07 ppm. A negative signal at 37.35 ppm was assigned to a methylene of C6. A negative signal of a methylene carbon was found at 50.63 ppm. A positive signal of a methine carbon, C7 was found at 52.09 ppm. Three positive signals of the three methyl carbons C3, C2 and C1 were found at 56.10 ppm, 61.28 ppm and 61.42 ppm respectively. A positive signal of the alpha carbon of prolinol was found at 62.23 ppm. A negative signal of a methylene (CH_2) of carbon adjacent to the OH group was found at 64.15 ppm. A positive signal of a methine carbon assigned to C4 was found at 107.41 ppm. A positive signal of the methine carbon of C11 was found at 113.25 ppm. A methine carbon of C8 was found at 123.66 ppm. A positive signal was assigned to methine CH carbon of C12 found at 138.31 ppm. The remaining quaternary carbon signals of colchicine (ring A, B and C) were found at 126.22, 129.85, 134.72, 141.52, 150.18, 151.33, 152.95, 156.23 and 176.73 ppm. A quaternary carbon of carbonyl group of C13 (acetamide) was found at 169.94 ppm (**Figure 2.13**)

2.4.2 Synthesis of Colchicine-Prolinol-TPP (AM2)



Reagents and conditions: (i) Col-Pro (AM1), TPP, DCC, DMAP, CH₂Cl₂ (dichloromethane), rt, 24 h.

Figure 2. 14 Synthesis of Col-prolinol-TPP (AM2) from Col-Pro (AM1).

To synthesise AM2 (Col-Prolinol-TPP), AM1 (Col-Prolinol-OH) was conjugated with TPP by an esterification reaction between the carboxylic acid group (COOH) of TPP and hydroxyl (OH) group of prolinol in AM1, where the carboxylic group of TPP was activated by DCC as a coupling agent and DMAP (as a basic catalyst) and enhancer. These bases induce coupling between an alcohol or amide and a carboxyl group and initiate formation of an active ester or an amide bond (**Figure 2.14**). Activated TPP was added to AM1 dissolved in dichloromethane (CH₂Cl₂). The progress of the reaction was monitored by TLC. Once the reaction was completed solvent extraction (Chloroform/water) was performed to remove extra TPP or unreacted TPP and to convert DCC into DCU that then was removed by filtration. TLC was performed that showed successful formation of the new AM2 product as a yellow spot running lower than AM1 (starting material) in the product lane. The crude compound AM2 was purified by silica gel chromatography (chloroform: methanol, 9:1 and 4:1) with order of increased polarity. All the fractions containing AM1 (confirmed by TLC) were eluted but some solid crystals of DCU and water was present in all the fraction. So, anhydrous sodium sulfate drying agent was added to the combined fractions. The filtered fractions were evaporated, cooled over ice bath and finally diethyl ether was added to get precipitates of pure AM2 compound. AM2 was characterised by its MS (ESI+) mass spectrum that showed a signal at m/z 813.36 Da (M+H)⁺ for the cationic species [C₄₉H₅₄N₂O₇P]⁺ and confirmed the molecular mass of 892.29 Da (**Figures 2.15 and 2.16**)

NAPMIN388-OJ-HNESP #33-46 RT: 0.74-1.04 AV: 12 SM: 7G NL: 4.69E8
T: FTMS + p NSI Full ms [140.00-1935.00]

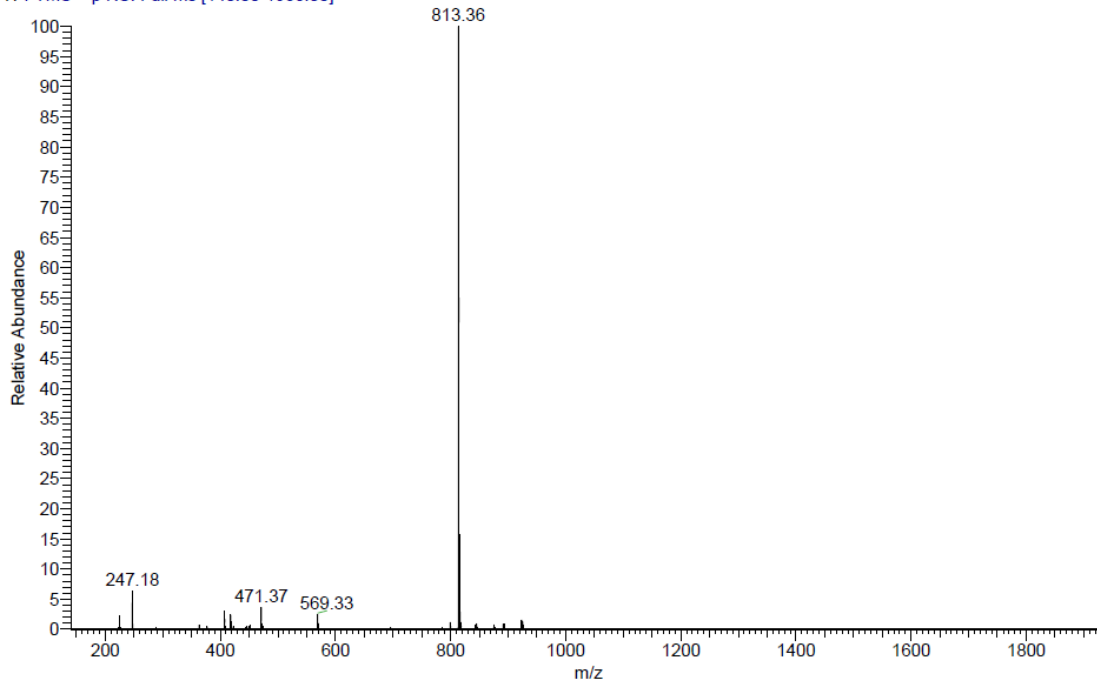
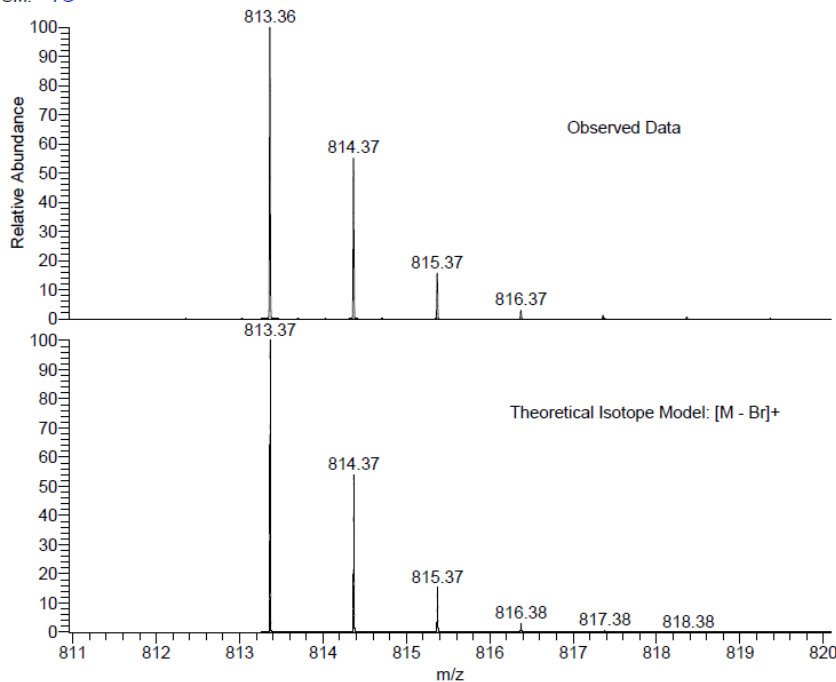


Figure 2. 15 ESI (+) Mass spectrum of AM1 (Col-prolinol)



NL:
4.69E8
NAPMIN388-OJ-HNESP#33-46
RT: 0.74-1.04 AV: 12 T:
FTMS + p NSI Full ms
[140.00-1935.00]

NL:
1.34E4
C₄₉ H₅₄ N₂ O₇ P:
C₄₉ H₅₄ N₂ O₇ P₁
p (gss, s /p:40) Chrg 1
R: 100000 Res .Pwr . @FWHM

Figure 2. 16 Comparison of the observed data with the theoretical isotope model of AM2.

The structure of the compound was also confirmed by its ^1H NMR spectrum.

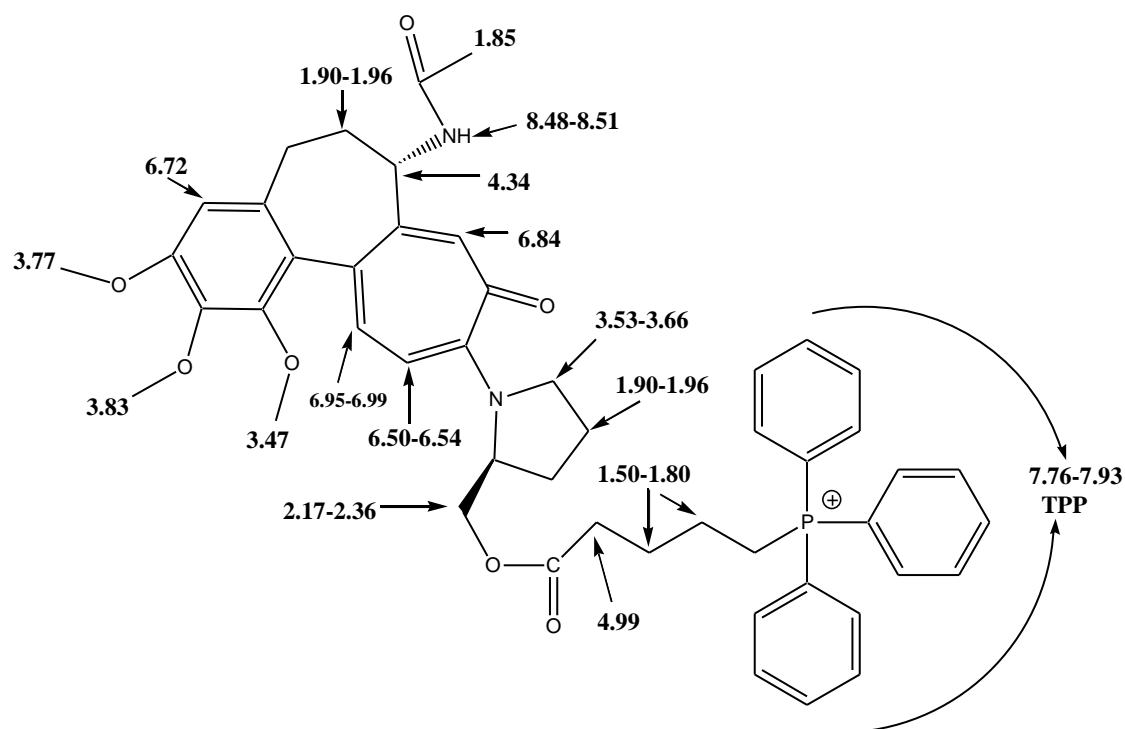


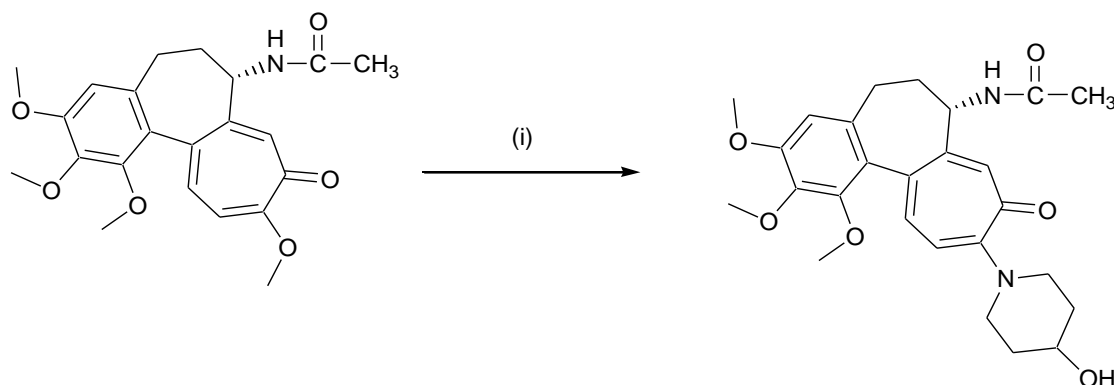
Figure 2. 17 ^1H NMR signals and assignments (ppm values) and atomic numbering.

A five proton multiplet at 1.50-1.80 ppm was assigned to two methylene CH_2 groups of $\text{OCOCH}_2\text{-CH}_2\text{-CH}_2\text{-CH}_2\text{-P}$ and one of the methylene CH_2 of C6. The three-proton singlet was assigned to the methyl group of acetamide at 1.85 ppm. The five-proton multiplet at 1.90-1.96 ppm was assigned to the methylene CH_2 of C5, and of prolinol $\text{NCH}_2\text{-CH}_2$ and methine CH of C6. A three-proton triplet at 2.17-2.36 ppm was assigned to a methylene of $\text{CH}_2\text{-CO}$. A three protons singlet at 3.47 ppm was assigned to the methoxy group of C1 (C1-OCH_3). A four-proton multiplet at 3.54 - 3.66 ppm was assigned to the one of the methylene CH_2 of prolinol ($\text{N-CH}_2\text{-CH}_2\text{-CH}_2$) and to a methylene adjacent to N (N-CH_2). A methoxy proton at C3 was assigned to a three-proton singlet at 3.77 ppm. A three-proton, singlet at 3.83 ppm was assigned to the methoxy group of C2. One-proton multiplet at 4.34 ppm was assigned to the methine of C7 (H-7). A one-hydrogen multiplet at 4.99 ppm was assigned to methine CH adjacent to $\text{CH}_2\text{-CH}_2\text{-OCO}$. One-proton doublet at 6.50-6.52 ppm, with $J=12$ Hz was assigned to the aromatic of H-11 (C11) proton. A methine proton of C4 was assigned to one-proton singlet found at 6.72 ppm. A methine proton of C8 was assigned to one-proton multiplet found at 6.84 ppm. A one-proton, doublet with $J = 12$ Hz, centred at 6.95-6.99 ppm was assigned to the aromatic methine of C12 (or H-12). A fifteen-proton

multiplet was assigned to TPP at 7.76-7.93 ppm. A doublet was assigned to a proton, attached to nitrogen of acetamide NH (acetamide nitrogen) (**Figure 2.17**).

2.4.3 Synthesis of Colchicine-4-hydroxypiperidine (AM3)

AM3 (Colchicine-4-hydroxypiperidine) was synthesised by reacting colchicine with an excess of 4-hydroxypiperidine in DMF, then the reaction mixture was stirred and kept for 48 h at room temperature. (**Figure 2.18**).



Reagents and conditions: (i) 4-hydroxypiperidine, DMF, rt, 48 h.

Figure 2.18 Synthesis of Colchicine-4-hydroxypiperidine (AM3) from Colchicine.

Solvent extraction was performed to remove excess amount of unreacted amino alcohol used in the reaction (because it was found that 4-hydroxypiperidine was soluble in the water) and DMF with chloroform/water mixture. White solid particles were found in the reaction therefore filtration was performed before extraction to remove those white solid particles. The progress of the reaction was monitored by TLC which showed completion of the reaction with a new yellow spot in the product lane running lower than the starting material (colchicine as reference).

Crude product (AM3) was purified by silica gel column chromatography, firstly, chloroform was used as a mobile phase to remove the front running impurities in the mixture and unreacted colchicine, then chloroform: methanol (9:1) and (4:1) was used to elute AM3. All the fractions containing pure AM1 (confirmed by TLC) were eluted, combined and filtered to remove silica, evaporated to reduce the volume, cooled over ice bath and finally diethyl ether was added into the mixture to get a yellow precipitate of Col-4-hydroxypiperidine (AM3). The precipitate was filtered and dried to get yellow solid AM3 in a good yield. AM3 was characterised by MS (ESI) mass spectrum that showed a signal at m/z 469.23 Da in $(M+H)^+$ for the cationic species $[C_{26}H_{32}N_2O_6]^+$

and its sodium adduct 491.21 (M+Na)⁺ and confirmed the molecular mass of 468.23 Da. (Figures 2.19 and 2.20)

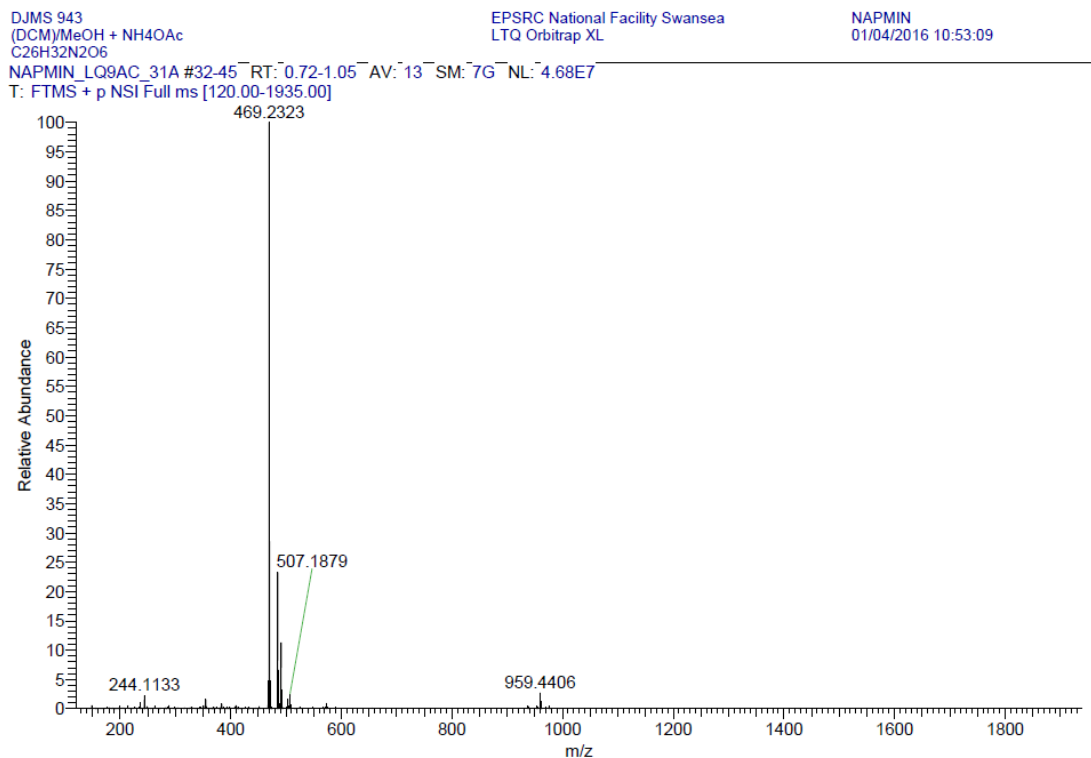


Figure 2. 19 ESI (+) Mass spectrum of AM3 (Col--4-hydroxypiperidine).

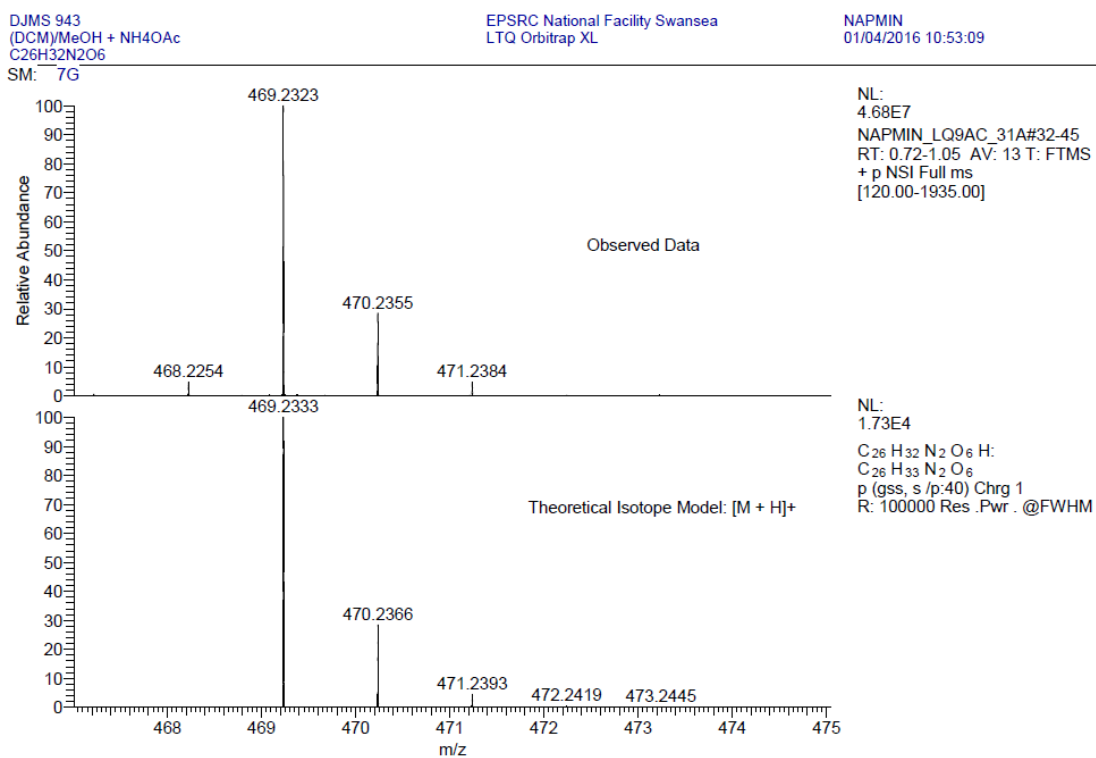


Figure 2. 20 Comparison of the observed data with the theoretical isotope model of AM3.

The structure of the compound was also confirmed by its ^1H NMR spectrum.

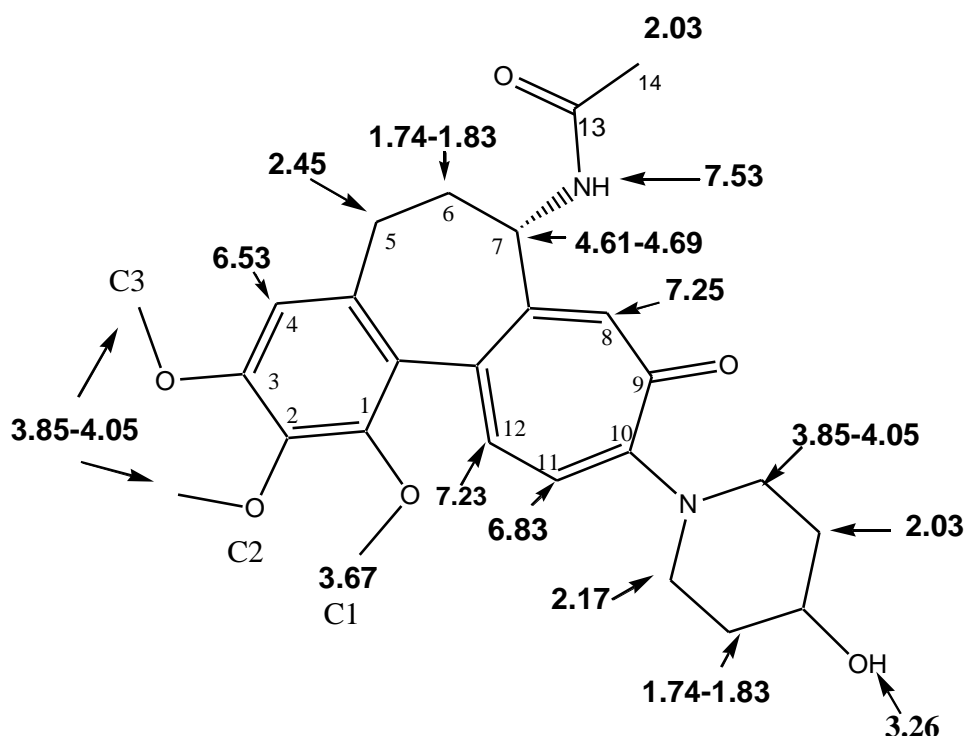


Figure 2. 21 ^1H NMR signals and assignments (ppm values) and atomic numbering.

A three-proton multiplet at 1.74-1.83 ppm was assigned to a methylene of $\text{N-CH}_2\text{-CH}_2$ and one of the CH of C6. A five-proton singlet was assigned to the methyl group of acetamide and methylene of $\text{N-CH}_2\text{-CH}_2$ at 2.03 ppm. The three-proton multiplet at 2.17 ppm was assigned to methine (CH) of C6 and methylene (CH_2) of $\text{N-CH}_2\text{-CH}_2$ (the other side of the hydroxypiperidine). A two-proton multiplet at 2.45 ppm was assigned to the methylene CH_2 of C5. A one-proton multiplet at 3.26 ppm was assigned to OH of hydroxypiperidine (CH-OH). A three protons singlet at 3.67 ppm was assigned to the methoxy group of C1 (C1-OCH_3). Eight proton singlets were found at 3.85-4.05 ppm was assigned to two methoxy groups (OCH_3) of C3 and C2 and a methylene of N-CH_2 . A proton multiplet at 4.61-4.69 ppm was assigned to methine of C7 (H7) adjacent to acetamide CH-NHCOCH_3 . A methine proton of C4 was assigned to one-proton singlet found at 6.53 ppm. One-proton doublet at 6.83 ppm, with $J=12$ was assigned to the aromatic of H-11 (C11) proton. A one-proton, doublet with $J=12$, at 7.23 ppm was assigned to the aromatic methine of C12 (or H-12). A methine proton of C8 was assigned to one-proton singlet found at 7.25 ppm. A doublet was assigned

to a proton attached to nitrogen of acetamide (NH-COCH_3) found at 7.53 ppm that is adjacent to C7 (**Figure 2.21**).

Additionally, ^{13}C NMR spectrum showed signals from all the carbon atoms.

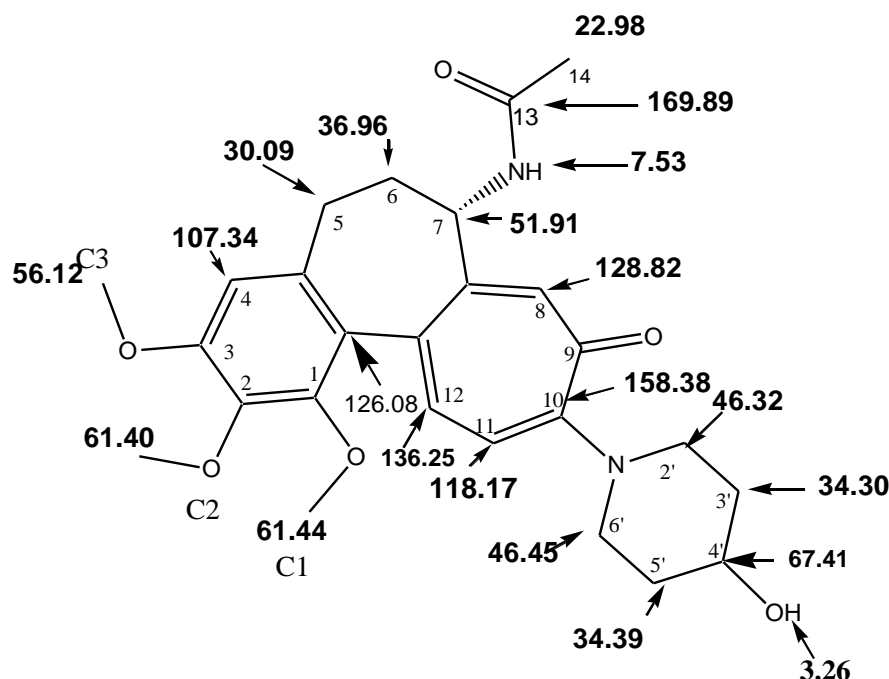
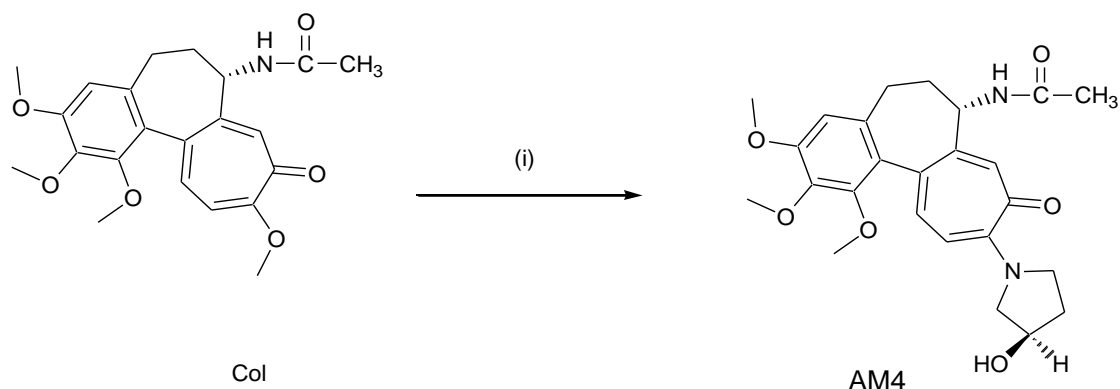


Figure 2. 22 ^{13}C NMR with assignments (ppm values) and atomic numbering

A DEPT experiment differentiated the methyl, methylene and methine carbons from the remaining quaternary carbon group signals. A positive signal at 22.98 ppm was assigned to the methoxy C14 carbon. A methylene CH_2 and a negative signal was assigned to C5 carbon at 30.09 ppm. A negative signal at 34.30 ppm and 34.39 ppm was assigned to methylene CH_2 carbon of C3' and C5'. A negative signal at 36.96 ppm was assigned to a methylene of C6 carbon. Two negative signals at 46.32 ppm and 46.45 ppm were assigned to methylene CH_2 of C2' and C6'. A positive signal of a methine carbon, C7 was found at 51.91 ppm. Three positive signals of the three methyl carbons C3, C2 and C1 were found at 56.12 ppm, 61.40 ppm and 61.44 ppm respectively. A positive signal of alpha carbon C4' of hydroxypiperidine was found at 67.41 ppm. A positive signal of a methine carbon assigned to C4 was found at 107.34 ppm. A positive signal of the methine carbon of C11 was found at 118.17 ppm. A methine carbon of C8 was found at 128.82 ppm. A positive signal was assigned to methine CH carbon of C12 found at 136.25 ppm. The remaining quaternary carbon

signals of colchicine (ring A, B and C) were found at 126.08, 133.84, 134.40, 141.60, 149.72, 151.29, 153.11 and 158.38 ppm. A quaternary carbon of carbonyl group of C9 and C13 (acetamide) was found at 181.32 and 169.89 ppm respectively (**Figure 2.22**).

2.4.4 Synthesis of Colchicine-(R)-3-Pyrrolidinol (AM4)



Reagents and conditions: (i) (*R*)-3-Pyrrolidinol, DMF, rt, 1 h.

Figure 2.23 Synthesis of Colchicine-(*R*)-3-Pyrrolidinol (AM4) from colchicine.

AM4 (Colchicine-(*R*)-3-Pyrrolidinol) was synthesised by reacting colchicine and (*R*)-3-pyrrolidinol in DMF, then the reaction mixture was stirred and kept for 1 hour at room temperature (**Figure 2.23**). The progress of the reaction was monitored by TLC which showed completion of the reaction with a new yellow spot in the product lane running lower than the starting material (colchicine) reference.

Crude product (AM4) was purified by silica gel column chromatography, firstly, dichloromethane was used as a mobile phase to remove the high running impurities in the mixture and unreacted colchicine, then dichloromethane: ethanol (9.5: 0.5) and dichloromethane: methanol (9:1) was used to elute out the pure AM4 compound. All the fractions containing pure AM4 (confirmed by TLC) were eluted, combined and filtered to remove silica and evaporated to reduce the volume. It was noticed that brownish sticky material was present after vacuum evaporation in the RBF. It was anticipated that it could be the unreacted amino alcohol (*R*)-3-pyrrolidinol) or DMF. The excess amount of DMF and amino alcohol was removed by solvent extraction (chloroform/water). AM4 solution in chloroform was evaporated to reduce its volume, cooled over an ice bath and finally diethyl ether was added into the mixture to get a

yellow precipitate of Col-(*R*)-3-pyrrolidinol (AM4). The precipitate was filtered and dried to get yellow solid AM4 in a good yield.

AM4 was characterised by MS (ESI+) mass spectrum that showed a signal at m/z 455.22 Da ($M+H$)⁺ for the cationic species [C₂₅H₃₁N₂O₆]⁺ and its sodium adduct 477.20 ($M+Na$)⁺ and confirmed the molecular mass of 454.22 Da. (**Figures 2.24** and **2.25**)

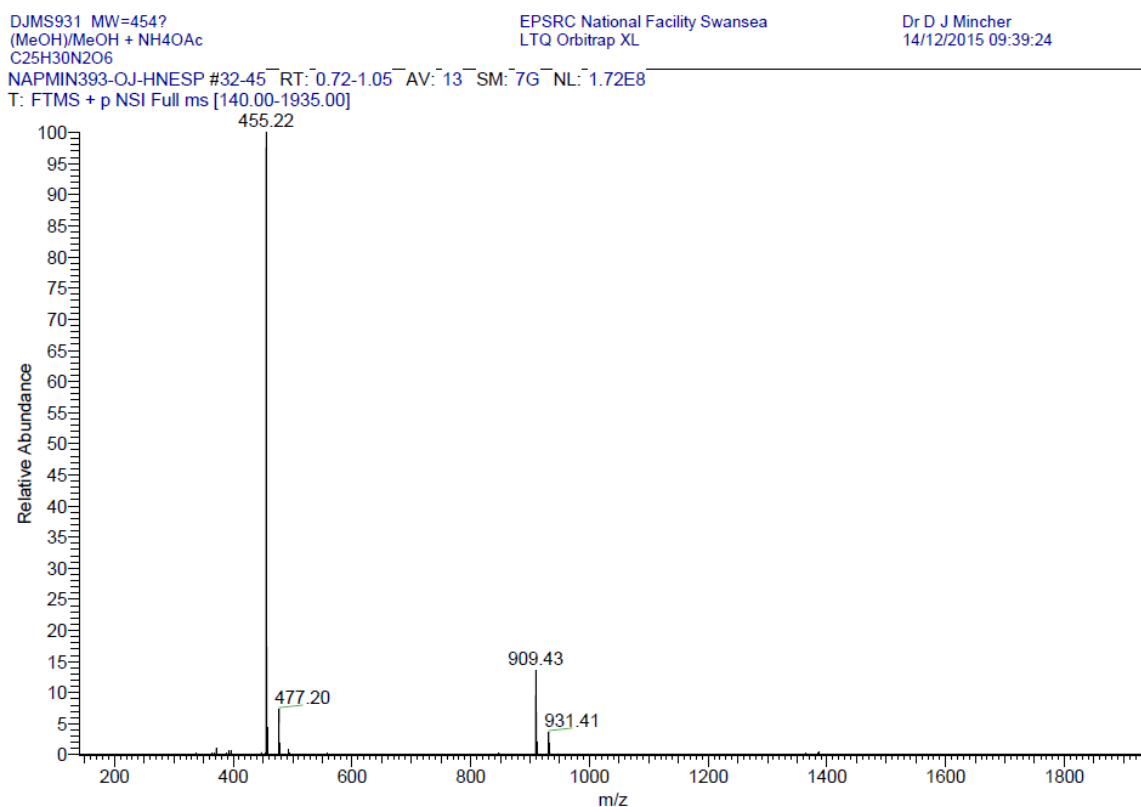
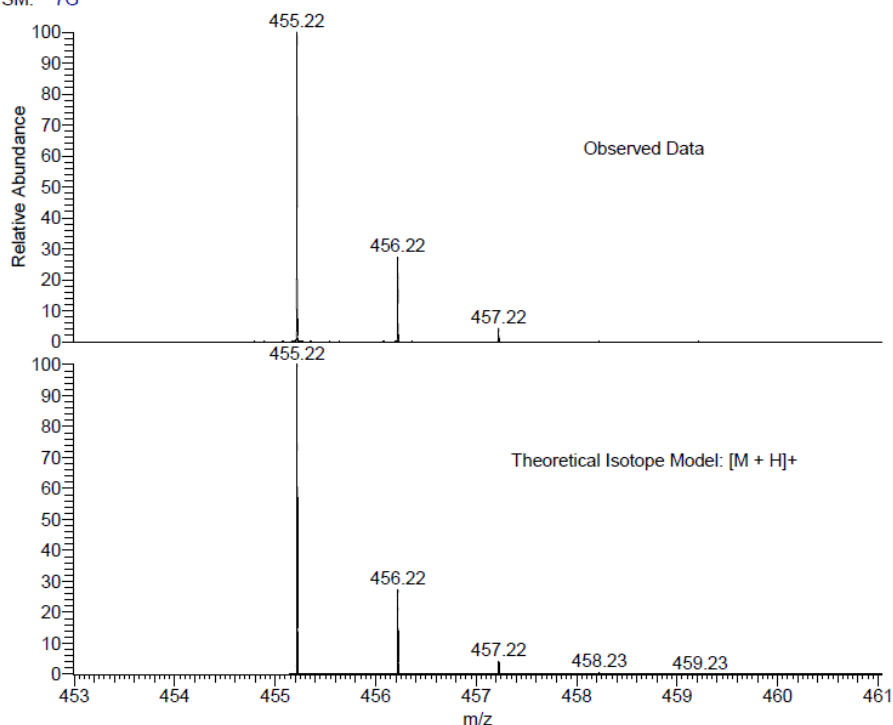


Figure 2. 24 ESI (+) Mass spectrum of AM4 (Col-(*R*)-3-Pyrrolidinol).

SM: 7G



NL:
1.72E8
NAPMIN393-OJ-HNESP#32-45
RT: 0.72-1.05 AV: 13 T:
FTMS + p NSI Full ms
[140.00-1935.00]

NL:
1.75E4
C₂₅ H₃₀ N₂ O₆ H:
C₂₅ H₃₁ N₂ O₆
p (gss, s /p.40) Chrg 1
R: 100000 Res .Pwr . @FWHM

Figure 2. 25 Comparison of the observed data with the theoretical isotope model of AM4.

The structure of the compound was also confirmed by its ¹H NMR spectrum.

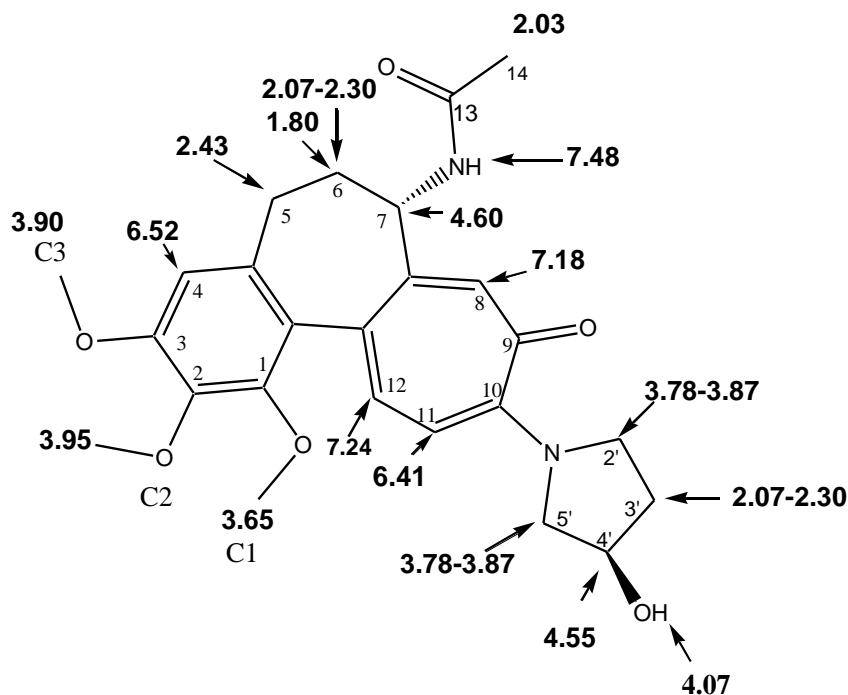


Figure 2. 26 ¹H NMR assignments (ppm values) and atomic numbering.

A proton multiplet was assigned to one of CH of C6 at 1.80 ppm. A three-proton singlet was assigned to the methyl group of acetamide at 2.03 ppm. A three-proton multiplet at 2.07-2.30 ppm was assigned to a methylene of N-CH₂-CH₂ and one of the CH of C6. A two-proton multiplet at 2.43 ppm was assigned to the methylene CH₂ of C5. A three protons singlet at 3.67 ppm was assigned to the methoxy group of C1 (C1-OCH₃). A four-proton multiplet was assigned to two of the methylene (CH₂) adjacent to N (2xN-CH₂) at 3.78-3.87 ppm. A three-proton singlet at 3.90 ppm was assigned to the methyl of C3. A three-proton singlet of the methyl of C2 were found at 3.95 ppm. A proton doublet was assigned to OH adjacent to CH found at 4.07 ppm. A proton multiplet at 4.55 ppm was assigned to the methine CH attached to OH. A proton multiplet at 4.60 ppm was assigned to methine of C7 (H7) adjacent to acetamide CH-NHCOCH₃. One-proton doublet at 6.41 ppm was assigned to the aromatic of H-11 (C11) proton. A methine proton of C4 was assigned to one-proton singlet found at 6.52 ppm. A methine proton of C8 was assigned to one-proton singlet found at 7.13 ppm. A one-proton, doublet with at 7.24 ppm was assigned to the aromatic methine of C12 (or H-12). A doublet was assigned to a proton attached to nitrogen of acetamide (NH-COCH₃) found at 7.48 ppm that is adjacent to C7 (**Figure 2.26**).

Additionally, ¹³C NMR spectrum showed signals from all the carbon atoms.

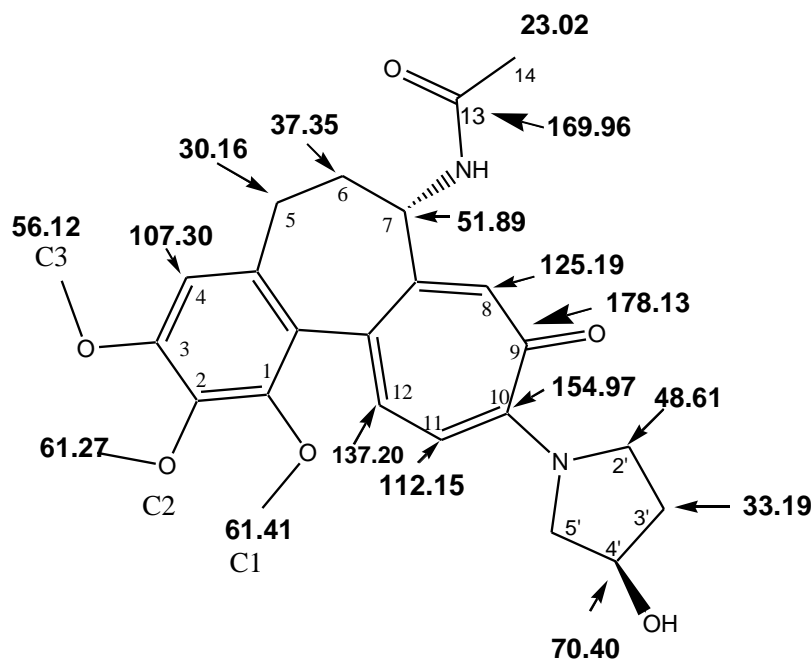
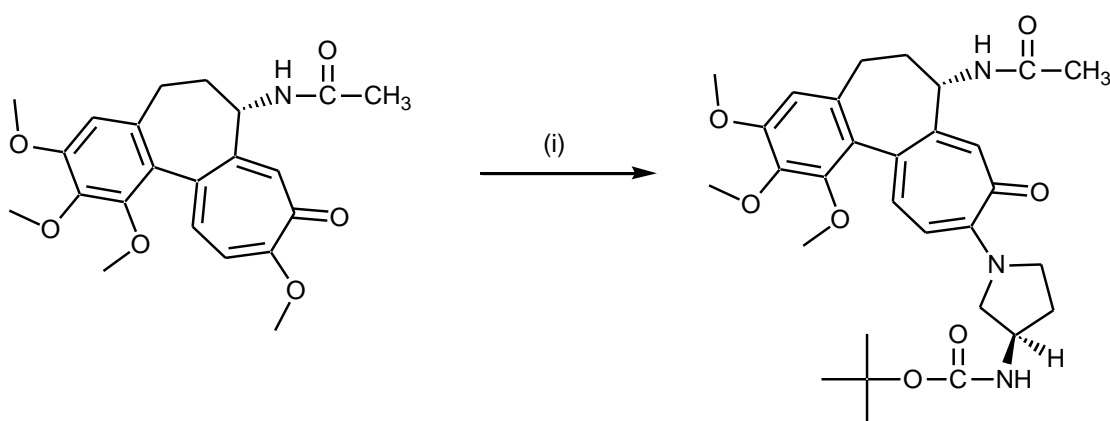


Figure 2.27 ¹³C NMR with assignments (ppm values) and atomic numbering.

A DEPT experiment differentiated the methyl, methylene and methine carbons from the remaining quaternary carbon group signals. A positive signal at 23.02 ppm was assigned to the methoxy C14 carbon. A methylene CH₂ and a negative signal was assigned to C5 carbon at 30.16 ppm. Three negative signals at 33.19 and 48.61 ppm were assigned to methylene CH₂. A negative signal at 37.35 ppm was assigned to a methylene of C6 carbon. A positive signal of a methine carbon, C7 was found at 51.89 ppm. Three positive signals of the three methyl carbons C3, C2 and C1 were found at 56.12 ppm, 61.27 ppm and 61.44 ppm respectively. A negative signal of methylene at 58.85 ppm was assigned to CH₂ adjacent to N-CH₂. A positive signal of alpha carbon C4' (CH-OH) of hydroxypiperidine was found at 70.40 ppm. A positive signal of a methine carbon assigned to C4 was found at 107.30 ppm. A positive signal of the methine carbon of C11 was found at 112.15 ppm. A positive signal of the methine carbon of C8 was found at 125.19 ppm. A positive signal was assigned to methine CH carbon of C12 found at 137.20 ppm. The remaining quaternary carbon signals of colchicine (ring A, B and C) were found at 126.57, 129.10, 134.55, 141.51, 149.58, 151.25, 152.76 and 154.97 ppm. A quaternary carbon of carbonyl group of C9 and C13 (acetamide) was found at 178.13 and 169.96 ppm respectively (**Figure 2.27**).

2.4.5 Synthesis of Colchicine-(R)-3-(Boc-aminopyrrolidine) (AM5)



Reagents and conditions: (i) (R)-3-(Boc-aminopyrrolidine), DMF, rt, 24 h.

Figure 2. 28 Synthesis of Colchicine-(R)-3-(Boc-aminopyrrolidine) (AM5) from colchicine.

To synthesise AM5 [Colchicine-(R)-3-(Boc-aminopyrrolidine)] colchicine was conjugated with a diamine (*R*)-3-(Boc-aminopyrrolidine) in DMF as a solvent (**Figure 2.28**). The reaction mixture was stirred and kept for 24 hours at room temperature. The progress of the reaction was monitored by TLC which showed completion of the reaction with a new yellow spot in the product lane running higher than the starting material (colchicine) reference. The excess amount of DMF and unreacted diamine was removed by Solvent extraction (chloroform/water) and dried by adding anhydrous sodium sulfate to remove moisture content. Crude product (AM5) was purified by silica gel column chromatography [chloroform: methanol: acetic acid, 9:1: 1 ml] to elute out the pure AM5 compound. All the fractions containing pure AM5 (confirmed by TLC) were eluted, combined and filtered to remove silica and evaporated to reduce the volume, cooled over ice bath and finally diethyl ether was added into the mixture to get a yellow precipitate of Col-(R)-3-Boc-amino pyrrolidine (AM5). The precipitate was filtered and dried to get yellow solid AM5 in a good yield.

The structure of the compound was confirmed by its ^1H NMR spectrum.

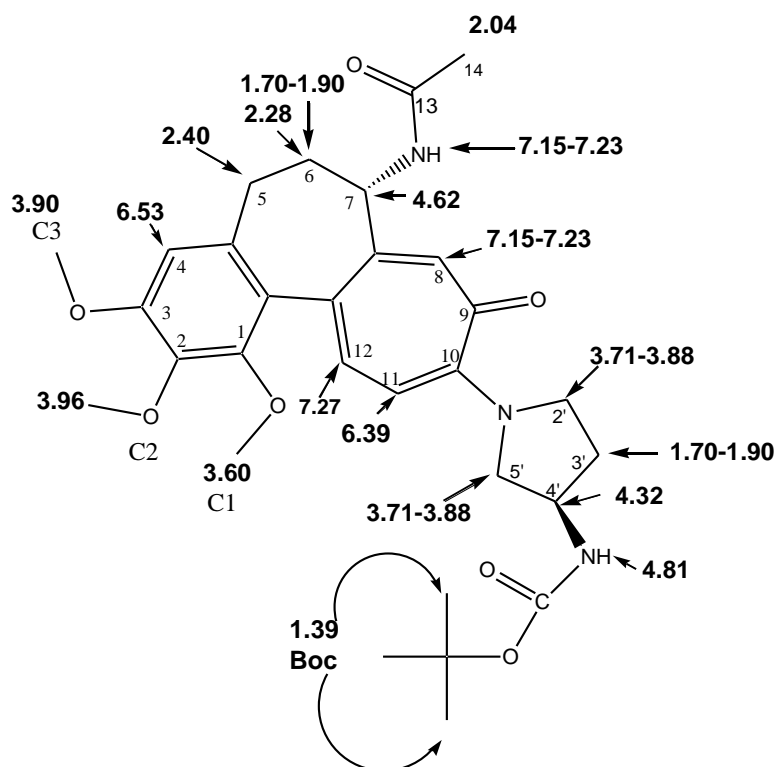


Figure 2. 29 ^1H NMR assignments (ppm values) and atomic numbering for AM5.

A nine-proton singlet at 1.49 ppm was assigned to three methyl CH₃ of Boc group. A three-proton multiplet at 1.70-1.90 ppm was assigned to a methylene of N-CH₂-CH₂ and one of the CH of C6. A three-proton singlet was assigned to the methyl group of acetamide at 2.04 ppm. A proton multiplet was assigned to one of CH of C6 at 2.28 ppm. A two-proton multiplet at 2.40 ppm was assigned to the methylene CH₂ of C5. A three protons singlet at 3.60 ppm was assigned to the methoxy group of C1 (C1-OCH₃). A four-proton multiplet was assigned to two of the methylene (CH₂) adjacent to N (2 x N-CH₂) at 3.71-3.88 ppm. A three-proton singlet at 3.90 ppm was assigned to the methyl of C3. A three-proton singlet of the methyl of C2 were found at 3.96 ppm. A proton multiplet at 4.32 ppm was assigned to the methine CH attached to Boc-NH-CH. A proton multiplet at 4.62 ppm was assigned to methine of C7 (H7) adjacent to acetamide CH-NHCOCH₃. A one-proton singlet was assigned to NH adjacent to Boc at 4.81 ppm. One-proton doublet at 6.39 ppm was assigned to the aromatic of H-11 (C11) proton. A methine proton of C4 was assigned to one-proton singlet found at 6.53 ppm. A methine proton of C8 and a proton attached to nitrogen of acetamide (NH-COCH₃) was assigned to a two-proton multiplet found at 7.15-7.23 ppm. A one-proton, doublet with at 7.27 ppm was assigned to the aromatic methine of C12 (or H-12) (Figure 2.29).

Additionally, ¹³C NMR spectrum showed signals from all the carbon atoms.

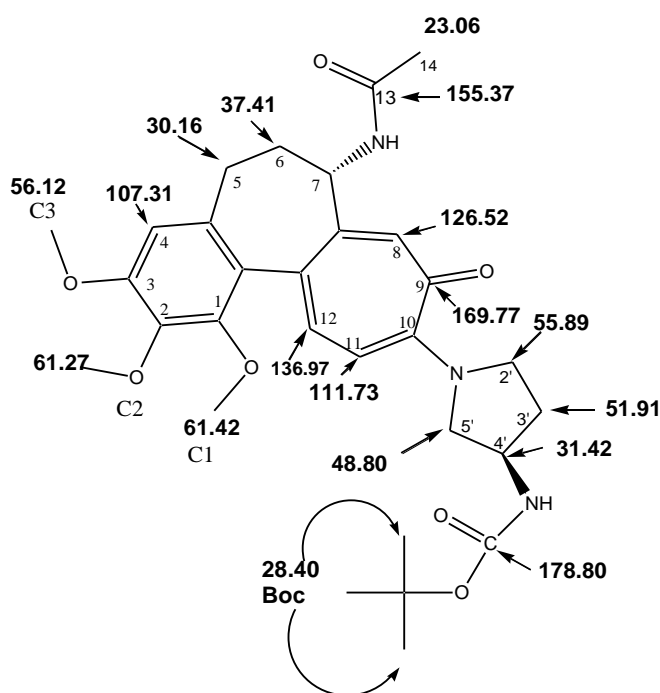
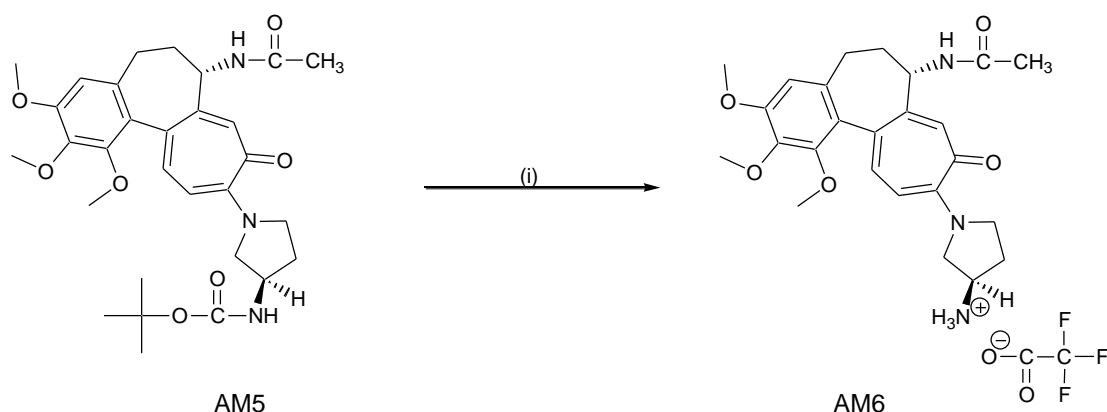


Figure 2. 30 ¹³C NMR with assignments (ppm values) and atomic numbering for AM5.

A DEPT experiment differentiated the methyl, methylene and methine carbons from the remaining quaternary carbon group signals. A positive signal at 23.06 ppm was assigned to the methoxy C14 carbon. A positive signal at 28.40 ppm was assigned to three methyl of Boc. A methylene CH₂ and a negative signal was assigned to C5 carbon at 30.16 ppm. Three negative signals at 31.42 and 48.80 and 55.89 ppm were assigned to methylene CH₂. A negative signal at 37.41 ppm was assigned to a methylene of C6 carbon. A positive signal of a methine carbon, C7 was found at 51.91 ppm. Three positive signals of the three methyl carbons C3, C2 and C1 were found at 56.12 ppm, 61.27 ppm and 61.42 ppm respectively. A positive signal of a methine carbon assigned to C4 was found at 107.31 ppm. A positive signal of the methine carbon of C11 was found at 111.73 ppm. A positive signal of the methine carbon of C8 was found at 126.52 ppm. A positive signal was assigned to methine CH carbon of C12 found at 136.97 ppm. The remaining quaternary carbon signals of colchicine (ring A, B and C) were found at 129.44, 134.52, 141.59, 149.70, 151.36, 152.80 and 154.79 ppm. A quaternary carbon of carbonyl group of C9 and C13 (acetamide) and carbonyl carbon adjacent to Boc was found at 169.77 and 155.37 and 178.80 ppm respectively (**Figure 2.30**)

2.4.6 Synthesis of Colchicine-(R)-3-(aminopyrrolidine)-TFA (AM6):



Reagents and conditions: (i) TFA, rt, 30 min.

Figure 2. 31 Synthesis of Colchicine-(R)-3-(aminopyrrolidine)-TFA (AM6) from AM5 (Colchicine-(R)-3-(Boc-aminopyrrolidine) (removal of Boc group)

To synthesise AM6 [Colchicine-(R)-3-amino-Pyrrolidine-TFA] (a TFA salt) Boc group was removed from AM5 (Colchicine-(R)-3-(Boc-amino) pyrrolidine) by reacting AM5 with TFA (trifluoroacetic acid) for 30 minutes at room temperature. The reaction mixture was then evaporated to remove TFA by addition of ethanol that would help in evaporation of TFA from the mixture. The AM6 compound was filtered, dried to get solid precipitates of AM6 compound (**Figure 2.31**).

AM6 was characterised by MS (ESI+) mass spectrum that showed a signal at m/z 454.23 Da in $(M+H)^+$ for the cationic species $[C_{25}H_{32}N_3O_5]^+$ and its sodium adduct 476.21 $(M+Na)^+$ and confirmed the molecular mass of 567.22 Da because in positive ion mode it only read positive ion specie and TFA was negatively charged molecule. (**Figures 2.32 and 2.33**)

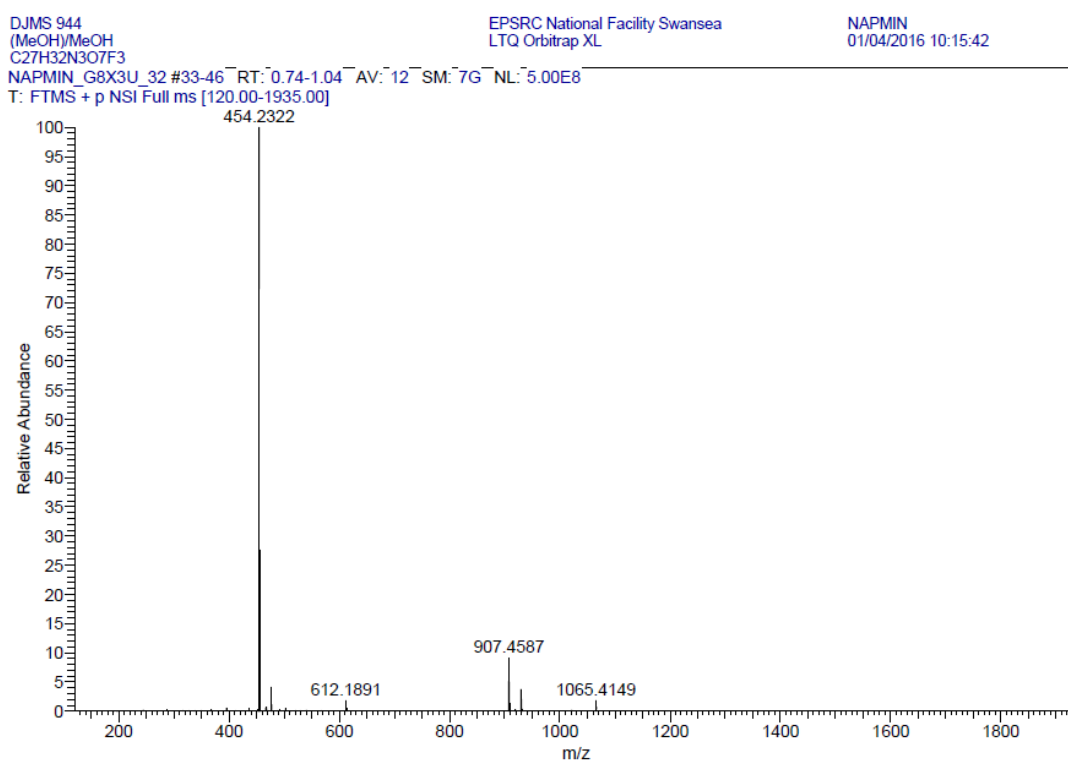


Figure 2. 32 ESI (+) Mass spectrum of AM6 (Col-(R)-3-aminopyrrolidine-TFA).

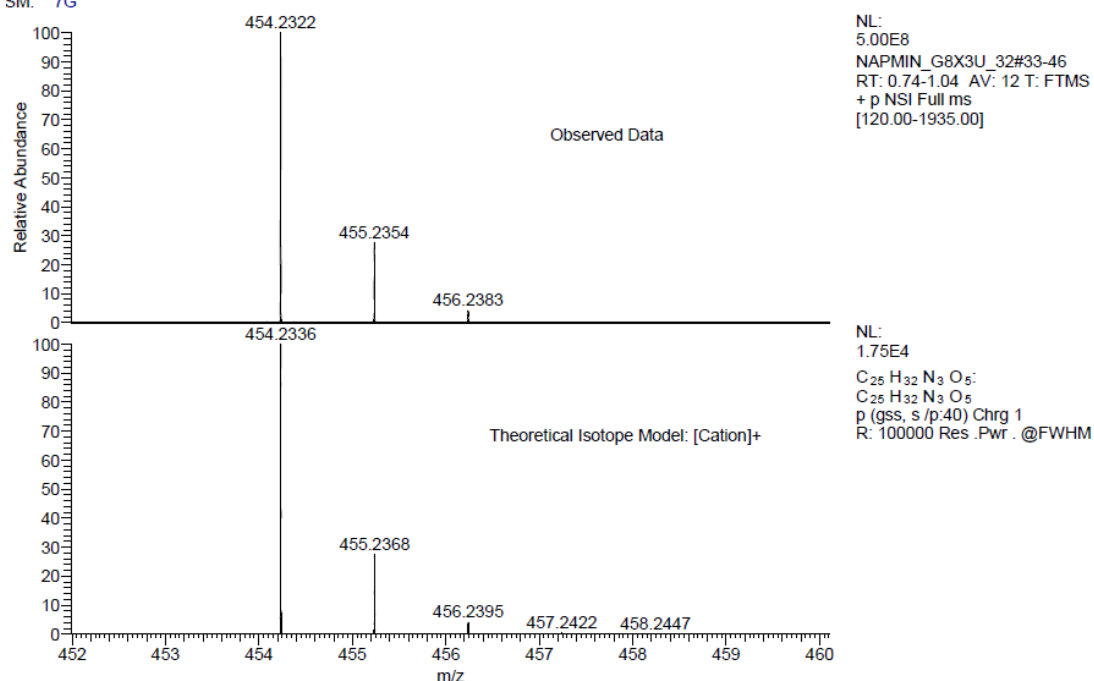


Figure 2.33 Comparison of the observed data with the theoretical isotope model of AM6.

The structure of the compound was also confirmed by its ¹H NMR spectrum.

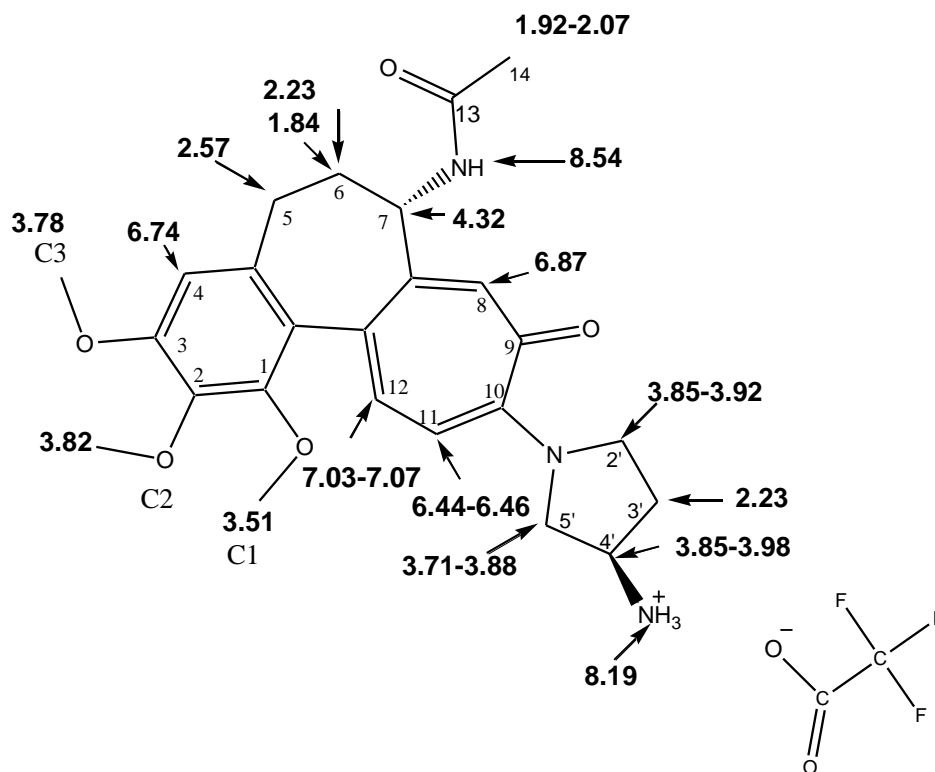


Figure 2.34. ¹H NMR assignments (ppm values) and atomic numbering for AM6.

A proton multiplet was assigned to one of methylene protons at C6 at 1.80 ppm. A three-proton singlet was assigned to the methyl group of acetamide at 1.92-2.07 ppm. A three-proton multiplet at 2.23 ppm was assigned to a methylene of N-CH₂-CH₂ and one of the CH of C6. A two-proton multiplet at 2.57 ppm was assigned to the methylene CH₂ of C5. A three protons singlet at 3.51 ppm was assigned to the methoxy group of C1 (C1-OCH₃). A two-proton multiplet at 3.70 ppm was assigned to methylene adjacent to nitrogen (N-CH₂). A three-proton singlet at 3.78 ppm was assigned to the methyl of C3. A three-proton singlet of the methyl of C2 were found at 3.82 ppm. A three-proton multiplet at 3.85-3.98 ppm was assigned to a methylene (C10-N-CH₂) and a methine next to NH₃ (CH-NH₃). A proton multiplet at 4.32 ppm was assigned to methine of C7 (H7) adjacent to acetamide CH-NHCOCH₃. One-proton doublet at 6.44-6.46 ppm was assigned to the aromatic of H-11 (C11) proton with J= 12 Hz. A methine proton of C4 was assigned to one-proton singlet found at 6.74 ppm. A proton singlet at 6.87 ppm was assigned to methine of C8. A one-proton, doublet with at 7.03 -7.07 ppm was assigned to the aromatic methine of C12 (or H-12) with J= 12 Hz. A three-proton multiplet was assigned to three hydrogen atoms of NH₃ at 8.19 ppm. A proton doublet at 8.54 ppm was assigned to NH of acetamide (**Figure 2.34**).

Additionally, ¹³C NMR spectrum showed signals from all the carbon atoms.

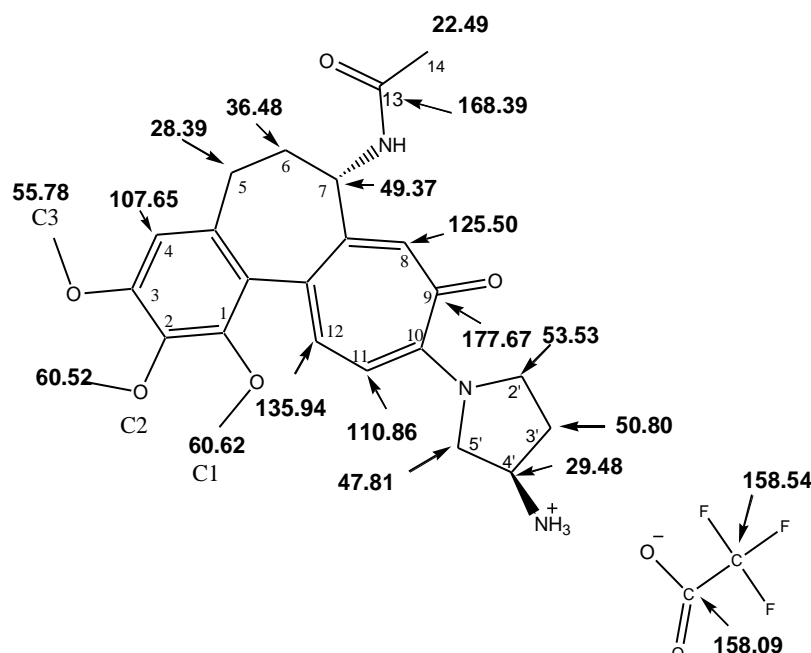
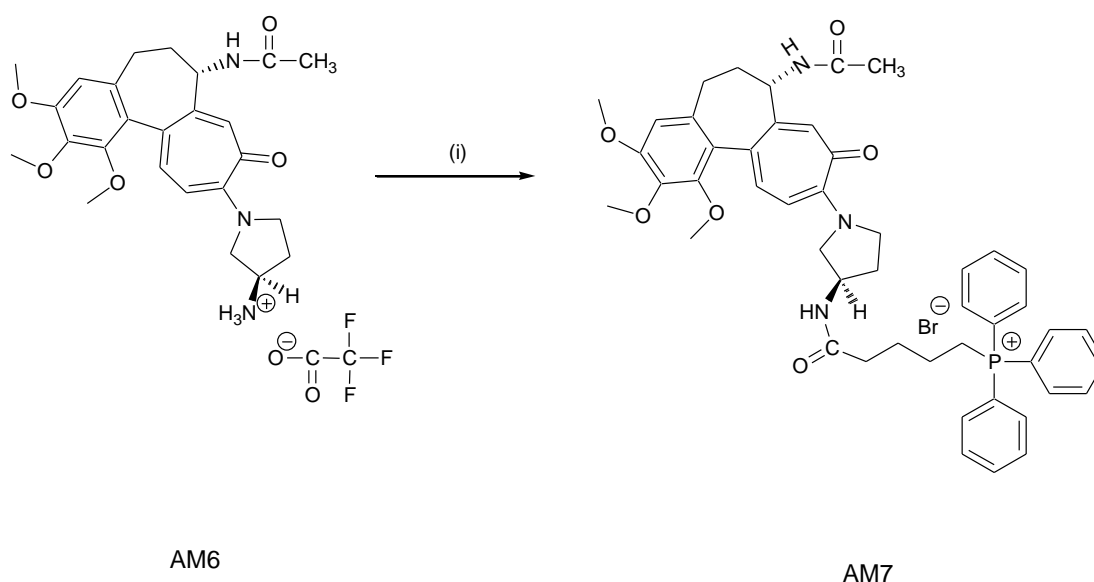


Figure 2.35 ¹³C NMR with assignments (ppm values) and atomic numbering for AM6.

A DEPT experiment differentiated the methyl, methylene and methine carbons from the remaining quaternary carbon group signals. A positive signal at 22.49 ppm was assigned to the methoxy C14 carbon. A methylene CH₂ and a negative signal was assigned to C5 carbon at 28.39 ppm. Three negative signals at 29.48, 47.81 and 53.53 ppm were assigned to methylene CH₂. A negative signal at 36.48 ppm was assigned to a methylene of C6 carbon. A positive signal was found at 49.37 for methine. A positive signal of a methine carbon, C7 was found at 50.80 ppm. Three positive signals of the three methyl carbons C3, C2 and C1 were found at 55.78 ppm, 60.52 ppm and 60.62 ppm respectively. A positive signal of a methine carbon assigned to C4 was found at 107.65 ppm. A positive signal of the methine carbon of C11 was found at 110.86 ppm. A positive signal of the methine carbon of C8 was found at 125.50 ppm. A positive signal was assigned to methine CH carbon of C12 found at 135.94 ppm. The remaining quaternary carbon signals of colchicine (ring A, B and C) were found at 126.14, 128.43, 134.40, 140.69, 149.25, 150.44, 152.32 and 153.67 ppm. A part of quartet carbon was assigned to 158.09. CF₃ carbon was assigned to 158.54 ppm. A quaternary carbon of carbonyl group of C13 (acetamide) and C9 were found at 168.39 and 177.67 ppm respectively (**Figure 2.35**).

2.4.7 Synthesis of Colchicine-(*R*)-3-aminopyrrolidine-TPP (**AM7**)



Reagents and conditions: (i) TPP (triphenylphosphonium bromide) PyBOP, DIPEA, HOBt, DMF, rt, 24h.

Figure 2. 36 Synthesis of Col-(*R*)-3-aminopyrrolidine-TPP (**AM7**) from AM6 (Col-(*R*)-3-aminopyrrolidine-TFA) (Addition of TPP).

To synthesise AM7 (Col-(*R*)-3-aminopyrrolidine-TPP), AM6 (Col-(*R*)-3-aminopyrrolidine-TFA) was conjugated with TPP by an amidation reaction between carboxylic acid group (COOH) of TPP and amino (NH) group of (*R*)-3-aminopyrrolidine in AM6 by a standard coupling method of peptides in DMF. In the reaction the carboxylic acid group of TPP was activated by PyBOP, DIPEA and HOBT through an esterification reaction to synthesise or produce the title compound AM7, a TPP conjugate prodrug (**Figure 2.36**).

Activated TPP was added to AM6 in DMF and reaction was set for 24 hours at room temperature. The progress of the reaction was monitored by TLC. TLC showed successful formation of AM7 product as yellow spot running higher than AM6 (starting material) in the product lane. Once the reaction was completed solvent extraction (Chloroform/water) was performed to remove excess TFA salt, unreacted TPP and DMF. Anhydrous sodium sulfate was added to mixture and stirred to remove moisture. The crude compound AM7 was purified by silica gel chromatography, the mobile phase (chloroform: methanol, 9:1) was used to elute AM7. All the fractions containing AM7 (confirmed by TLC) were eluted, combined, filtered to remove silica, evaporated to reduce the volume, cooled over ice bath and finally diethyl ether was added to get precipitates of pure AM7 compound in a good yield.

AM7 was characterised by MS (ESI+) mass spectrum that showed a signal at m/z 798.36 Da in $(M+H)^+$ for the cationic species $[C_{48}H_{53}N_3O_6P]^+$ and confirmed the molecular mass of 877.29 Da that includes the mass of bromide ion an anionic specie. (**Figures 2.37** and **2.38**).

NAPMIN_U2VQ4_33#33-46 RT: 0.74-1.04 AV: 12 SM: 7G NL: 2.40E8
T: FTMS + p NSI Full ms [120.00-1935.00]

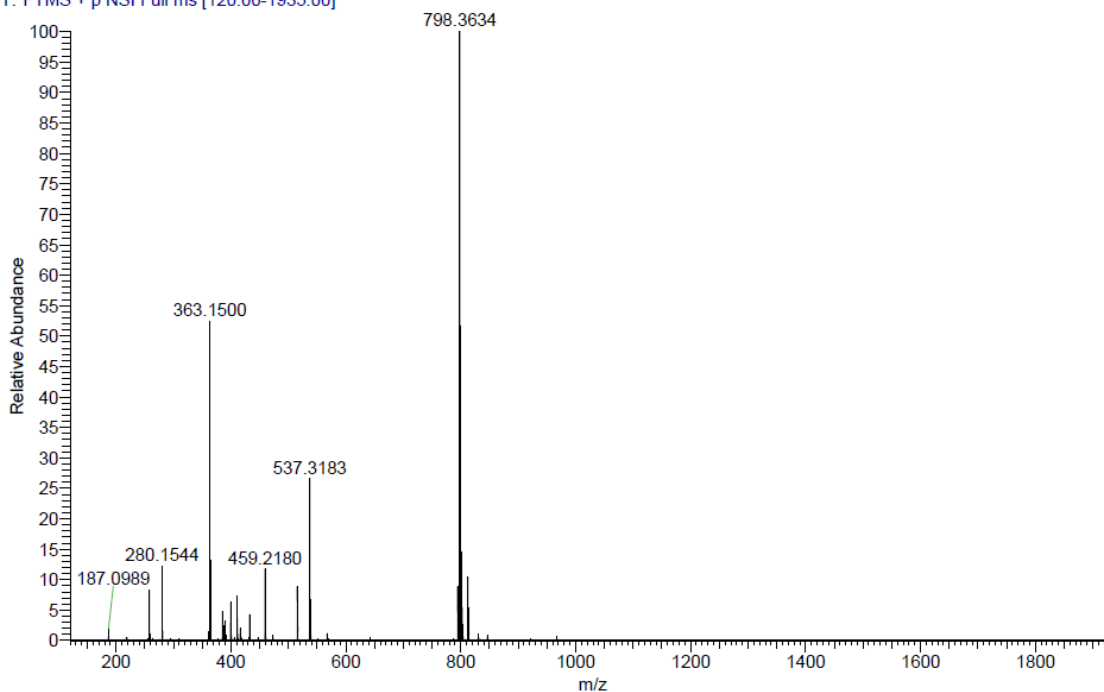
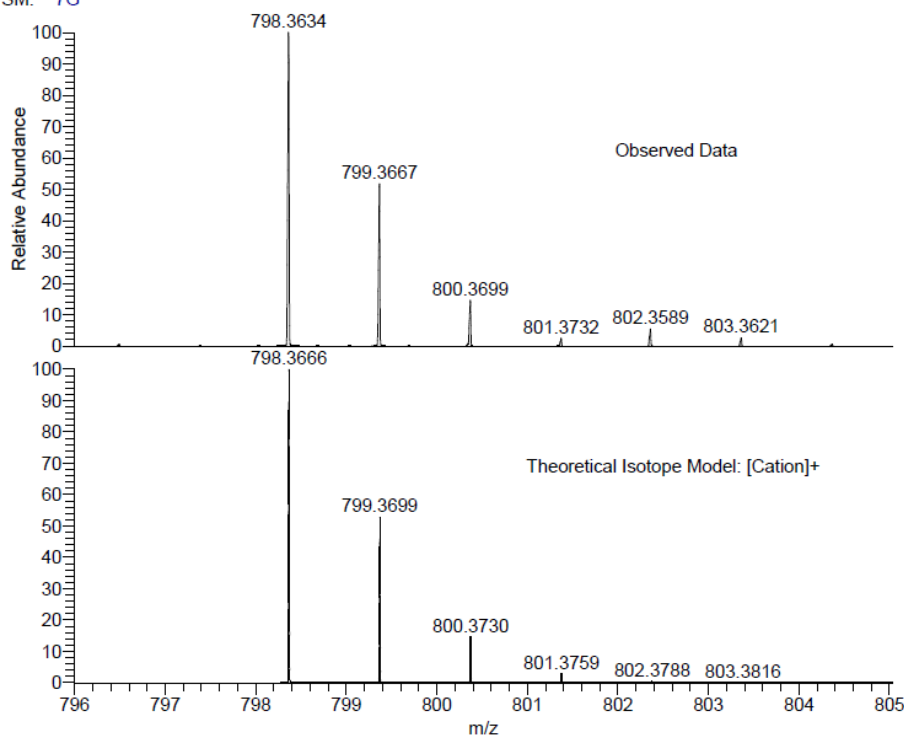


Figure 2. 37 ESI (+) Mass spectrum of AM7 (Col-(R)-3-aminopyrrolidine-TPP).

SM: 7G



NL:
2.40E8
NAPMIN_U2VQ4_33#33-46
RT: 0.74-1.04 AV: 12 T: FTMS
+ p NSI Full ms
[120.00-1935.00]

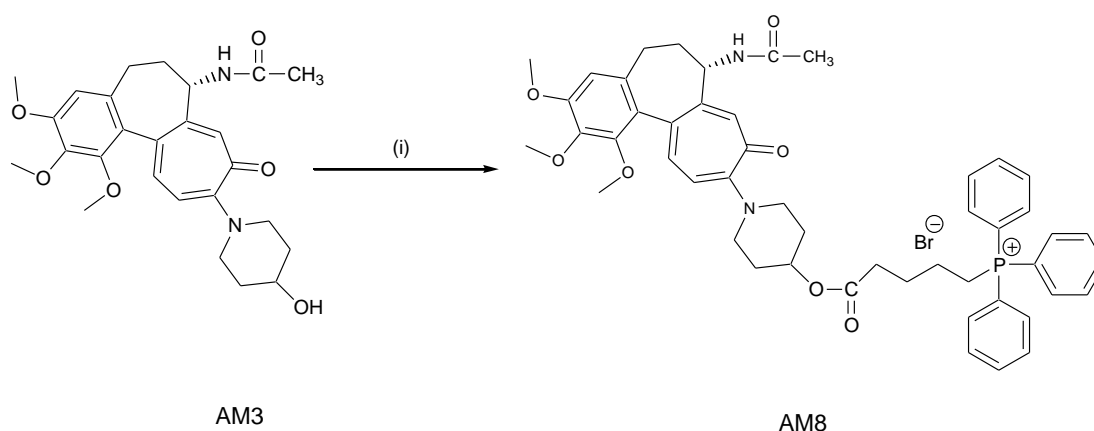
NL:
1.36E4
C₄₈H₅₃N₃O₆P:
C₄₈H₅₃N₃O₆P₁
p (gss, s /p:40) Chrg 1
R: 100000 Res .Pwr . @FWHM

Figure 2. 38 Comparison of the observed data with the theoretical isotope model for AM7.

The structure of the compound was also confirmed by its ¹H NMR spectrum.

An eight-proton multiplet was assigned to two methylene (P-CH₂-CH₂-CH₂), a methylene of acetamide (NHCO-CH₃) and a hydrogen of C6 (CH) at 1.50-1.85 ppm. A three-proton multiplet at 2.01-2.23 ppm was assigned to a methylene of N-CH₂-CH₂ and one of the CH of C6. A two-hydrogen triplet was assigned to the methylene next to carbonyl group (CH₂-COO) at 2.34 ppm. A two-proton multiplet at 2.50 ppm was assigned to the methylene CH₂ of C5. A two-proton singlet was assigned to the methylene attached to P (P-CH₂) at 3.02 ppm. A three protons singlet at 3.50 ppm was assigned to the methoxy group of C1 (C1-OCH₃). A two-proton multiplet at 3.60 ppm was assigned to methylene adjacent to nitrogen (C10-N-CH₂). A three-proton singlet at 3.80 ppm was assigned to the methyl of C3. A three-proton singlet of the methyl of C2 were found at 3.85 ppm. A three-hydrogen multiplet was assigned to the methylene N-CH₂-CH₂ and methine attached to TPP (CH-TPP) at 4.20 ppm. A proton multiplet at 4.39 ppm was assigned to methine of C7 (H7) adjacent to acetamide CH-NHCOCH₃. One-proton doublet at 6.35 ppm was assigned to the aromatic of H-11 (C11) proton with J= 11 Hz. A methine proton of C4 was assigned to one-proton singlet found at 6.71 ppm. A proton singlet at 6.85 ppm was assigned to methine of C8. A one-proton, doublet with at 7.00 ppm was assigned to the aromatic methine of C12 (or H-12) with J= 11 Hz. A fifteen hydrogen multiplet was assigned to TPP at 7.80 ppm. A proton doublet at 8.15 ppm was assigned to the NH of acetamide.

2.4.8 Synthesis of Colchicine-4-hydroxypiperidine-TPP (AM8)



Reagents and conditions: (i) TPP, DCC, DMAP, CH₂Cl₂ (dichloromethane), rt, 24 h.

Figure 2. 39 Synthesis of AM8 (Colchicine-4-hydroxypiperidine-TPP) from AM3 (Colchicine-4-hydroxypiperidine) (Addition of TPP)

AM8 (Colchicine-4-hydroxypiperidine-TPP) was synthesised by conjugating TPP with AM3 (Colchicine-4-hydroxypiperidine) by an esterification reaction between carboxylic acid group (COOH) of TPP and hydroxyl (OH) group of 4-hydroxypiperidine in AM3, where carboxylic group of TPP was activated by DMAP (as a catalyst base) and DCC as a coupling enhancer. These bases induce coupling between an alcohol and a carboxyl group and initiate formation of an active ester (**Figure 2.39**).

Activated TPP was added to AM3 dissolved in dichloromethane (CH₂Cl₂). The progress of the reaction was monitored by TLC. Once the reaction was completed solvent extraction (chloroform/water) was performed to remove extra TPP and to convert DCC into DCU that then was removed by filtration. TLC was performed that showed successful formation of AM8 product as yellow spot running lower than AM3 (starting material) in the product lane. The crude compound AM8 was purified by silica gel chromatography by mobile phase dichloromethane, dichloromethane: methanol, 9:1 and 4:1 with order of increased polarity. All the fractions containing AM8 (confirmed by TLC) were eluted but some solid crystals of DCU was present in two of the fractions. The fractions of compound AM8 were filtered to remove silica and DCU, evaporated to reduce the volume, cooled over ice bath and finally diethyl ether was added to get precipitates of pure AM8 compound in a good yield.

AM8 was characterised by MS (ESI+) mass spectrum that showed a signal at m/z 813.36 Da in (M+H)⁺ for the cationic species [C₄₉H₅₄N₂O₇P]⁺ and confirmed the molecular mass of 892.29 Da including mass of anionic bromide ion. (**Figures 2.40 and 2.41**).

NAPMIN_E9B0F_34#33-46 RT: 0.74-1.04 AV: 12 SM: 7G NL: 1.11E9
T: FTMS + p NSI Full ms [120.00-1935.00]

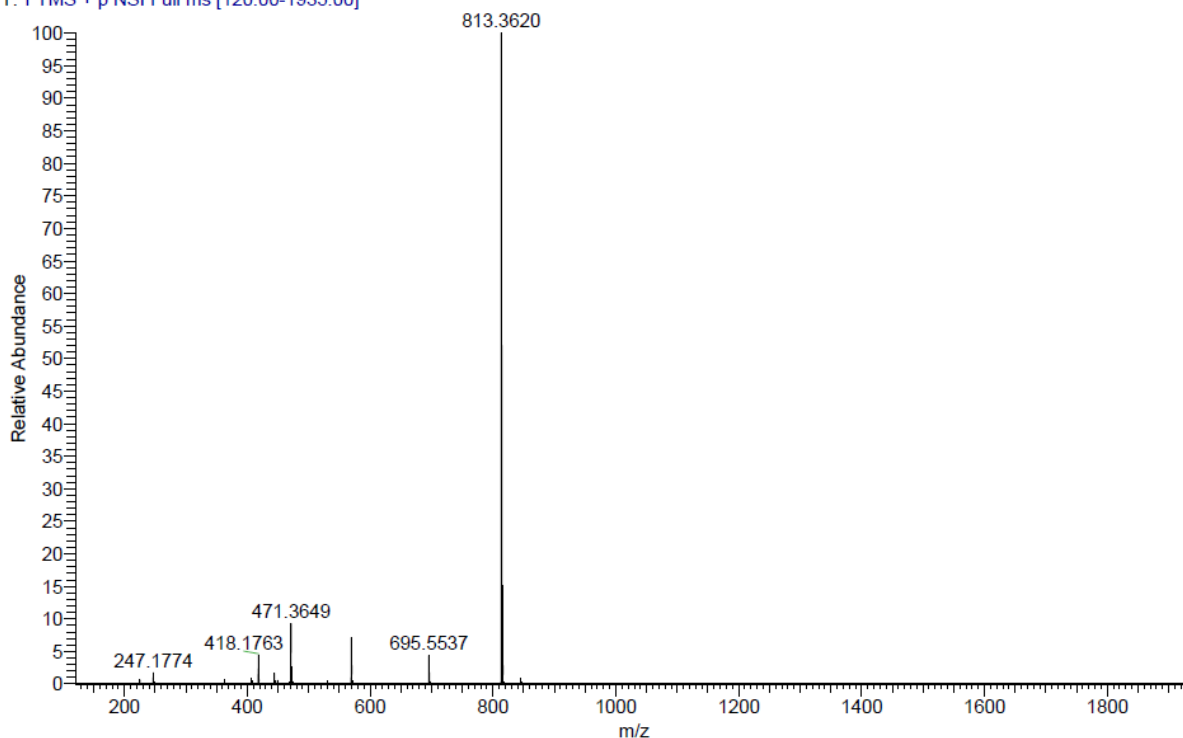
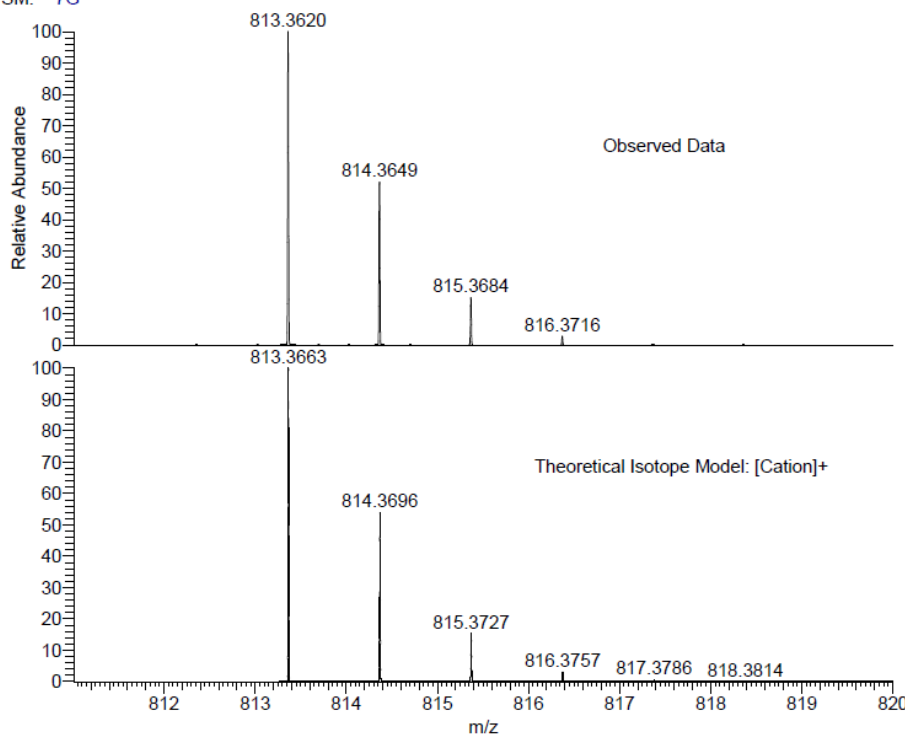


Figure 2. 40 ESI (+) Mass spectrum of AM8 (Col--4-hydroxypiperidine-TPP).

SM: 7G



NL:
1.11E9
NAPMIN_E9B0F_34#33-46
RT: 0.74-1.04 AV: 12 T: FTMS
+ p NSI Full ms
[120.00-1935.00]

NL:
1.34E4
C₄₉H₅₄N₂O₇P:
C₄₉H₅₄N₂O₇P₁
p (gss, s /p:40) Chrg 1
R: 100000 Res .Pwr . @FWHM

Figure 2. 41 Comparison of the observed data with the theoretical isotope model of AM8

The structure of the compound was also confirmed by its ^1H NMR spectrum.

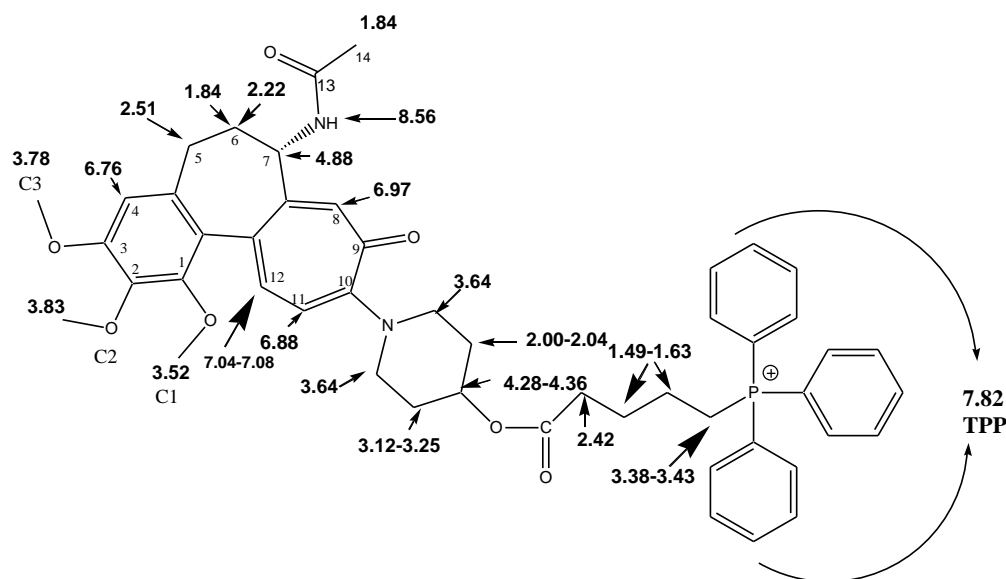


Figure 2. 42 ^1H NMR assignments (ppm values) and atomic numbering for AM8.

An eight-proton multiplet was assigned to two methylene ($\text{P-CH}_2\text{-CH}_2\text{-CH}_2$) at 1.49-1.63 ppm. A four-proton singlet was assigned to a methyl of acetamide (NHCO-CH_3) and a hydrogen of C6 (CH) at 1.84 ppm. A two-proton multiplet at 2.00-2.04 ppm was assigned to a methylene of $\text{N-CH}_2\text{-CH}_2$. A two-hydrogen triplet was assigned to the methylene next to carbonyl group ($\text{CH}_2\text{-COO}$) at 2.42 ppm. A two-proton multiplet at 2.51 ppm was assigned to the methylene CH_2 of C5. A two-hydrogen multiplet was assigned to the methylene $\text{N-CH}_2\text{-CH}_2$ at 3.12-3.25 ppm. A two-proton multiplet was assigned to the methylene attached to P (P-CH_2) at 3.38-3.43 ppm. A three protons singlet at 3.52 ppm was assigned to the methoxy group of C1 (C1-OCH_3). A four-proton multiplet at 3.64 ppm was assigned to two methylene adjacent to nitrogen ($2\times\text{N-CH}_2$). A three-proton singlet at 3.78 ppm was assigned to the methyl of C3. A three-proton singlet of the methyl of C2 were found at 3.83 ppm. A one-proton multiplet was assigned to CH adjacent to OCO at 4.28-4.36 ppm. A proton multiplet at 4.88 ppm was assigned to methine of C7 (H7) adjacent to acetamide CH-NHCOCH_3 . A methine proton of C4 was assigned to one-proton singlet found at 6.76 ppm. One-proton doublet at 6.88 ppm was assigned to the aromatic of H-11 (C11) proton with $J=11$ Hz. A proton singlet at 6.97 ppm was assigned to methine of C8. A one-proton, doublet with at 7.04-7.08 ppm was assigned to the aromatic methine of C12 (or H-12) with $J=$

11 Hz. A fifteen hydrogen multiplet was assigned to TPP at 7.82 ppm. A proton doublet at 8.56 ppm was assigned to NH of acetamide (**Figure 2.42**).

Additionally, the ^{13}C NMR spectrum showed signals from all the carbon atoms.

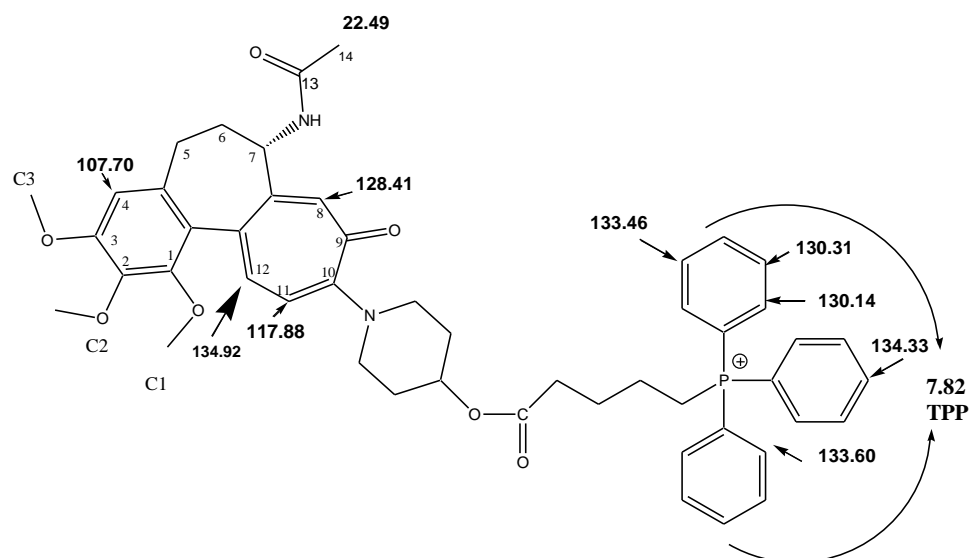
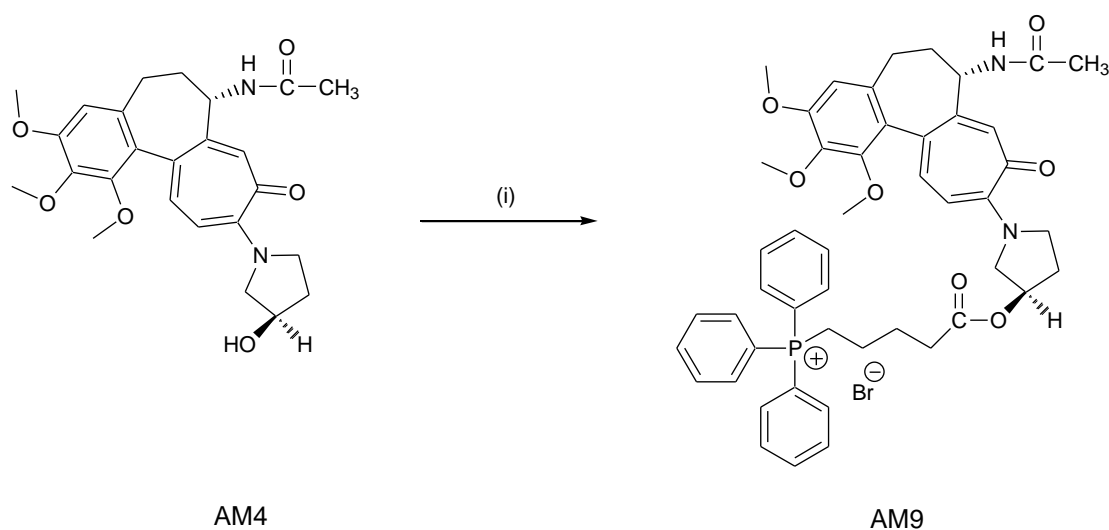


Figure 2. 43 ^{13}C NMR with assignments (ppm values) and atomic numbering for AM8.

A DEPT experiment differentiated the methyl, methylene and methine carbons from the remaining quaternary carbon group signals. A positive signal at 22.49 ppm was assigned to the methoxy C14 carbon. Seven negative signals at 24.43, 25.30, 30.35, 32.81, 33.31, 36.11 and 45.25 ppm were assigned to methylene CH_2 . A positive signal was found at 50.86 ppm for methine. Three quaternary carbon signals were found at 55.82 ppm 60.64 ppm and 60.69 ppm. A positive signal for the methine was found at 69.30 ppm. A positive signal of a methine carbon assigned to C4 was found at 107.70 ppm. A positive signal of the methine carbon of C11 was found at 117.88 ppm. Two signals were found at 119.02 and 125.71 (unspecified). A positive signal of the methine carbon of C8 was found at 128.41 ppm. Two positive signals for ortho and meta methine of TPP were found at 130.14 ppm and 130.31 ppm. Two positive signals for ortho and meta methine of TPP were found at 133.46 ppm and 130.60 ppm. A positive signal of the para methine of TPP was found at 134.33. A positive signal was assigned to methine CH carbon of C12 found at 134.92 ppm. The remaining quaternary carbon

signals of colchicine (ring A, B and C) were found at 119.02 ppm, 125.71 ppm, 132.59 ppm, 140.68 ppm, 149.03 ppm, and 150.44 ppm (**Figure 2.43**).

2.4.9 Synthesis of Colchicine-(*R*)-3-Pyrrolidinol)-TPP (AM9)



Reagents and conditions: (i) TPP, DCC, DMAP, CH₂Cl₂ (dichloromethane), rt, 24 h.

Figure 2. 44 Synthesis of Colchicine-(*R*)-3-Pyrrolidinol)-TPP (AM9) from AM4 (Colchicine-(*R*)-3-Pyrrolidinol)

AM9 (Colchicine-(*R*)-3-Pyrrolidinol)-TPP) was synthesised by conjugating TPP with AM4 (Colchicine-(*R*)-3-Pyrrolidinol) by an esterification reaction between carboxylic acid group (COOH) of TPP and hydroxyl (OH) group of (*R*)-3-pyrrolidinol in AM4, where carboxylic group of TPP was activated by DMAP (as a catalyst base) and DCC as a coupling enhancer (**Figure 2.44**).

Activated TPP was added to AM4 dissolved in dichloromethane (CH₂Cl₂). The progress of the reaction was monitored by TLC. Once the reaction was completed solvent extraction (chloroform/water) was performed to remove extra TPP and to convert DCC into DCU that then was removed by filtration. TLC was performed that showed successful formation of AM9 product as yellow spot running lower than AM4 (starting material) in the product lane. The crude compound AM9 was purified by silica gel chromatography by mobile phase dichloromethane, dichloromethane: methanol, 9:1 and 4:1. All the fractions containing AM9 (confirmed by TLC) were eluted, filtered

to remove silica and DCU, evaporated to reduce the volume, cooled over ice bath and finally diethyl ether was added to get precipitates of pure AM9 compound in a good yield. AM9 was characterised by MS (ESI+) mass spectrum that showed a signal at m/z 799.34 Da in $(M+H)^+$ for the cationic species $[C_{48}H_{52}N_2O_7P]^+$ and confirmed the molecular mass of 878.27 Da that includes the mass of anionic bromide ion. (**Figures 2.45 and 2.46**).

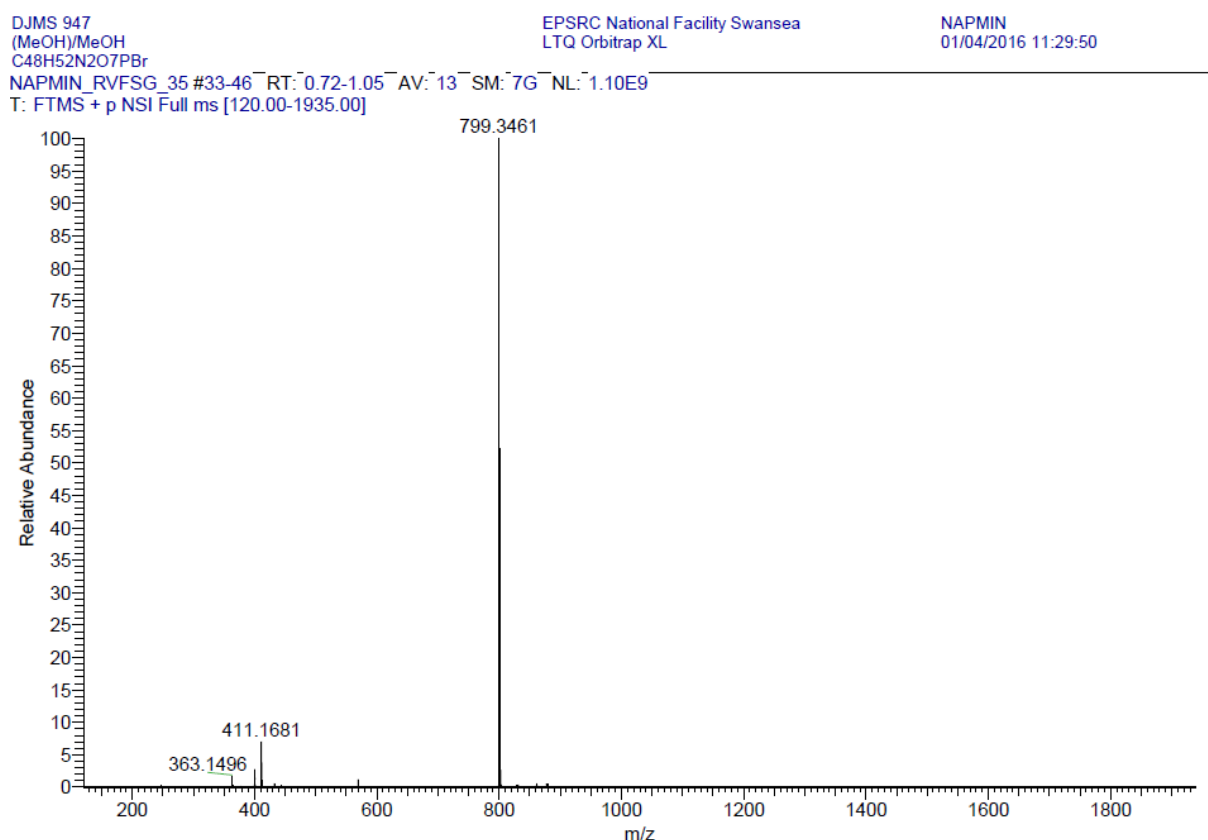


Figure 2. 45 ESI (+) Mass spectrum of AM9 (Col-(*R*)-3-Pyrrolidinol-TPP).

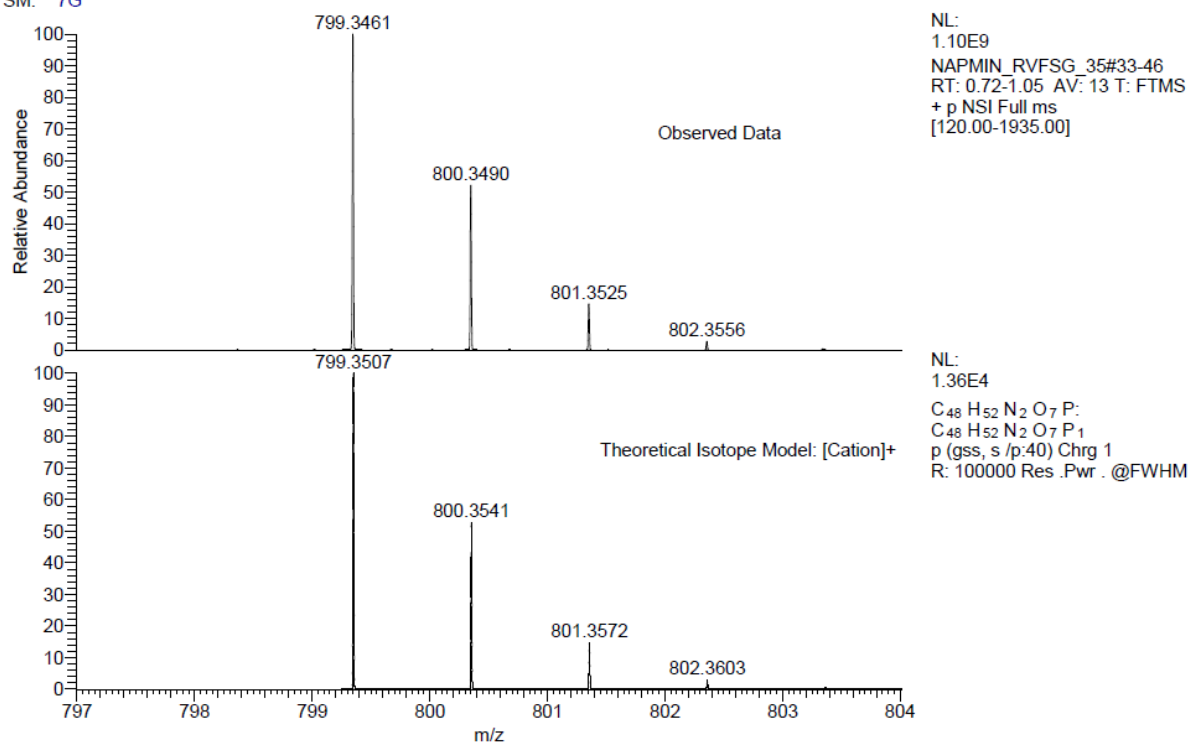


Figure 2. 46 Comparison of the observed data with the theoretical isotope model of AM9.

The structure of the compound was also confirmed by its ^1H NMR spectrum.

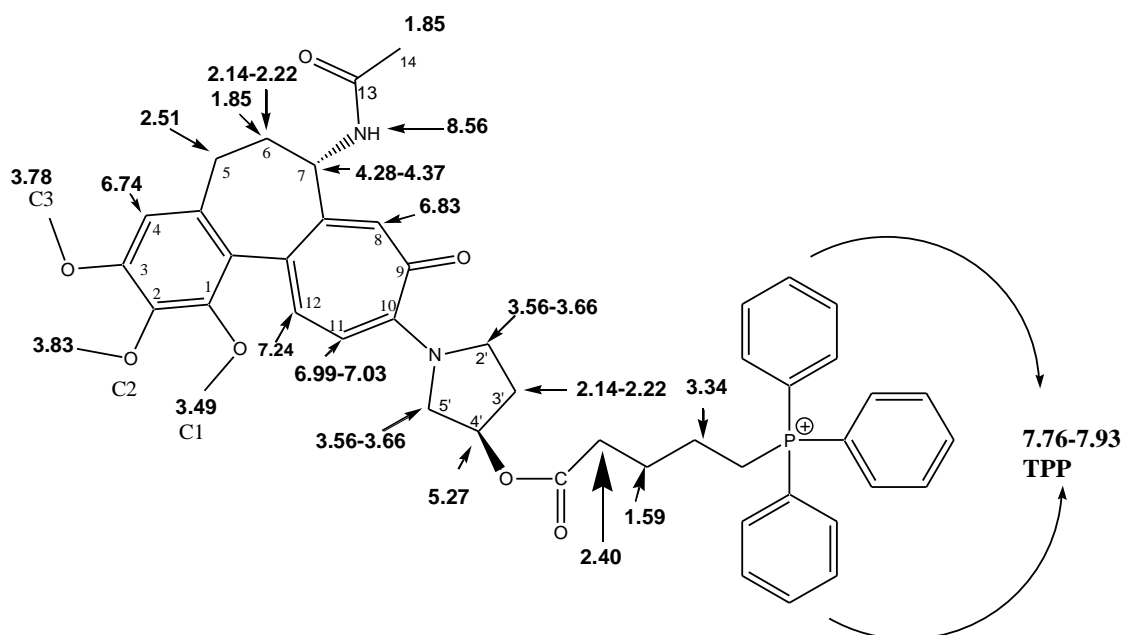


Figure 2. 47 ^1H NMR assignments (ppm values) and atomic numbering for AM9.

A two-proton multiplet was assigned to the methylene group (COCH₂-CH₂-CH₂-CH₂-P) at 1.59 ppm. A two-proton multiplet was assigned to the methylene (COCH₂-CH₂-CH₂-CH₂-P) at 1.73 ppm. A four-proton singlet was assigned to a methyl of acetamide (NHCO-CH₃) and a hydrogen of C6 (CH) at 1.85 ppm. A three-proton multiplet was assigned to the methylene N-CH₂-CH₂ and CH of C6 at 2.14-2.22 ppm. A two-hydrogen triplet was assigned to the methylene next to carbonyl group (CH₂-COO) at 2.40 ppm. A two-proton multiplet at 2.51 ppm was assigned to the methylene CH₂ of C5. A two-proton multiplet was assigned to the methylene attached to P (P-CH₂) at 3.34 ppm. A three protons singlet at 3.49 ppm was assigned to the methoxy group of C1 (C1-OCH₃). A four-proton multiplet at 3.56-3.66 ppm was assigned to two methylene adjacent to nitrogen (2 x N-CH₂). A three-proton singlet at 3.78 ppm was assigned to the methyl of C3. A three-proton singlet of the methyl of C2 were found at 3.83 ppm. A proton multiplet at 4.28-4.37 ppm was assigned to methine of C7 (H7) adjacent to acetamide CH-NHCOCH₃. A one-proton singlet was assigned to CH adjacent to OCO at 5.27 ppm. One-proton doublet at 6.39-6.43 ppm was assigned to the aromatic of H-11 (C11) proton with J=11 Hz. A methine proton of C4 was assigned to one-proton singlet found at 6.74 ppm. A proton singlet at 6.83 ppm was assigned to methine of C8. A one-proton, doublet with at 6.99-7.03 ppm was assigned to the aromatic methine of C12 (or H-12) with J=11 Hz. A fifteen hydrogen multiplet was assigned to TPP at 7.76 -7.93 ppm. A proton doublet at 8.50-8.52 ppm was assigned to NH of acetamide (**Figure 2.47**).

2.5 Distribution Coefficient Studies

The physicochemical properties of novel colchicine derivatives (AM1, AM3, AM4, AM5 and AM6) and TPP-conjugated colchicine derivatives (AM2, AM7, AM8 and AM9) were studied to determine the distribution coefficient.

Distribution coefficient is an important parameter that determines if the given drug compound is hydrophobic “water hating” or hydrophilic “water loving” in nature. This is the crucial predictor of drug distribution inside the body. Pharmacokinetics studies reveals that hydrophilic compounds will most likely to be distributed in the aqueous compartments of the body such as blood or plasma, whereas a hydrophobic compound will be distributed in the lipid or fatty compartments of the body such as lipid bilayer cellular membrane (Markovsky *et al.*, 2012).

Distribution coefficient define as the ratio of the concentration of a drug molecule or a compound (solute) in a mixture of two immiscible solvents at equilibrium. It is represented by log D or log P. However, log P only predicts partition of uncharged or unionised or neutral drug molecule (solute molecules) therefore it is not a true determinant of hydrophilicity or hydrophobicity of an ionised species inside a body where pH is always changing. Whereas, the distribution coefficient, log D, accurately determines concentration of ionised and unionised drug moieties and is pH dependent. A polar or hydrophilic compound would always favour aqueous or a polar phase such as PBS buffer (pH. 7.4) and a non-polar or hydrophobic compound always favours non-polar or an organic phase such as octanol (Andrés *et al.*, 2015)(Pajouhesh and Lenz, 2005).

Octanol is used as an organic solvent (phase) in distribution coefficient experiment because its 8-carbon atoms are highly hydrophobic and are like hydrophobic lipid bilayer of cell membrane according to the biological data obtained in vivo. And, it has a hydrophilic hydroxyl group (OH) that favours hydrogen bonding with solute. So, it gives the closest balance to that found in human cell membrane. PBS represents the aqueous zone of the body such as blood plasma. Hence the distribution coefficient can be a true predictor of main elements of ADME that is, absorption, distribution and elimination (Hinderliter and Saghir, 2014).

As the main drug target of the current study is mitochondria, an important organelle of the cell with lipid bilayer membrane and it was already discussed in the introduction of this project that TPP-conjugates of colchicine derivatives needs to be hydrophobic or lipophilic in order to cross lipid bilayer of cell membrane and mitochondrial membrane. So, distribution coefficient experiment was performed to check whether TPP-linked colchicine derivatives (AM2, AM7, AM8 and AM9) are hydrophobic in nature in comparison with their non-TPP-linked colchicine derivatives (AM1, AM3, AM4, AM5 and AM6).

2.5.1 Determination of distribution coefficient (Log D) method

Distribution coefficient experiments were performed and log D results for AM compounds (AM1-AM9) were obtained by using the shake-flask octanol/PBS partition coefficient method. To plot the calibration curves for each compound, two sets of cuvettes were prepared at different concentration ranging from 0 μ M to 25 μ M for all the compounds (AM1-AM9). In one set of cuvettes (5 in total) the compound was diluted in PBs (buffer, pH 7.4) and in other set the drug compound was diluted with octanol to get the specific concentration. The absorbance reading was in a range of 0-0.85 in case of octanol calibration for all the drug compounds and graph showed a linear line of best fit for all the compounds. The equations derived from octanol calibration curves are as follows: AM1 ($y=0.0237x-0.003$), AM2 ($y=0.0201x+0.003$), AM3 ($y=0.0188x+0.0066$), AM4 ($y=0.0337x+0.0076$), AM5 ($y=0.0293x+0.0041$) AM6 ($y= 0.0164x+0.0081$), AM7 ($y=0.0097x+0.0019$), AM8 ($y=0.0154x+0.0006$) and AM9 ($y=0.0199x+0.0059$) (**Appendix figures A.1.1 to A.1.5**).

For PBS calibration curves, the absorbance reading was in a range of 0-0.89 for all the drug compounds and graph showed a linear line of best fit for all the compounds. (Figures calibration curves). The equations derived from PBS calibration curves are as follows: AM1 ($y= 0.0258x + 0.0046$), AM2 ($y = 0.0208x + 0.0034$), AM3 ($y = 0.0213x + 0.005$), AM4 ($y = 0.0353x + 0.0063$), AM5 ($y = 0.029x + 0.0104$), AM6 ($y = 0.0181x - 0.0017$), AM7 ($y = 0.0097x + 0.0019$), AM8 ($y = 0.0139x + 0.0019$) and AM9 ($y = 0.0199x + 0.005$) (**Appendix Figures A.1.1 to A.1.5**).

The absorbance readings from distributed samples of AM1-AM9 are listed in the tables (**Appendix Table A.2.1-A.2.9**), using these absorbance values, equation obtained from calibration curve data and considering the dilution factor for each concentration the log D value were calculated for all the colchicine derivatives and their TPP-conjugates using the equation given below:

$$\log D_{\text{oct/water}} = \log \left(\frac{[\text{solute}]_{\text{octanol}}}{[\text{solute}]_{\text{ionised water}} + [\text{solute}]_{\text{neutral water}}} \right)$$

Log D values for all aminocolchicine derivatives were AM1 (log D=1.69) (**Appendix Table A.2.1**), AM3 (log D=1.64) (**Appendix Table A.2.3**), AM4 (log D=1.65) (**Appendix Table A.2.4**) AM5 (log D=1.63) (**Appendix Table A.2.5**) and AM6 (log D=1.28) (**Appendix Table A.2.6**).

Table 2. 1 Log D values for aminocolchicine derivatives (Appendix A.2.1-Appendix A.2.6).

Amino-colchicine derivatives	Log D values
AM1	1.69 ± 0.06
AM3	1.64 ± 0.02
AM4	1.65 ± 0.04
AM5	1.63 ± 0.005
AM6	1.28 ± 0.03

Results were as expected as their clinical comparator colchicine itself has a log P value of 2.34 making it a lipophilic compound (Swissadme.ch, 2019).

All the aminocolchicine derivatives were mainly partitioned in the octanol (organic) layer, since these compounds predominantly found in organic layer that means they are lipophilic or hydrophobic in nature. Ionization of the compounds greatly affects octanol/water partitioning. Where AM1 emerged as most hydrophobic agent in aminocolchicine derivatives with log D value of 1.69. Lipophilicity or hydrophobicity is low under 12 pH because at this pH majority of the compound exist in ionized form. Negative log D values (-1.44 to 0) in the physiological pH range (1-8) lead us to conclude that the compound has higher water solubility or is hydrophilic/lipophobic in

nature that means poor membrane permeability. Positive log D values (1-5) predict higher lipophilicity of drug compounds (Bhal, 2007; Lipinski, 2000).

The log D values for TPP-conjugated aminocolchicine were; AM2 (1.34) (**Appendix Table A.2.2**), AM7 (0.72) (**Appendix Table A.2.7**), AM8 (1.28) (**Appendix Table A.2.8**) and AM9 (1.37) (**Appendix Table A.2.9**).

Table 2. 2 Log D values for TPP-conjugated aminocolchicine (Appendix A.2.2-Appendix A.2.9).

Tpp-conjugated aminocolchicine	Log D
AM2	1.34 ± 0.26
AM7	0.72 ± 0.11
AM8	1.28 ± 0.05
AM9	1.37 ± 0.04

Results demonstrated that TPP-conjugated aminocolchicine derivatives were also predominantly found in octanol layer hence proved to be hydrophobic/lipophilic in nature, but these TPP-conjugates are less hydrophobic in comparison of their non-conjugated compounds. This was unexpected because compounds with TPP supposed to be more hydrophobic due to presence of lipophilic cation TPP. AM7 (a TPP-conjugated aminocolchicine derivative of AM6) turned out to be the least hydrophobic compound among all the amino-colchicine derivatives with a log D value of 0.72.

However, all amino-colchicine derivatives with or without TPP showed a moderate degree of hydrophobicity except AM7 (0.72), that predicted easy passage of these compounds from cell and mitochondrial lipid bilayer membranes.

2.6 Effect of Novel targeted anthelmintic prodrugs on *C. elegans*

TPP is a lipophilic cationic drug delivery vehicle that directs drug molecules to the target site (mitochondria) when conjugated with the compounds (drug compounds) due to its unique characteristics such as delocalised positive charge and its lipophilicity (as discussed previously in detail in section 1.4.2.1) that not only attracts TPP base compounds towards the matrix of mitochondria but also ensure the easy passage from the lipid bilayer of cell and mitochondrial membrane (Finichiu *et al.*, 2013)

In the current study TPP-conjugated colchicine derivatives were synthesised as potential anthelmintic agents to target colchicine derivatives (active drug) to the target site i.e. “the worm’s mitochondria”. In doing so, it was anticipated that they not only provide targeted delivery to the site and possibly circumvent the resistance against colchicine but also reduce the toxic effects to the host by achieving selectivity. In order to prove this concept and to prove the efficacy of TTP-conjugated compounds (AM2, AM7, AM8 and AM9) in comparison with the non-conjugated compounds (AM1, AM3, AM4, AM5 and AM6), *C. elegans* worm was selected as a model organism because of its close resemblance with helminths parasite to see the potential of these drugs as novel anthelmintic agents.

2.6.1 *C. elegans* viability assay

For this purpose, L4 worms were chosen from wild type *C. elegans* synchronised population and were exposed to different concentrations of Colchicine derivatives and their TPP-conjugates to establish comparison. Two novel colchicine derivatives AM1 and AM2 were chosen for the experiment. Where AM1 (Col-Pro) is the colchicine derivative with prolinol and AM2 (Col-Pro-TPP) is an ester-linked TPP-conjugate of AM1. L4 were exposed to different concentrations of AM1 and AM2 for 24 hours at start (n=1 experiment). The result demonstrated that at 100 µM, TPP-conjugate, AM2 showed 2% worm survival as compared with its non-conjugated form AM1 (**Figure 2.49**). Whereas, 10 µM, 1 µM, and 0.1 µM of both AM1 and AM2 did not appear to be

different from each other and more than 96% worm survival was monitored after treatment exposure.

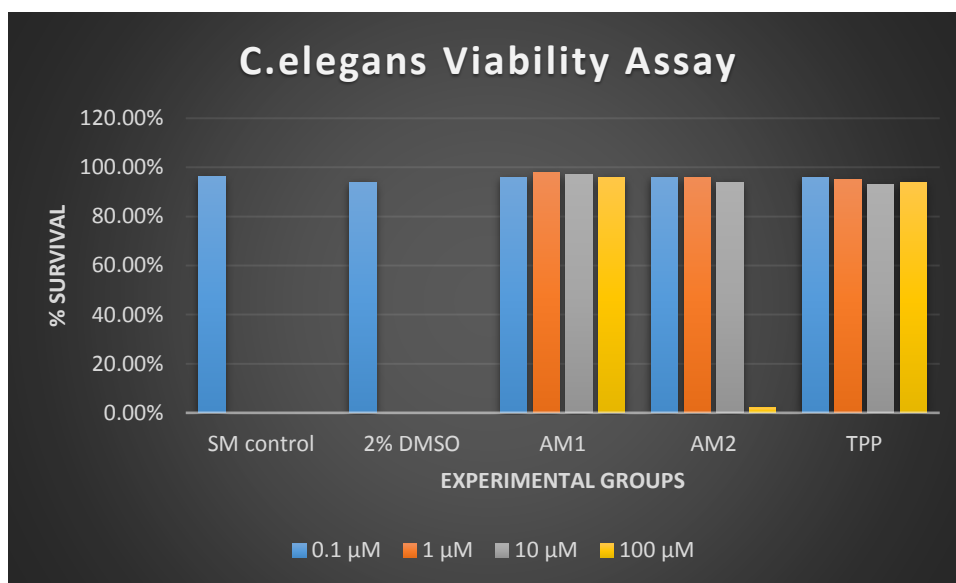


Figure 2. 48 % survival of *C. elegans* for AM1 and AM2 at different concentrations (0.1 μM, 1 μM, 10 μM and 100 μM in the presence of negative controls (*S. medium* control and DMSO control) at 22h. % survival of *C.elegans* was calculated by considering number of live worms and divided by sum of live and dead worms multiplied by 100 to get % of survival. The experiment was repeated in triplicates with n=3.

The aim of the results described in the worm viability assay was to enlighten the efficacy of TPP-conjugated colchicine derivatives in anthelmintic therapy. AM2 (a TPP-conjugate, a magic bullet) most likely to possess anthelmintic activity given the fact that 98% worms died in the first exposure (n=1) for 24 hours at 100 μM (**Figure. 2.48**). Results have shown a trend of toxicity of TPP conjugated prodrug AM2 as 2% worm's survival in comparison with AM1 with 96% worm survivals. It suggested that TPP is likely responsible for the results described in the figure due to its high affinity for the mitochondria because of the ability of TPP to cross membrane of a cell and mitochondria without needing a transporter mechanism (Ross *et al.*, 2005). It allows easy a quick uptake of AM2 compound in the worm's mitochondria where TPP-conjugate would release active drug following cleavage of ester bond between TPP and Colchicine derivative by worm esterase. This result gives us a strong ground for proof of concept for TPP-conjugated colchicine derivatives being developed as promising agents in anthelmintic therapy.

However, when the same experiment was performed in n=3, and with increased time of exposure (48 to 72 hours) the results obtained were not as promising as the first

preliminary study. There was a level of toxicity from these agents towards *C. elegans* worms and this was approaching significance.

Another study was conducted on the same agents AM1 and AM2 where behavioural assay was performed. In the behavioural assay, worm viability was tested in terms of motility measurement of the worms after exposing worms to treatment (AM1 & AM2) with the negative controls (S. medium and DMSO). Motility was measured by counting the total number of turns (bends) by an individual worm per minutes. (BDPM). Results were recorded at 2 hours and 24 hours and data was presented in mean of the total number of body-turns per minute/worm. The experiment was performed in n=4. The Results obtained from the experiment indicated a difference in worm motility, however statistical significance ($P < 0.05$) was not achieved for both AM1 and TPP-conjugate AM2, the effects were time dependent i.e. increased effect after 24-hour exposure. Results showed that motility of worms decreased after 24-hour exposure for both the agents and AM2 the TPP-conjugated prodrug is more potent in terms of decreasing motility and viability of worms as compared to AM1 as shown in the figure. These results further provided support for our concept of TPP-conjugated magic bullets having the potential to be targeted novel anthelmintic prodrugs (**Figure 2.49**).

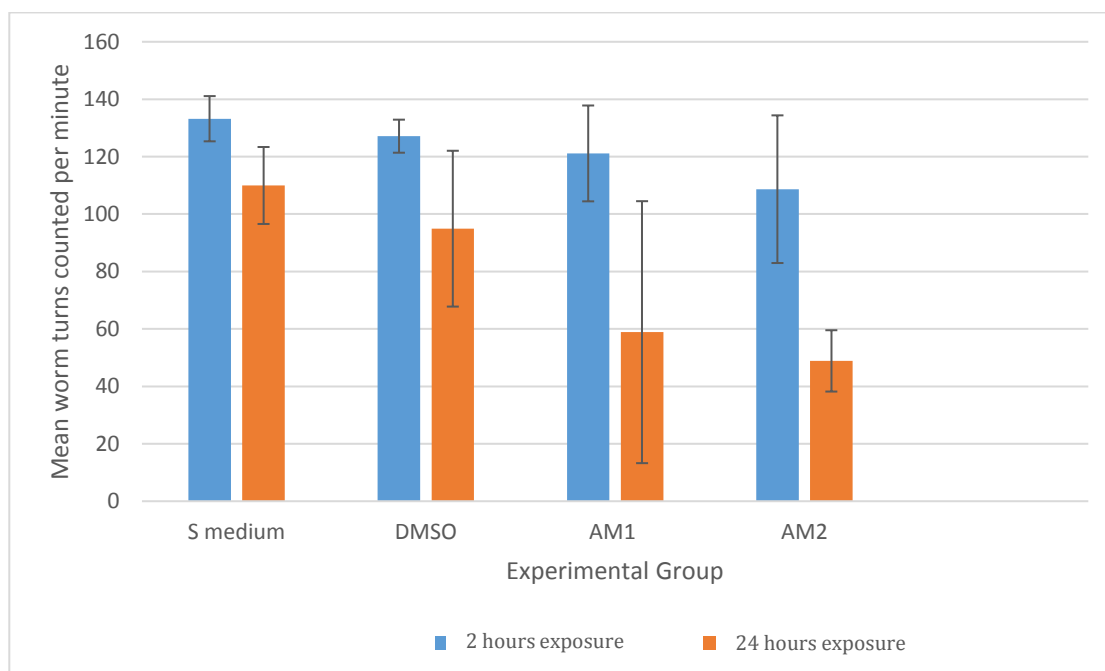


Figure 2. 49 The comparison between effects AM1 and TPP-conjugate AM2 on worm's viability in terms of motility at 2 h and 24 h exposure, with both negative controls; s. medium and DMSO. Motility was measured by total number of turns per individual worm per minute, data shown in mean of number of turns per minute. Experiment was performed in duplicate with n=4. (Adopted from the results provided by Dr. Lorna Proudfoot).

The same experiment was also performed on other two agents of the AM series: AM6 (Colchicine-(*R*)-3-amino-Pyrrolidine-TFA) and its TPP conjugate AM7 (Colchicine-(*R*)-3-amino-Pyrrolidine-TPP) and it was decided to increase the exposure time to 48 hours this time as it was shown in the results that motility was decreased but worms were not dead or immobilised. Results obtained from the experiment showed that both AM6 and its TPP conjugate reduced the motility of the worms, so they have the potential to affect the viability of the worms. However, the theory of increasing time exposure was proven wrong because at 24 hours the motility of the worms was lowest (reduced) but after 48 hours exposure of the treatments the motility increased and also the worms count was highest at the point. These results also showed that prolong time exposure of these agents can lead to decrease in their effects on the viability of worms (Figure 2.50).

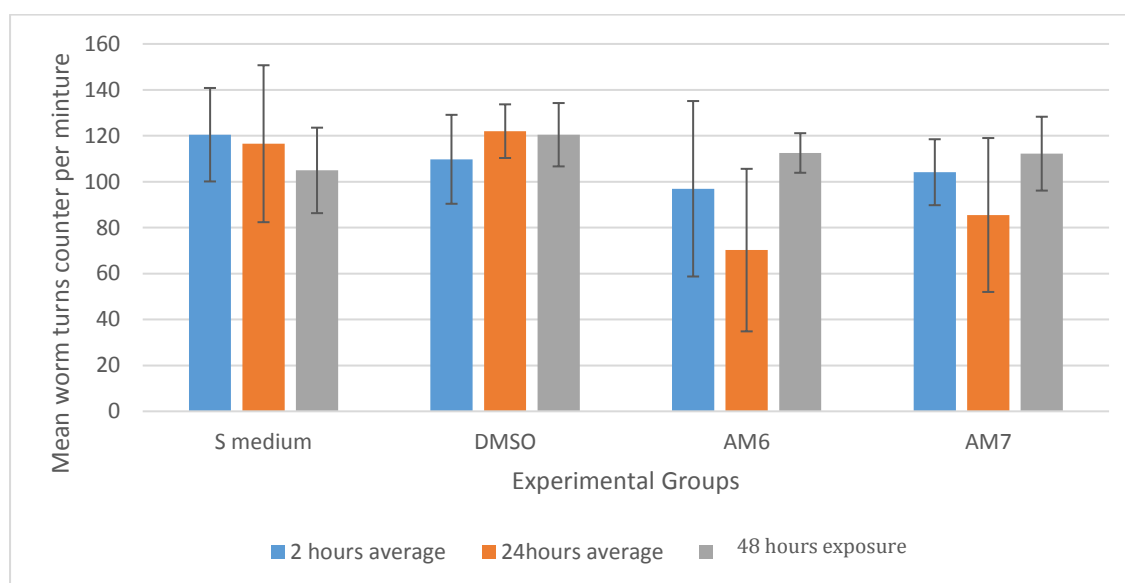


Figure 2. 50 The comparison between effects AM6 and TPP-conjugate AM7 on worm viability in terms of motility at 2 h, 24 h and 48 h exposure, with both negative controls; s. medium and DMSO. Motility was measured by total number of turns per individual worm per minute, data shown in mean of number of turns per minute. Experiment was performed in duplicate with n=4. (Adopted from the results provided by Dr. Lorna Proudfoot).

All the results obtained from worm viability assay using these novel colchicine TPP-conjugated prodrugs demonstrated that there is a strong effect on worm viability, but the effect of these prodrugs decreased by the time. One possible reasoning for this is that may be *C. elegans* is not a suitable model for these agents and a true helminth

parasite model can be considered for further testing on these agents to get a clear idea of their effect on helminth viability. *C.elegans* live in soil where they deal with extreme and constant osmotic pressure or stress. *C. elegans* recovered from the shock very quickly and return to their normal motion as the time passes. Their ability to survive after the shock and come out of stress is very impressive. They have ability to sense and reverse changes in the cell and survive extreme conditions in the laboratory due to their ability to adapt these changes and turgor pressure (Lamitina, 2004). It can be possible that a strain of *C. elegans* is sensitive to chemical stress and another strain is completely resistant to the same chemical. This variation in the different strains of *C. elegans* have been studied many times to elaborate their survival and come back from stress. Mutations can be developed in then *c. elegans* against toxicity of various chemicals such as toxicity produced by Zinc (Zn) (Bruinsma *et al.*, 2008)

Another reason could be the solubility of these agents in solvents. Although AM1 and AM2 were soluble in the DMSO still some of the viability assay showed traces of solid crystals in the treatment wells which may have been attributable to the drugs slowly coming out of solution.

2.7 Molecular Docking

Technological advancements such as molecular docking, can be employed to obtain the atomic information of protein-ligand complex interaction and has and presented a new platform for the drug design and development for specific targets. It helps to predict the best possible interaction between drug molecules and target sites. Molecular docking is an efficient tool and is playing a very important significant role in the rationale of drug design. It is a computational way to look for a suitable ligand (a drug molecule) that has the suitable fit profile for the binding site (a protein molecule or an enzyme) in fixed orientation and in order of internal geometry. Just like a 3D puzzle, or ligand receptor lock and key model, where one molecule such as a drug molecule or a ligand has the binding affinity for the pocket of another molecule, a protein receptor. If the structure of the protein is known, different conformations of the selected ligand can be easily seen in the protein molecule (Ferreira *et al.*, 2015; Guedes *et al.*, 2014; Kholod *et al.*, 2018).

A preliminary study has been performed for novel amino-colchicines AM1 (Col-Prolinol), AM3 (Col-4hydroxypiperidine), AM4 (Col-(*R*)-3-pyrrolidinol), AM6 (Col-aminopyrrolidine) and a reference compound CN2 (N-deacetyl-N-(2-mercaptoacetyl)-colchicine) that is a known tubulin binder and a colchicine binding site inhibitor (CBSI) (Ravelli *et al.*, 2004). Docking studies revealed binding energies for all these compounds that showed these agents have binding affinity for tubulin molecule (**Figure 2.51 & 2.52**), where AM6 showed strong tubulin binding with binding energy - 9.84 KJ in comparison with the reference compound CN2 (which is a CBSI) that has binding energy of -9.01 Kcal/mol (**Table 2.1**). A negative or low energy refers to the strong binding of ligand into protein (receptor) pocket, means the ligand and protein complex is stable and most likely to interact with each other whereas a higher or positive binding energy means more energy needed by the complex for interaction hence weak binding (Ferreira *et al.*, 2015).

These preliminary studies indicate that this is a promising area in drug design and development.

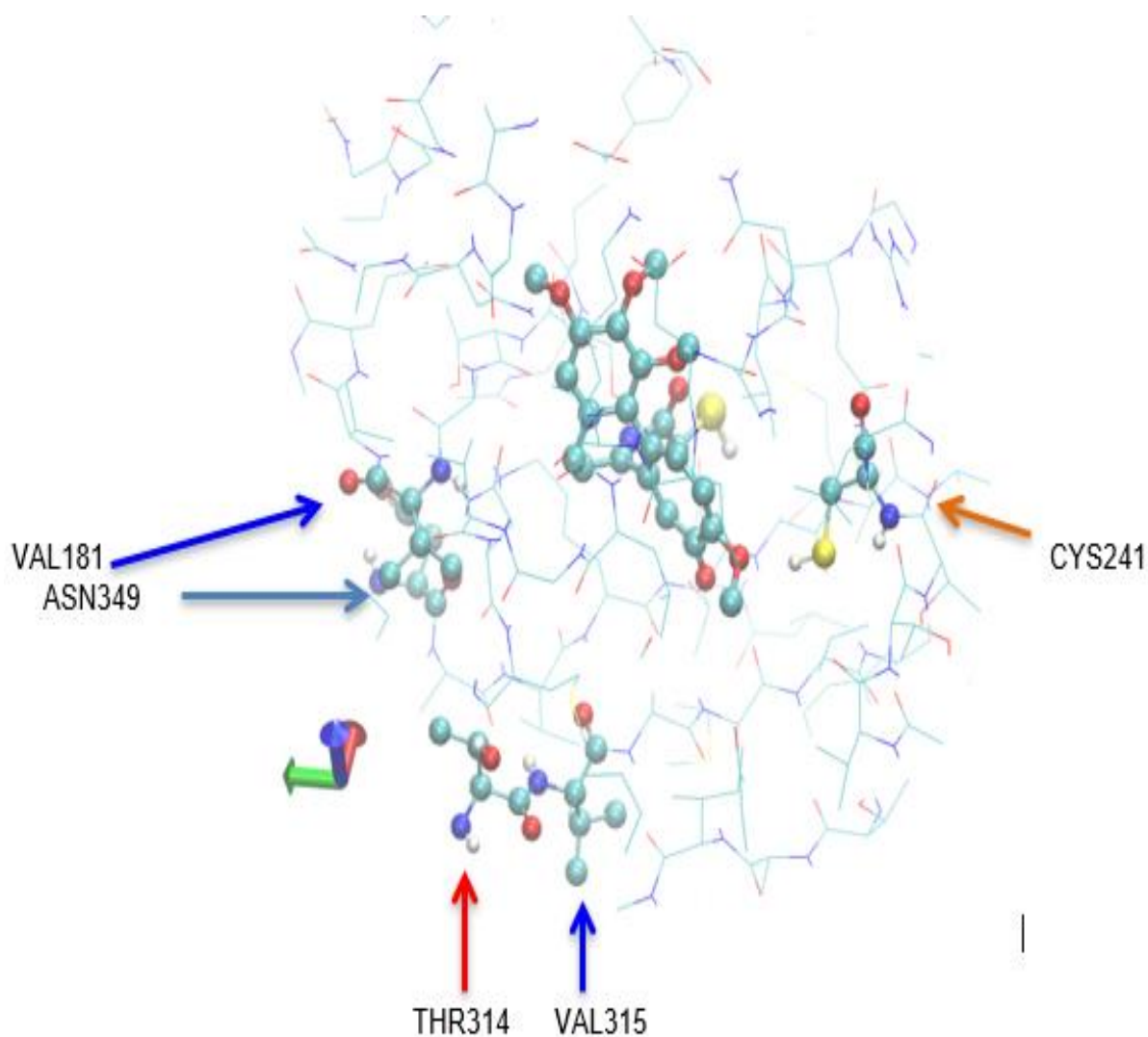


Figure 2. 51 CN2 (N-deacetyl-N-(2-mercaptoacetyl)-colchicine in complex with X-ray crystal structure of bovine α , β -tubulin in the colchicine binding pocket. Crystal structure obtained from the protein database in the pdb form.

AutoDock4 software was employed to generate binding models for CN2 compound that is a tubulin modulator and CBSI (colchicine binding site inhibitor). **Figure 2.51** showing binding of the ligand CN2 in the tubulin molecule at the interface of chain A and chain B, the methoxy group on the ring A of colchicine facilitates interaction with CYS241 residue (please note that CYS241 residue is very important for the interaction in case of CBS (colchicine binding site)). Ligand CN2 also showed interaction with residues VAL181, THR314, ASN349 and VAL315. In this picture, Line model is alpha and beta chain of tubulin, LIG, CN2 (ligand and its code is CN2), CYS241 (cysteine 241 on chain B of tubulin molecule), VAL181 (Valine residue on chain A of tubulin

molecule), VAL315 (on chain B), ASN349 (Asparagine residue on chain B), THR314 (Threonine residue on chain B of tubulin).VMD software has been used to create this representation after obtaining docking results from AutoDock software.

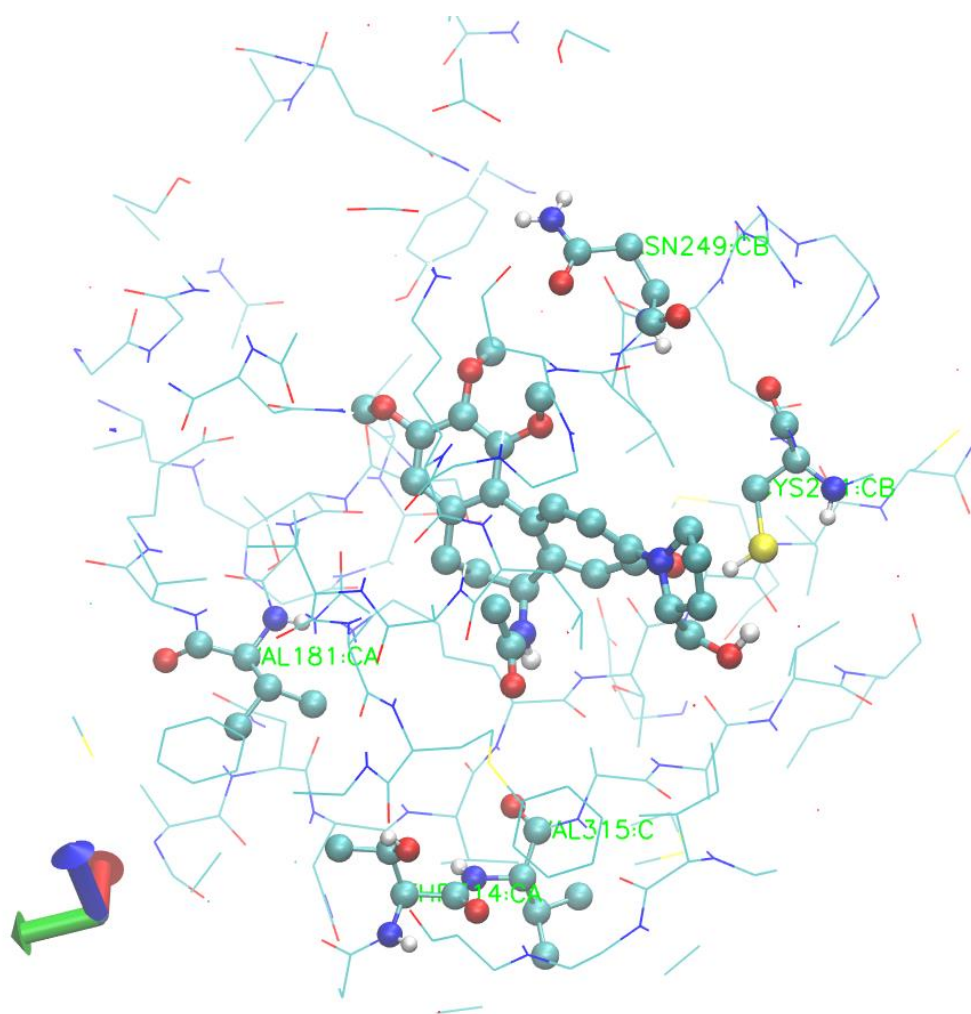


Figure 2. 52 Binding model of compound AM1 (Col-Pro) (a potential tubulin modulator), in the colchicine binding pocket; top ranked pose.

AutoDock4 results shows that AM1 binds in the same colchicine binding pocket at the interface of alpha and beta chains of tubulin molecule as CN2 and interacting with the same residues as did CN2. Here one thing is clear that we use CN2 as our reference compounds to compare our results with. The methoxy group on the ring A of colchicine

facilitates interaction with CYS241 residue (please note that CYS241 residue is very important for the interaction in case of CBS (colchicine binding site). Line model is alpha and beta chain of tubulin, LIG, AM1 (ligand and its code is AM1), CYS241 (cysteine 241 on chain B of tubulin molecule), VAL181 (Valine residue on chain A of tubulin molecule), VAL315 (on chain B), ASN349 (Asparagine residue on chain B), THR314 (Threonine residue on chain B of tubulin). VMD software has been used to create this representation after obtaining docking results from AutoDock software.

Table 2. 3 Binding energies of AM1, AM3, AM4, AM6 and CN2 (the reference compound).

Compounds	Lowest binding energies (Kcal/mol)
AM1	-9.00
	-8.82
	-7.50
AM3	-8.59
	-7.98
AM4	-8.93
	-8.75
	-8.50
AM6	-9.84
	-8.86
CN2	-9.01

AM6 shown the lowest binding energy with -9.86 Kcal, demonstrate that it has a strong binding affinity for tubulin as compared to reference compound CN2 (-9.01) and AM1 (-9.00 kCal) shown to have same binding energy as CN2; important to note here that both the compounds share almost same lowest binding energies (we already know that CN2 is a tubulin modulator). *(Ravelli *et al.*, 2004).

2.8 Conclusion & Future work:

Resistance is a major issue when it comes to the efficacy of traditional anthelmintic agents and a huge reason of their failure in resistant helminths. This hallmark affects the world economy a great deal. Prodrug strategy is one solution of this major problem by targeting drug compounds directly to the site of action by inclusion of a targeting moiety. For this purpose, novel amino-colchicines (AM1, AM3, AM4, AM5, AM6) have been synthesised that are further conjugated with a TPP targeting moiety to develop novel anthelmintic prodrugs (AM2, AM7, AM8, AM9) to achieve selectivity and circumvent developing resistance. TPP is the lipophilic cationic drug delivery vehicle that takes the advantage of negative membrane potential of cell and mitochondrial membrane and it is highly lipophilic, facilitating both cellular uptake of the drug-TPP complex and accumulation in the matrix of mitochondria, hence potentially achieving selectivity and bypass of resistance. Novel amino-colchicines that can disrupt the assembly of microtubules, leading to dysfunction of mitochondria and apoptosis in the cell. TPP was linked with amino-colchicines with an ester bond that could be cleaved by an esterase in the worm mitochondria releasing active drug to initiate drug activity. The worm viability assay revealed that the TPP-conjugated AM2 prodrug showed toxicity towards *C. elegans* worms that was used as a model organism in this research, hence has the potential to be used as an anthelmintic agent in the treatment of helminth diseases. Preliminary molecular docking studies also showed that these novel amino-colchicines have affinity for tubulin and AM6 showed strong tubulin binding with low binding energy of -9.84, indicating strong binding. These novel agents have the strong potential to be used as anthelmintic agents in helminth therapy.

Further work could include inclusion of a true parasite as a model system to check the helminth viability and toxic profile of these novel agents towards parasites. Technological advancements such as molecular docking can be employed to obtain the atomic information of protein-ligand complex interaction and has presented a new platform for the drug design and development for the specific targets. It helps to predict the best possible interaction between drug molecules and target sites. More work can be done on docking studies of TPP conjugates of aminocolchicine (AM2, AM7, AM8 and AM9) to monitor drug-target interactions and then results can be compared with in this area for this purpose. Structural modification can be done to these novel amino-

colchicines to develop more efficient prodrugs or small molecules that have higher potential as anthelmintic agents, for example, further modification at C-10 or C-7 positions of colchicine ring. Work can be done to check the cytotoxicity of these novel agents against cancer cells, preliminary work has already been done on these novel drugs using MCF-7 cancer breast carcinoma cell line where they showed some toxicity in MTT assay (data not shown).

3 Chapter

3.0 Experimental

3.1 Analytical Methods

3.1.1 Thin layer chromatography

Pre-coated aluminium Kieselgel 60 F₂₅₄ silica plates (Merck) were used for TLC (Thin Layer Chromatography). Uncoloured compounds were visualised by UV light (250-390 nm). Solvent systems used for thin layer chromatography were A) chloroform: methanol (CHCl₃-MeOH) 4:1; B) chloroform: methanol (CHCl₃-MeOH) (9:1, v/v), (C) butanol: glacial acetic acid: water (n-Bu-AcOH-H₂O) (4:5:1, v/v/v). TLC was used to assess compound purity. Compounds were deemed to be pure when observed as single spots (homogeneous) by TLC. Percentage yields are reported for the purified compounds.

3.1.2 Column chromatography

Kieselgel 60 (0.063-0.0200 mm) silica gel was used in column chromatography. Sometimes a small pump was used to apply air pressure to the column.

3.1.3 Mass spectrometry

High resolution mass spectrometry-electrospray ionization (HRMS-ESI) were carried out using a ThermoFisher LTQ Orbitrap XL or a Waters ZQ4000 instrument. UV-vis spectra were measured on a Beckman DU800 spectrophotometer; scan speed 1200 nm min⁻¹ and wavelength range 400 to 800 nm. Mass spectra were recorded on a ThermoFisher LTQ Orbitrap XL or a Waters ZQ4000 spectrometer.

3.1.4 Proton and carbon nuclear magnetic resonance (¹H and ¹³C NMR)

¹H and ¹³C NMR were recorded on either a Bruker AC300 or a Bruker AC400 NMR spectrometer at 25°C at 300.1 MHz and 75.47 MHz, respectively from samples dissolved either in deuterated DMSO or deuterated chloroform. In ¹³C, a DEPT (Distortionless Enhancement by Polarization Transfer) experiment was conducted to differentiate between quaternary, methylene carbons, methine and methyl carbons

3.1.5 Chemical reagents

Colchicine 95% dry weight was purchased from Alfa Aesar. All other reagents were obtained from Sigma-Aldrich Merck (Gillingham, UK) Purity of compounds was assessed as 95 %.

3.2 Synthesis of colchicine-based small molecule compounds (AM series):

3.2.1 Synthesis of Colchicine-Prolinol {N-[10-(2-Hydroxymethyl-pyrrolidin-1-yl)-1,2,3-trimethoxy-9-oxo-5,6,7,9-tetrahydro-benzo[α]heptalene-7-yl]-acetamide} (AM1)

To a solution of colchicine (0.25 g, 0.625 mmol) in DMF (1 ml) was added prolinol (168 μ l, 6.26 mmol, 10 eq) at rt After 24 h, the mixture was extracted with CHCl₃ and H₂O (1:1, 100 ml). The combined organic layers were dried over anhydrous Na₂SO₄, filtered and the filtrate was concentrated *in vacuo*. The residue was purified by silica gel column chromatography (chloroform: methanol, 9:1 and 4:1). The desired fractions of product were combined, filtered, concentrated to dryness under reduced pressure and the residue was triturated with ether to give the desired AM1 compound as a yellow solid (0.276 g; 94 %).

TLC (chloroform: methanol, 9: 1) R_f. 0.42.

HRMS (ESI+) m/z: 491.21 (14%) (M+Na)⁺ 470.23 (29%), 469.23 (100%) (M+H)⁺ .
Calcd for [C₂₆H₃₂N₂O₆]⁺ 468.23; found 469.23.

¹H NMR (DMSO-*d*₆, 300 MHz): δ (ppm) 1.69-1.90 (m, 3H, C₆-CH₂, N-CH₂-CH₂), 2.03 (s, 3H, NH-COCH₃), 2.38 (m, 3H, C₆-CH₂, C₅-CH₂), 3.40-3.50 (m, 2H, N-CH₂-CH₂-CH₂), 3.64 (s, 3H, C₁-OCH₃), 3.76 (m, 3H, N-CH₂), 3.90 (s, 3H, C₃-OCH₃), 3.95 (s, 3H, C₂-OCH₃), 4.57 (m, 1H, C₇-CH), 6.49 (d, 1H, C₁₁-CH, J 12 Hz), 6.54 (s, 1H, C₄-CH), 7.24 (m, 1H, C₈-CH), 7.30 (d, 1H, C₁₂-CH, J 12 Hz), 7.66 (d, 1H, NH-COCH₃).

¹³C NMR (DMSO-*d*₆, 75.5 MHz): δ (ppm) 22.46 (+ve, CH₂), 22.93 (+ve, C₁₄-CH₃), 28.07 (-ve, CH₂), 30.07 (-ve, C₅-CH₂), 37.35 (-ve, CH₂-C₆), 50.63 (-ve, CH₂), 52.09 (+ve, CH-C₇), 56.10 (+ve, C₃-CH₃), 61.28 (+ve, C₂-CH₃), 61.42 (+ve, C₃-CH₃), 62.23 (+ve, CH), 64.15 (-ve, CH₂-OH), 107.41 (+ve, CH-Ar-C₄), 113.25 (+ve, C₁₁, CH-Ar), 123.66 (+ve, CH-Ar, C₈), 138.31 (+ve, CH-Ar, C₁₂), 126.22 (absent), 129.85 (absent), 134.72 (absent), 141.52 (absent), 150.18 (absent), 151.33 (absent), 152.95 (absent), 156.23 (absent), 176.73 (absent), 169.94 (COO, C₁₃).

3.2.2 Synthesis of Colchicine-Prolinol-TPP {4-[1-(7-Acetylamino-1,2,3-trimethoxy-9-oxo-5,6,7,9-tetrahydro-benzo[α]heptalene-10-yl)-pyrrolidin-2-ylmethoxycarbonyl]-butyl}-triphenyl-phosphonium; bromide} (AM2)

To a solution of TPP (0.196 g, 0.442 mmol, 1.3 eq) in dichloromethane (3 ml) was added solid colchicine-prolinol (AM1) (0.16 g, 0.341 mmol) and DMAP (25 nano g). To this mixture was added DCC (0.105 g, 0.509 mmol, 1.5 eq) in dichloromethane and stirred at rt. After 24 h, the mixture was extracted with CHCl₃ and H₂O (1:1, 100 ml). The combined organic layers were dried over anhydrous Na₂SO₄, filtered and the filtrate was concentrated *in vacuo*. The residue was purified by silica gel column chromatography (chloroform: methanol, 9:1 and 4:1). The desired fractions of product were combined, filtered, concentrated to dryness under reduced pressure and the residue was triturated with ether to give the desired title product colchicine-prolinol-TPP (AM2) as a yellow solid (0.203 g; 73 %). TLC (chloroform: methanol, 9: 1) R_f. 0.5.

HRMS (ESI) m/z: 815.37 (14%) (M+Na)⁺ , 814.37 (54%), 813.36 (100%) (M+H)⁺ .
Calcd for [C₄₉ H₅₄ N₂ O₇]⁺ 892.29; found 813.36.

¹H NMR (DMSO-*d*₆, 300 MHz): δ (ppm) 1.50-1.80 (m, 6H, OCOCH₂-CH₂-CH₂-CH₂-P, C₆-CH), 1.85 (s, 3H, NHCO-CH₃), 1.90-1.96 (m, 5H, C₆-CH, NCH₂-CH₂, C₅-CH₂), 2.17-2.36 (t, 3H, CH₂-CO), 3.47 (s, 3H, C1-OCH₃), 3.54 - 3.66 (m, 4H, N-CH₂, N-CH₂-CH₂-CH₂), 3.77 (s, 3H, C₃-OCH₃), 3.83 (s, 3H, C₂-OCH₃), 4.34 (m, 1H, C₇-CH-NH), 4.99 (m, 1H, CH-CH₂-OCO), 6.50-6.52 (d, 1H, C₁₁-CH, J 11 Hz), 6.72 (s, 1H, C₄-CH), 6.84 (s, 1H, C₈-CH), 6.95-6.99 (d, 1H, C₁₂-CH, J 11 Hz), 7.76-7.93 (m, 15H, TPP), 8.48-8.51 (d, 1H, NH-CO).

3.2.3 Synthesis of Colchicine-4-hydroxypiperidine {(S)-N-(10-(4-hydroxypiperidin-1-yl)-1,2,3-trimethoxy-9-oxo-5,6,7,9-tetrahydrobenzo[α]heptalene-7-yl)acetamide} (AM3)

To a solution of colchicine (0.25g, 0.625 mmol) in DMF (1 ml) was added 4-hydroxypiperidine (0.94 g, 9.3 mmol, 15 eq) at rt. After 24 h, the mixture was extracted with CHCl₃ and H₂O (1:1, 100 ml). The combined organic layers were dried over anhydrous Na₂SO₄, filtered and the solvent was concentrated *in vacuo*. The residue was purified by silica gel column chromatography (chloroform: methanol, 9:1 and 4:1). The desired fractions of product were combined, filtered, concentrated to dryness under reduced pressure and the residue was triturated with ether to give the title compound AM3 as a yellow solid (0.261 g; 89 %). TLC (chloroform: methanol, 9: 1). R_f 0.33.

HRMS (ESI) m/z: 491.2135 (10%) (M+Na)⁺, 485.2266 (22%), 469.2323 (100 %) (M+H)⁺. Calcd for C₂₆H₃₂N₂O₆ 468.23; Found 469.2323.

¹H NMR (DMSO-*d*₆, 300 MHz): δ (ppm) 1.74-1.83 (m, 3H, C₆-CH, N-CH₂-CH₂), 2.03 (s, 5H, NHCO-CH₃, N-CH₂-CH₂), 2.17 (m, 3H, N-CH₂-CH₂, C₆-CH), 2.45 (m, 2H, C₅-CH₂), 3.26 (m, 1H, CH-OH), 3.67 (s, 3H, C1-OCH₃), 3.91 OR 3.85-4.05 (s, 8H, C₃-OCH₃, C₂-OCH₃, N-CH₂), 4.61-4.69 (m, 1H, C₇-CH-NHCOCH₃), 6.53 (s, 1H, C₄-CH), 6.83 (d, 1H, C₁₁-CH, J Hz), 7.23 (d, 1H, C₁₂-CH J Hz), 7.25 (s, 1H, C₈-CH), 7.53 (d, 1H, NH-CO-CH₃).

^{13}C NMR (DMSO-d_6 , 75.5 MHz): δ (ppm) 22.98 (+ve, C14- $\underline{\text{C}}\text{H}_3$), 30.09 (-ve, C5- $\underline{\text{C}}\text{H}_2$), 34.30 (-ve, $\underline{\text{C}}\text{H}_2$), 34.39 (-ve, $\underline{\text{C}}\text{H}_2$), 36.96 (-ve, $\underline{\text{C}}\text{H}_2\text{-C6}$), 46.32 (-ve, $\underline{\text{C}}\text{H}_2$), 46.45 (-ve, $\underline{\text{C}}\text{H}_2$), 51.91 (+ve, $\underline{\text{C}}\text{H-C7}$), 56.12 (+ve, C3- $\underline{\text{C}}\text{H}_3$), 61.40 (+ve, C2- $\underline{\text{C}}\text{H}_3$), 61.44 (+ve, C1- $\underline{\text{C}}\text{H}_3$), 67.41 (+ve, $\underline{\text{C}}\text{H}$), 107.34 (+ve, $\underline{\text{C}}\text{H-Ar-C4}$), 118.17 (+ve, C11, $\underline{\text{C}}\text{H-Ar}$), 128.82 (+ve, $\underline{\text{C}}\text{H-Ar}$, C8), 136.25 (+ve, $\underline{\text{C}}\text{H-Ar}$, C12), 126.08 (absent), 133.84 (absent), 134.40 (absent), 141.60 (absent), 149.72 (absent), 151.29 (absent), 153.11 (absent), 158.38 (absent), 169.89 (absent, C13), 181.32 ($\underline{\text{C}}\text{OO}$, C9).

3.2.4 Synthesis of Colchicine-(R)-3-Pyrrolidinol {1-(7-Acetylamino-1,2,3-trimethoxy-9-oxo-5,6,7,9-tetrahydro-benzo[α]heptalen-10-yl)-pyrrolidin-3-yl-ammonium;trifluoro-acetate} (AM4)

To a solution of colchicine (0.25g, 0.626 mmol) in DMF (1 ml) was added (R)-3-Pyrrolidinol (0.545 g, 6.26 mmol, 10 eq) at room temperature. After 1 h, the mixture was extracted with CHCl_3 and H_2O (1:1, 100 ml). The combined organic layers were dried over Na_2SO_4 , filtered and the solvent was concentrated *in vacuo*. The residue was purified by silica gel column chromatography (chloroform: methanol, 9:1 and 4:1). The desired fractions of product were combined, filtered, concentrated to dryness under reduced pressure at 20 °C and the residue was triturated with ether to give the title compound AM4 as a yellow solid (0.275 g; 96 %).

TLC (chloroform: methanol, 9: 1). R_f 0.19.

HRMS (ESI) m/z : 457.22 (5%) (M+Na^+), 456.22 (26%), 455.22 (100 %) (M+H^+). Calcd for $\text{C}_{25}\text{H}_{31}\text{N}_2\text{O}_6$ 454.21; Found 455.22.

^1H NMR (DMSO-d_6 , 300 MHz): δ (ppm) 1.8 (m, 1H, C6- $\underline{\text{C}}\text{H}$), 2.03 (s, 3H, $\text{NHCO-}\underline{\text{C}}\text{H}_3$), 2.07-2.3 (m, 3H, C6- $\underline{\text{C}}\text{H}$ and N- $\underline{\text{C}}\text{H}_2\text{-}\underline{\text{C}}\text{H}_2$), 2.43 (m, 2H, C5- $\underline{\text{C}}\text{H}_2$), 3.65 (s, 3H, C1- $\text{O}\underline{\text{C}}\text{H}_3$), 3.78-3.87 (m, 4H, 2 X N- $\underline{\text{C}}\text{H}_2$), 3.90 (s, 3H, C3- $\text{O}\underline{\text{C}}\text{H}_3$), 3.95 (s, 3H, C2- $\text{O}\underline{\text{C}}\text{H}_3$), 4.07 (d, 1H, $\underline{\text{C}}\text{H-OH}$), 4.55 (m, 1H, $\underline{\text{C}}\text{H-OH}$), 4.6 (m, 1H, C7- $\underline{\text{C}}\text{H-NH}$), 6.41 (d, 1H, C11- $\underline{\text{C}}\text{H}$), 6.52 (s, 1H, C4- $\underline{\text{C}}\text{H}$), 7.13 (s, 1H, C8- $\underline{\text{C}}\text{H}$), 7.24 (d, 1H, C12- $\underline{\text{C}}\text{H}$). 7.48 (d, 1H, NH-COCH_3).

^{13}C NMR (DMSO-d_6 , 75.5 MHz): δ (ppm) 23.02 (+ve, C14- $\underline{\text{C}}\text{H}_3$), 30.16 (-ve, C5- $\underline{\text{C}}\text{H}_2$), 33.19 (-ve, $\underline{\text{C}}\text{H}_2$), 37.35 (-ve, $\underline{\text{C}}\text{H}_2\text{-C6}$), 48.61 (-ve, $\underline{\text{C}}\text{H}_2$), 51.89 (+ve, $\underline{\text{C}}\text{H-C7}$), 56.12

(+ve, C3-CH₃), 58.85 (-ve, CH-OH), 61.27 (+ve, C2-CH₃), 61.41 (+ve, C1-CH₃), 70.40 (+ve, CH), 107.30 (+ve, CH-Ar-C4), 112.15 (+ve, C11, CH-Ar), 125.19 (+ve, CH-Ar, C8), 137.20 (+ve, CH-Ar, C12), 126.57 (absent), 129.10 (absent), 134.55 (absent), 141.51 (absent), 149.58 (absent), 151.25 (absent), 152.76 (absent), 154.97 (absent), 169.96 (absent, C13), 178.13 (COO, C9).

3.2.5 Synthesis of Colchicine-(R)-3-(Boc-amino) Pyrrolidine {1-(7-Acetylamino-1,2,3-trimethoxy-9-oxo-5,6,7,9-tetrahydro-benzo[α]heptalene-10-yl)-pyrrolidin-3-yl]-carbamic acid ter-butyl ester} (AM5)

To a solution of colchicine (0.25g, 0.626 mmol) in DMF (1 ml) was added (R)-3-(Boc-amino) Pyrrolidine (0.582 g, 3.13 mmol, 5 eq) at rt and stirred. After 24 h, the mixture was extracted with CHCl₃ and H₂O (1:1, 100 ml). The combined organic layers were dried over anhydrous Na₂SO₄, filtered and the solvent was concentrated *in vacuo*. The residue was purified by silica gel column chromatography (chloroform, chloroform: methanol: acetic acid, 9:1: 2 drops). The desired fractions of product were combined, filtered, concentrated to dryness under reduced pressure and the residue was triturated with ether over an ice bath to give the title compound AM5 as a yellow solid (0.310 g, 89 %).

TLC (chloroform: methanol, 9: 1). R_f 0.8.

¹H NMR (DMSO-*d*₆, 300 MHz): δ (ppm) 1.49 (s, 9H, CH₃-BoC), 1.7-1.9 (m, 3H, C₆-CH₂, N-CH₂-CH₂), 2.04 (s, 3H, NHCO-CH₃), 2.28 (m, 1H, C₆-CH), 2.4 (m, 2H, C₅-CH), 3.6 (s, 3H, C₁-OCH₃), 3.71-3.88 (m, 4H, 2 x N-CH₂), 3.9 (s, 3H, C₃-OCH₃), 3.96 (s, 3H, C₂-OCH₃), 4.32 (m, 1H, BoC-NH-CH), 4.62 (m, 1H, C₇-CH-NHCOCH₃), 4.81 (s, 1H, CH-NH-BoC), 6.39 (d, 1H, C₁₁-CH, J= 11 Hz), 6.53 (s, 1H, C₄-CH), 7.15-7.23 (m, 2H, C₈-CH, NH-CO-CH), 7.27 (d, 1H, C₁₂-CH, J= 11 Hz).

¹³C NMR (DMSO_{d6}, 75.5 MHz): δ (ppm) 23.06 (+ve, C14-CH₃), 28.40 (+ve, CH₃x3)Boc), 30.16 (-ve, C5-CH₂), 31.42 (-ve, CH₂), 37.41 (-ve, CH₂-C6), 48.80 (-ve, CH₂), 51.91 (+ve, CH-C7), 55.89 (-ve, CH₂), 56.12 (+ve, C3-CH₃), , 61.27 (+ve, C2-CH₃), 61.42 (+ve, C1-CH₃), 107.31 (+ve, CH-Ar-C4), 111.73 (+ve, C11, CH-Ar),

126.52 (+ve, $\underline{\text{C}}\text{H-Ar}$, C8), 136.97 (+ve, $\underline{\text{C}}\text{H-Ar}$, C12), 129.44 (absent), 134.52 (absent), 141.59 (absent), 149.70 (absent), 151.36 (absent), 152.80 (absent), 154.79 (absent), 155.37 (absent, C13), 169.77 (C9), 178.80 ($\underline{\text{C}}\text{OO}$, Boc).

3.2.6 Synthesis of AM6 (Col-(R)-3-(amino) Pyrrolidine-TFA) {1-(7-Acetylamino-1,2,3-trimethoxy-9-oxo-5,6,7,9-tetrahydro-benzo[α]heptalene-10-yl)-pyrrolidin-3-yl-ammonium; trifluoro-acetate} (AM6)

The Boc protected compound AM5 (Colchicine-(R)-3-(Boc-aminopyrrolidine) (0.28 g, 0.5 mmol) was treated with TFA (5 ml) for 30 min at rt. After 30 min, the mixture was concentrated in the presence of ethanol *in vacuo*, triturated with ether, and filtered to give a solid precipitate of desired compound AM6 (0.275 g, 95 %).

TLC (chloroform: methanol, 9: 1) R_f .

HRMS (ESI) m/z : 456.2383 (5%) ($\text{M}+\text{Na}$)⁺, 456.2354 (28%), 454.2322 (100 %) ($\text{M}+\text{H}$)⁺. Calcd for $\text{C}_{27}\text{H}_{32}\text{N}_3\text{O}_7\text{F}_3$ 567.22; Found 454.2322.

^1H NMR ($\text{DMSO-}d_6$, 300 MHz): δ (ppm) 1.84 (m, 1H, $\text{C}_6\text{-CH}$), 1.92-2.07 (m, 3H, NHCO-CH_3), 2.23 (m, 3H, $\text{C}_6\text{-CH}$, $\text{N-CH}_2\text{-CH}_2$), 2.57 (m, 2H, $\text{C}_5\text{-CH}_2$), 3.51 (s, 3H, $\text{C}_1\text{-OCH}_3$), 3.7 (m, 2H, $\text{C}_{10}\text{-N-CH}_2\text{-CH}_2$), 3.78 (s, 3H, $\text{C}_3\text{-OCH}_3$), 3.82 (s, 3H, $\text{C}_2\text{-OCH}_3$), 3.85-3.98 (m, 3H, $\text{C}_{10}\text{-N-CH}_2\text{-CH}$ and CH-NH_3), 4.32 (m, 1H, $\text{C}_7\text{-CH-NHCOCH}_3$), 6.44-6.46 (d, 1H, $\text{C}_{11}\text{-CH}$), 6.74 (s, 1H, $\text{C}_4\text{-CH}$), 6.87 (s, 1H, $\text{C}_8\text{-CH}$), 7.03-7.07 (d, 1H, $\text{C}_{12}\text{-CH}$, $J=11$ Hz), 8.19 (m, 3H, NH_3^+), 8.54 (d, 1H, NH-COCH_3)

^{13}C NMR (DMSO_d6 , 75.5 MHz): δ (ppm) 22.49 (+ve, $\underline{\text{C}}\text{H}_3$ -14), 28.39 (-ve, $\text{C}_5\text{-CH}_2$), 29.48 (-ve, $\underline{\text{C}}\text{H}_2\text{-C}_4'$), 36.48 (-ve, $\text{C}_6\text{-CH}_2$), 47.81 (-ve, $\underline{\text{C}}\text{H}_2\text{-C}_5'$), 49.37 (+ve, $\text{C}_7\text{-CH}$), 50.80 (+ve, $\underline{\text{C}}\text{H}$), 53.53 (-ve, $\underline{\text{C}}\text{H}_2$), 55.78 (+ve, $\text{C}_3\text{-CH}_3$), 60.52 (+ve, $\text{C}_2\text{-CH}_3$), 60.62 (+ve, $\text{C}_1\text{-CH}_3$), 107.65 (+ve, $\underline{\text{C}}\text{H-Ar-C}_4$), 110.86 (+ve, C_{11} , $\underline{\text{C}}\text{H-Ar}$), 125.50 (+ve, $\underline{\text{C}}\text{H-Ar}$, C8), 126.14 (absent), 128.43 (absent), 134.40 (absent), 135.94 (+ve, CH-Ar , C12), 140.69 (absent), 149.25 (absent), 150.44 (absent), 152.32 (absent), 153.67 (absent),

158.09, 158.54 (parts of quaternary form, COOH-CF₃, 168.39 (absent, C13, COO), 177.67 (absent, C-9, COO).

3.2.7 Synthesis of AM7 (Col-(R)-3-(aminopyrrolidine-TPP) {(5-(((R)-1-((S)-7-acetamido-1,2,3-trimethoxy-9-oxo-5,6,7,9-tetrahydrobenzo[α]heptalene-10-yl)pyrrolidine-3-yl)amino)-5-oxopentyl)triphenylphosphonium; bromide (AM7)

To a solution of AM6 (Col-(R)-3-(amino) Pyrrolidine-TFA) (0.150 g, 0.264 mmol) in DMF (1 ml) was added TPP (0.198 g, 0.448 mmol, 1.7 eq), PyBOP (0.26 g, 0.501 mmol, 1.9 eq), HOBt (0.0676 g, 0.501 mmol, 1.9 eq) and DIPEA (0.180 g, 1.39 mmol, 5.3 eq) in DMF (4 ml). The mixture was stirred at rt. After 24 h, the mixture was extracted with CHCl₃ and H₂O (1:1, 100 ml). The combined organic layers were dried over anhydrous Na₂SO₄, filtered and the solvent was concentrated *in vacuo* and air dried for 1 h. The residue was purified by silica gel column chromatography (chloroform, chloroform: methanol, 9:1). The desired fractions of product were combined, filtered, concentrated to dryness under reduced pressure and the residue was triturated with ether over an ice bath then in the fridge (4 °C) overnight and vacuum dried to give the title compound AM7 (Col-(R)-3-(aminopyrrolidine-TPP) (0.117 g, 50 %).

TLC (chloroform: methanol, 4: 1). R_f 0.91.

HRMS (ESI) m/z: 800.3699 (15%) (M+Na)⁺, 799.3667 (52%), 798.3634 (100 %) (M+H)⁺. Calcd for C₄₈H₅₃N₃O₆PBr 877.29; Found 798.3634.

¹H NMR (DMSO-*d*₆, 300 MHz): δ (ppm) 1.50-1.85 (m, 8H, OCOCH₂-CH₂-CH₂-CH₂-P, NHCO-CH₃, C₆-CH), 2.01-2.23 (m, 3H, C₆-CH, N-CH₂-CH₂), 2.34 (t, 2H, CH₂-C=O), 2.50 (m, 2H, C₅-CH₂), 3.02 (s, 9H, P-CH₂), 3.50 (s, 3H, C1-OCH₃), 3.60 (m, 2H, C10-N-CH₂-CH₂), 3.80 (s, 3H, C₃-OCH₃), 3.85 (s, 3H, C₂-OCH₃), 4.20 (m, 3H, C₁₀-N-CH₂-CH, CH-TPP), 4.39 (m, 1H, C₇-CH-NHCO), 6.35 (d, 1H, C₁₁-CH, J= 11 Hz), 6.71 (s, 1H, C₄-CH), 6.85 (s, 1H, C₈-CH), 7.00 (d, 1H, C₁₂-CH, J= 11 Hz), 7.80 (m, 15H, TPP), 8.15 (d, 1H, NHCO).

3.2.8 Synthesis of Colchicine-4-hydroxypiperidine-TPP {4-[1-(7-Acetylamino-1,2,3-trimethoxy-9-oxo-5,6,7,9-tetrahydro-benzo[α]heptalene-10-yl)-piperidin-4-yloxy-carbonyl]-butyl}-triphenyl-phosphonium; bromide} (AM8)

To a solution of colchicine-4-hydroxypiperidine (AM3) (0.13 g, 0.277 mmol) in dichloromethane (3 ml) was added TPP (0.196 g, 0.443 mmol, 1.6 eq) and DMAP (25 ng). To this mixture was added DCC (0.105 g, 0.443 mmol, 1.6 eq) in dichloromethane and stirred at rt. After 24 h, the mixture was extracted with CHCl_3 and H_2O (1:1, 100 ml). The combined organic layers were dried over Na_2SO_4 , filtered and the solvent was concentrated *in vacuo*. The residue was purified by silica gel column chromatography (chloroform: methanol, 9:1 and 4:1). The desired fractions of product were combined, filtered, concentrated to dryness under reduced pressure and the residue was triturated with ether to give desired title product colchicine-4-hydroxypiperidine-TPP (AM8) as a yellow solid (0.203 g; 90 %).

TLC (chloroform: methanol, 9: 1) R_f 0.11. HRMS (ESI) m/z : 815.3684 (16%) ($\text{M}+\text{Na}$)⁺, 814.3649 (52%), 813.3620 (100%) ($\text{M}+\text{H}$)⁺. Calcd for $[\text{C}_{49} \text{H}_{54} \text{N}_2 \text{O}_7]^+$ 892.29; found 813.3620.

^1H NMR ($\text{DMSO-}d_6$, 300 MHz): δ (ppm) 1.49-1.63 (m, 8H, $\text{OCOCH}_2\text{-CH}_2\text{-CH}_2\text{-CH}_2\text{-P}$), 1.84 (s, 4H, NHCO-CH_3 and $\text{C}_6\text{-CH}$), 2.00-2.04 (m, 2H, $\text{N-CH}_2\text{-CH}_2$), 2.22 (m, 1H, $\text{C}_6\text{-CH}$), 2.42 (t, 2H, $\text{CH}_2\text{-C=O}$), 2.51 (m, 2H, $\text{C}_5\text{-CH}_2$), 3.12-3.25 (m, 3H, $\text{N-CH}_2\text{-CH}_2$), 3.38-3.43 (m, 2H, $\text{CH}_2\text{-P}$), 3.52 (s, 3H, $\text{C}_1\text{-OCH}_3$), 3.64 (m, 4H, $\text{N-CH}_2 \times 2$), 3.78 (s, 3H, $\text{C}_3\text{-OCH}_3$), 3.83 (s, 3H, $\text{C}_2\text{-OCH}_3$), 4.28-4.36 (m, 1H, CH-OCO), 4.88 (m, 1H, $\text{C}_7\text{-CH-NH}$), 6.76 (s, 1H, $\text{C}_4\text{-CH}$), 6.88 (d, 1H, $\text{C}_{11}\text{-CH}$, $J=11$ Hz), 6.97 (s, 1H, $\text{C}_8\text{-CH}$), 7.04-7.08 (d, 1H, $\text{C}_{12}\text{-CH}$, $J=11$ Hz), 7.82 (m, 15H, TPP), 8.56 (d, 1H, NH-COCH_3 , $J=7$).

^{13}C NMR (DMSO_d_6 , 75.5 MHz): δ (ppm) 22.49 (+ve, $\text{C}_{14}\text{-CH}_3$), 24.43 (-ve, CH_2), 25.30 (-ve, CH_2), 30.35 (-ve, CH_2), 32.81 (-ve, CH_2), 33.31 (-ve, CH_2), 36.11 (-ve, CH_2),

45.25 (-ve, $\underline{\text{C}}\text{H}_2$), 107.70 (+ve, $\underline{\text{C}}\text{H-Ar-C4}$), 117.88 (+ve, C11, $\underline{\text{C}}\text{H-Ar}$), 128.41 (+ve, $\underline{\text{C}}\text{H-Ar}$, C8), 130.14-130.31 (ortho, meta, $\underline{\text{C}}\text{H-TPP}$), 133.46-133.60 (ortho, meta, $\underline{\text{C}}\text{H-TPP}$), 134.33 (+ve, $\underline{\text{C}}\text{H-TPP}$, para), 134.92 (+ve, $\underline{\text{C}}\text{H-C12}$), 140.68 (absent), 149.03 (absent), 150.44 (absent).

3.2.9 Synthesis of Colchicine-(R)-3-Pyrrolidinol-TPP {4-[1-(7-Acetylamino-1,2,3-trimethoxy-9-oxo-5,6,7,9-tetrahydro-benzo[α]heptalene-10-yl)-pyrrolidin-3-yloxycarbonyl]-butyl}-trphenyl-phosphonium; bromide} (AM9)

To a solution of Colchicine-(R)-3-Pyrrolidinol (AM4) (0.145 g, 0.319 mmol) in dichloromethane (3 ml) was added TPP (0.183 g, 0.414 mmol, 1.3eq) and DMAP (25 ng). To this mixture was added DCC (0.098 g, 0.478 mmol, 1.5 eq) in dichloromethane and stirred at rt. After 24 h, the mixture was extracted with CHCl_3 and H_2O (1:1, 100 ml). The combined organic layers were dried over anhydrous Na_2SO_4 , filtered and the solvent was concentrated *in vacuo*. The residue was purified by silica gel column chromatography (dichloromethane: methanol, 9:1 and 4:1). The desired fractions of product were combined, filtered, concentrated to dryness under reduced pressure and the residue was triturated with ether to give the desired title product colchicine-(R)-3-pyrrolidinol-TPP (AM9) as a yellow solid (0.270 g; 96 %).

TLC (chloroform: methanol, 9: 1). R_f 0.15.

HRMS (ESI) m/z : 801.3525 (14%) ($\text{M}+\text{Na}$)⁺, 800.3490 (52%), 799.3461 (100%) ($\text{M}+\text{H}$)⁺. Calcd for $[\text{C}_{48} \text{H}_{52} \text{N}_2 \text{O}_7]^+$ 878.27; found 799.3461.

^1H NMR ($\text{DMSO-}d_6$, 300 MHz): δ (ppm) 1.59 (m, 2H, $\text{COCH}_2\text{-CH}_2\text{-CH}_2\text{-P}$), 1.73 (m, 2H, $\text{OCOCH}_2\text{-CH}_2\text{-CH}_2\text{-P}$), 1.85 (s, 4H, NHCO-CH_3 and $\text{C}_6\text{-CH}$), 2.14-2.22 (m, 3H, $\text{C}_6\text{-CH}$ and $\text{N-CH}_2\text{-CH}_2$), 2.40 (t, 2H, $\text{CH}_2\text{-C=O}$), 2.51 (m, 2H, $\text{C}_5\text{-CH}_2$), 3.34 (s, 2H, P-CH_2), 3.49 (s, 3H, $\text{C}_1\text{-OCH}_3$), 3.56-3.66 (m, 4H, 2 x N-CH_2), 3.78 (s, 3H, $\text{C}_3\text{-OCH}_3$), 3.83 (s, 4H, $\text{C}_2\text{-OCH}_3$), 4.28-4.37 (m, 1H $\text{C}_7\text{-CH-NH}$), 5.27 (s, 1H, CH-OCO), 6.39-6.43 (d, 1H, $\text{C}_{11}\text{-CH}$, $J=11$ Hz), 6.74 (s, 1H, $\text{C}_4\text{-CH}$), 6.83 (s, 1H, $\text{C}_8\text{-CH}$), 6.99-

7.03 (d, 1H, C₁₂-CH, J= 11 Hz), 7.76 -7.93 (m, 15H, TPP), 8.50-8.52 (d, 1H, NH-COCH₃).

3.3 Distribution coefficient measurement

Materials

- PBS buffer (pH 7.4):
Phosphate buffer 0.01M,
Potassium chloride 0.0027 M and
Sodium chloride 0.137 M),
- Octanol; 3 mL
- Quartz cuvette
- Test samples in DMSO: Colchicine-Prolinol (AM1) (1 mg ml⁻¹; 2134 μM) Colchicine-Prolinol-TPP (AM2) (1 mg mL⁻¹; 1227 μM); Colchicine-4-hydroxypiperidine (AM3) (1 mg ml⁻¹; 2134 μM); Colchicine-(*R*)-3-Pyrrolidinol (AM4) (1 mg ml⁻¹; 2200 μM); Colchicine-(*R*)-3-(Boc-aminopyrrolidine (AM5) (1 mg ml⁻¹; 1806 μM); Col-(*R*)-3-aminopyrrolidine-TFA (AM6) (1 mg ml⁻¹; 1762 μM); Col-(*R*)-3-aminopyrrolidine-TPP (AM7) (1 mg ml⁻¹; 1137 μM) Colchicine-4-hydroxypiperidine-TPP (AM8) (1 mg ml⁻¹; 1118 μM); Colchicine-(*R*)-3-Pyrrolidinol-TPP (AM9) (1 mg ml⁻¹; 1136 μM).
- Beckman DU800 Spectrophotometer.

3.3.1 Preparation of saturated solutions

PBS buffer (200 mL) was prepared by dissolving a PBS tablet in deionized water. Octanol (30 mL) and PBS buffer (30 mL) were combined and shaken for 24 h on a vortex. Layers of octanol and PBS buffer were separated in separating funnel.

3.3.2 Preparation of calibration curves

Stock solutions of the test sample compounds were prepared in DMSO Different concentrations of the test compounds were prepared from the 1 mg mL⁻¹ stock

solutions by diluting with either octanol saturated phosphate buffer and phosphate buffer saturated octanol to concentrations of 5, 10, 15, 20 and 25 μM for each test compound. Absorbance values were recorded at the maximum wavelength for each compound (between 0 and 0.7) in accordance with the Beer Lambert Law, by using a Beckman DU800 Spectrophotometer. Wavelength range and scanning speed were set at 320-500 nm and 1200 nm/min respectively. Each experiment was performed in triplicate $n=3$.

3.3.3 Distribution coefficient methods

Samples of each compound (1 mg) in triplicate were suspended in octanol (pre-saturated with PBS for 24 h) (900 μL) and in PBS buffer (pre-saturated with octanol for 24 h) (900 μL), mixed by vortex and shaken for 24 h at room temperature until dissolved, then the two layers were separated by centrifugation at 2000 g for 5 min. Each of the test samples were diluted as follows with either octanol or PBS to give a final volume of 3000 μL in a cuvette: for AM1, 30 μL of octanol layer and 800 μL of aqueous layer were removed and separately diluted to give 3000 μL (final volume of cuvette); for AM2, 30 μL of octanol layer and 400 μL of aqueous layer were removed and diluted to 3000 μL ; for AM3, 30 μL of octanol layer and 300 μL of aqueous layer; for AM4, 30 μL of octanol layer and 200 μL of aqueous layer; for AM5, 40 μL of octanol and 750 μL of aqueous layer; for AM6, 50 μL of octanol and 50 μL of aqueous layer; for AM7, 160 μL of octanol layer and 800 μL of aqueous layer; for AM8, 70 μL of octanol layer and 700 μL of aqueous layer and for AM9, 30 μL of octanol and 400 μL of aqueous layer. The absorbances were measured at maximum wavelength of 369 nm (AM1), 372 nm (AM2), 378 nm (AM3), 368 nm (AM4), 368 nm (AM5), 367 nm (AM6), 369 nm (AM7), 375 nm (AM8) and 371 nm (AM9) and the calibration curves used to determine the concentration in each layer. Distribution coefficients for different test compounds were calculated by taking the LOG of the concentration in octanol divided by the concentration in the aqueous phase with the log D equation given below.

$$\log D_{\text{oct/water}} = \log \left(\frac{[\text{solute}]_{\text{octanol}}}{[\text{solute}]_{\text{ionised water}} + [\text{solute}]_{\text{neutral water}}} \right)$$

3.4 Compound Lethality Treatments on *C. elegans* worms

3.4.1 Materials and Methods

3.4.1.1 *C. elegans* maintenance

C. elegans (wild-type, N2 strain) were obtained from the *Caenorhabditis* genetics centre, University of Minnesota. The *C. elegans* worms were kept on NGM plates seeded with worm food *Escherichia coli* OP50 at 20 °C in 60 mm or 100 mm diameter petri dishes from VWR, UK and Thermo Fischer Scientific, UK respectively. OP50, *E. coli* was obtained from Leibniz Institute DMSZ- German collection of microorganisms and cell cultures. The strain of nematodes was maintained by regular transfer of nematodes by chunking into fresh NGM plates seeded with OP50.

C. elegans at L1 and L2 stages were also stored at -80 °C in the freezer by moving starved stages (L1 and L2) into vials containing soft agar as freezing solution.

3.4.1.2 Synchronization

Synchronization protocol as described by Sulston & Hodgkin (1988) was adapted for the research work. Mixed culture and synchronized populations were prepared for the lethality experiments. L4 stage worms were specifically used for the assays. All the treatments were carried out in S medium which is standard liquid medium for the worm maintenance. Age specific worms (L4) were maintained at 20 °C in the incubator for 4 or 24 hours with the food source *E. coli* OP50.

3.4.2 Toxic assessment of AM series as novel anthelmintic agents

3.4.2.1 Drug Treatments

The novel potential anthelmintic agents AM1 (Colchicine-Prolinol) and AM2 (Col-Prolinol-TPP) were used as the main drugs in the worm lethality assay.

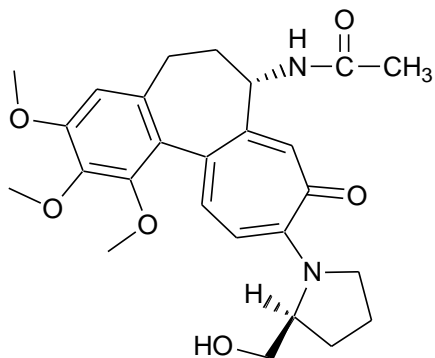
3.4.3 Anthelmintic worm viability assay

A range of different concentrations of colchicine (sigma, Aldrich), AM1 (col-Prolinol), AM2 (Col-Prolinol-TPP), TPP, Levamisole from 0 – 100 μ M were used for the lethality or worm viability assay. Negative control was L stage worms in S medium. DMSO 2%, 5% was another negative control used and was also the solvent for drug suspensions AM1 and AM2. 24-well plates sets were used for the assay containing worms and their food was exposed to all the drug treatments in the final volume of 1 ml. The exposure time for all the treatments was from 4 h to 24 h at the start then up to 72 h at 20 °C in the incubator, performed in staggered time points. Experiments were repeated three times, (n= 3). After the incubation time, results were read from samples in the well one by one at staggered time points, and percentage survival was calculated and plotted in a graph.

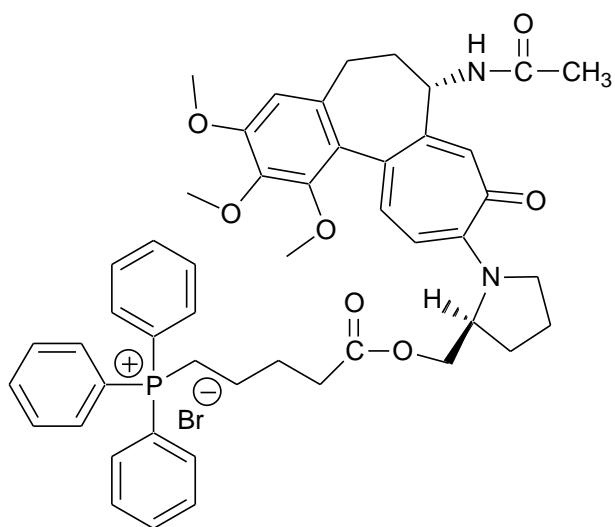
4 Chapter

4.1 Structure Library

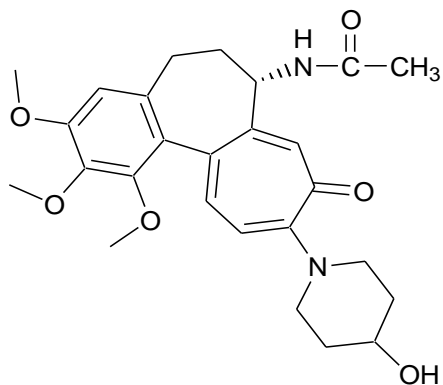
4.1.1 Structure of AM1



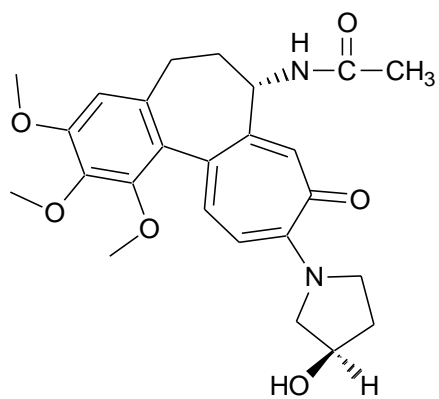
4.1.2 Structure of AM2



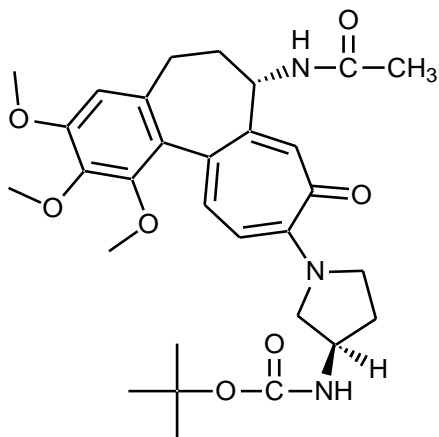
4.1.3 Structure of AM3:



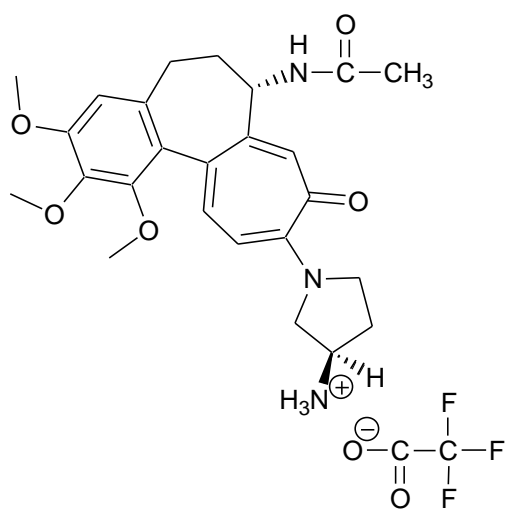
4.1.4 Structure of AM4



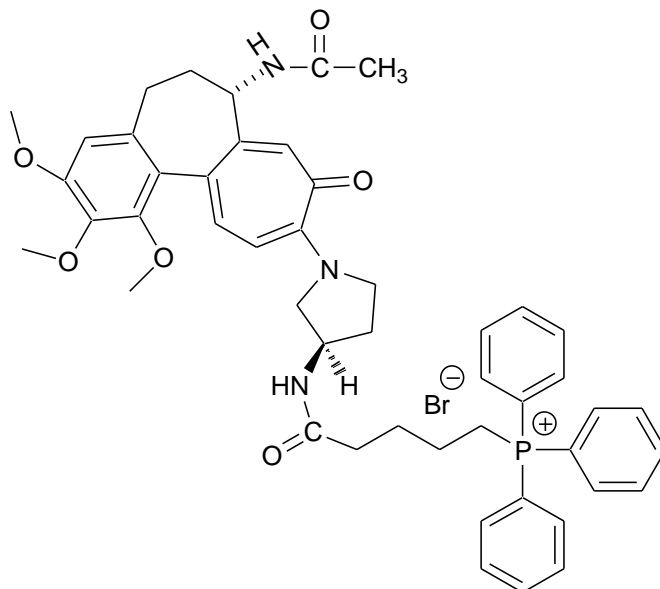
4.1.5 Structure of AM5



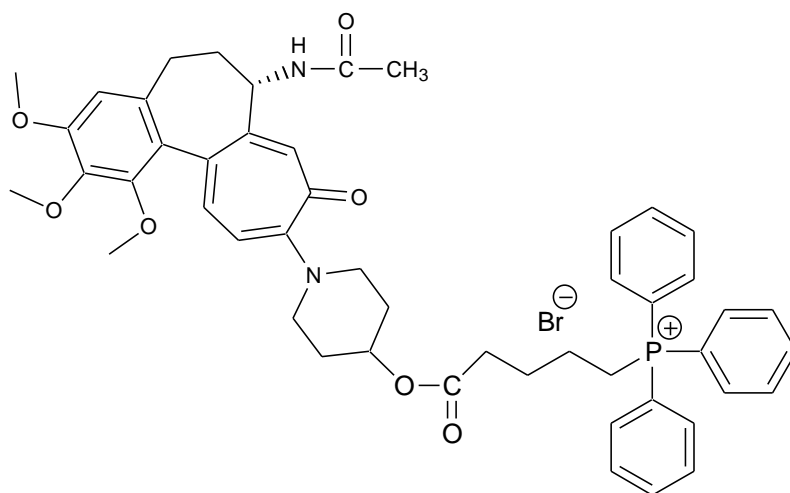
4.1.6 Structure of AM6



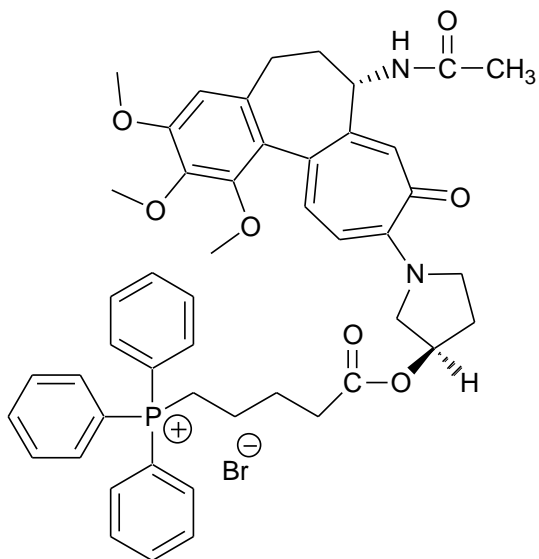
4.1.7 Structure of AM7:



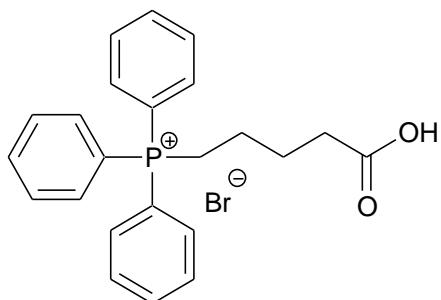
4.1.8 Structure of AM8:



4.1.9 Structure of AM9

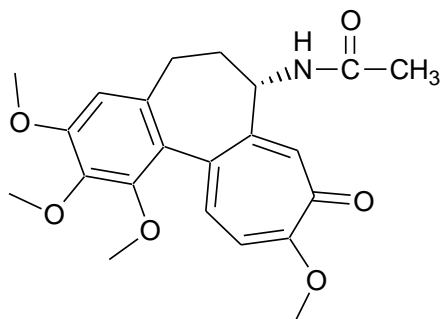


4.1.10 Structure of TPP



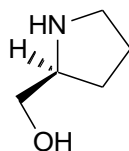
(4-Carboxy-butyl)-triphenyl-phosphonium; bromide

4.1.11 Structure of Colchicine (Col)

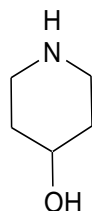


N-(1,2,3,10-Tetramethoxy-9-oxo-5,6,7,9-tetrahydro-benzo[*a*]heptalen-7-yl)-acetamide

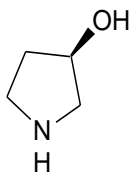
4.1.12 Structure of Prolinol (Pro)



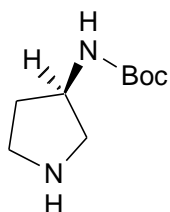
4.1.13 Structure of 4-hydroxypiperidine



4.1.14 Structure of *R*-3-pyrrolidinol



4.1.15 Structure of (*R*)-3-Boc-aminopyrrolidine



References

- Abebe, R., Abunna, F., Berhane, M., Mekuria, S., Megersa, B., Regassa, A., 2010. Fasciolosis: Prevalence, financial losses due to liver condemnation and evaluation of a simple sedimentation diagnostic technique in cattle slaughtered at Hawassa. *Ethiop. Vet. J.* 14, 39–51. <https://doi.org/10.4314/evj.v14i1.63868>
- Akhmanova, A., Steinmetz, M.O., 2015. Control of microtubule organization and dynamics: Two ends in the limelight. *Nat. Rev. Mol. Cell Biol.* 16, 711–726. <https://doi.org/10.1038/nrm4084>
- Aleyasin, H., Karuppagounder, S.S., Kumar, A., Sleiman, S., Basso, M., Ma, T., Siddiq, A., Chinta, S.J., Brochier, C., Langley, B., Haskew-Layton, R., Bane, S.L., Riggins, G.J., Gazaryan, I., Starkov, A.A., Andersen, J.K., Ratan, R.R., 2015. Antihelminthic Benzimidazoles Are Novel HIF Activators That Prevent Oxidative Neuronal Death via Binding to Tubulin. *Antioxid. Redox Signal.* 22, 121–134. <https://doi.org/10.1089/ars.2013.5595>
- Andrés, A., Rosés, M., Ràfols, C., Bosch, E., Espinosa, S., Segarra, V., Huerta, J.M., 2015. Setup and validation of shake-flask procedures for the determination of partition coefficients (log D) from low drug amounts. *Eur. J. Pharm. Sci.* 76, 181–191. <https://doi.org/10.1016/j.ejps.2015.05.008>
- Atkinson, H.J., Lilley, C.J., Urwin, P.E., 2012. Strategies for transgenic nematode control in developed and developing world crops. *Curr. Opin. Biotechnol.* 23, 251–256. <https://doi.org/10.1016/J.COPBIO.2011.09.004>
- Atkinson, H.J., Lilley, C.J., Urwin, P.E., 2012. Strategies for transgenic nematode control in developed and developing world crops. *Curr. Opin. Biotechnol.* 23, 251–256. <https://doi.org/10.1016/j.copbio.2011.09.004>
- Bachmann, F., Burger, K., Lane, H., 2015. BAL101553 (prodrug of BAL27862): The spindle assembly checkpoint is required for anticancer activity. *Cancer Res.* 75, 3789–3789.
- Balaban, R.S., Nemoto, S., Finkel, T., 2005. Mitochondria, oxidants, and aging. *Cell*

120, 483–495. <https://doi.org/10.1016/j.cell.2005.02.001>

Battogtokh, G., Choi, Y.S., Kang, D.S., Park, S.J., Shim, M.S., Huh, K.M., Cho, Y.-Y., Lee, J.Y., Lee, H.S., Kang, H.C., 2018. Mitochondria-targeting drug conjugates for cytotoxic, anti-oxidizing and sensing purposes: current strategies and future perspectives. *Acta Pharm. Sin. B* 8, 862–880. <https://doi.org/10.1016/J.APSB.2018.05.006>

Berezikov, E., 2004. Homologous gene targeting in *Caenorhabditis elegans* by biolistic transformation. *Nucleic Acids Res.* 32, 40e–40. <https://doi.org/10.1093/nar/gnh033>

Besier, R.B., Kahn, L.P., Sargison, N.D., Van Wyk, J.A., 2016. The Pathophysiology, Ecology and Epidemiology of *Haemonchus contortus* Infection in Small Ruminants. *Adv. Parasitol.* 93, 95–143. <https://doi.org/10.1016/bs.apar.2016.02.022>

Besier, R.B., Love, S.C.J., 2003. Anthelmintic resistance in sheep nematodes in Australia: The need for new approaches. *Aust. J. Exp. Agric.* 43, 1383–1391. <https://doi.org/10.1071/EA02229>

Bhal, S.K., 2007. Application Note: Lipophilicity Descriptors: Understanding When to Use LogP and LogD, ACD/Labs PhysChem Software Application Notes. Available online at: http://www.acdlabs.com/resources/knowledgebase/app_notes/physchem/ (accessed 09/09/15). <https://doi.org/2019>

Bhattacharya, S., Das, A., Datta, S., Ganguli, A., Chakrabarti, G., 2016. Colchicine induces autophagy and senescence in lung cancer cells at clinically admissible concentration: potential use of colchicine in combination with autophagy inhibitor in cancer therapy. *Tumor Biol.* 37, 10653–10664. <https://doi.org/10.1007/s13277-016-4972-7>

Brenner, S., 1974. The genetics of *Caenorhabditis elegans*. *Genetics* 77, 71–94. <https://doi.org/10.1002/cbic.200300625>

Broeks, A., Janssen, H.W.R.M., Calafat, J., Plasterk, R.H.A., 1995. A P-glycoprotein protects *Caenorhabditis elegans* against natural toxins. *Parasitol. Today* 11, 243.

[https://doi.org/10.1016/0169-4758\(95\)80199-5](https://doi.org/10.1016/0169-4758(95)80199-5)

Brophy, P.M., MacKintosh, N., Morphey, R.M., 2012. Anthelmintic metabolism in parasitic helminths: Proteomic insights. *Parasitology* 139, 1205–17. <https://doi.org/10.1017/S003118201200087X>

Bruinsma, J.J., Schneider, D.L., Davis, D.E., Kornfeld, K., 2008. Identification of mutations in *Caenorhabditis elegans* that cause resistance to high levels of dietary zinc and analysis using a genomewide map of single nucleotide polymorphisms scored by pyrosequencing. *Genetics* 179, 811–28. <https://doi.org/10.1534/genetics.107.084384>

Buckingham, S.D., Partridge, F.A., Sattelle, D.B., 2014. Automated, high-throughput, motility analysis in *Caenorhabditis elegans* and parasitic nematodes: Applications in the search for new anthelmintics. *Int. J. Parasitol. Drugs Drug Resist.* 4, 226–232. <https://doi.org/10.1016/j.ijpddr.2014.10.004>

Burns, R.J., Smith, R.A.J., Murphy, M.P., 1995. Synthesis and Characterization of Thiobutyltriphenylphosphonium Bromide, a Novel Thiol Reagent Targeted to the Mitochondrial Matrix. *Arch. Biochem. Biophys.* 322, 60–68. <https://doi.org/10.1006/ABBI.1995.1436>

Cacciatore, I., Ciulla, M., Marinelli, L., Eusepi, P., Di Stefano, A., 2018. Advances in prodrug design for Parkinson's disease. *Expert Opin. Drug Discov.* 13, 295–305. <https://doi.org/10.1080/17460441.2018.1429400>

Campbell, W.C., 1990. Benzimidazoles: Veterinary uses. *Parasitol. Today* 6, 130–133. [https://doi.org/10.1016/0169-4758\(90\)90231-R](https://doi.org/10.1016/0169-4758(90)90231-R)

Cancela, M., Ruétalo, N., Dell'Oca, N., da Silva, E., Smircich, P., Rinaldi, G., Roche, L., Carmona, C., Alvarez-Valín, F., Zaha, A., Tort, J.F., 2010. Survey of transcripts expressed by the invasive juvenile stage of the liver fluke *Fasciola hepatica*. *BMC Genomics* 11, 1–14. <https://doi.org/10.1186/1471-2164-11-227>

Cassada, R.C., Russell, R.L., 1975. The dauerlarva, a post-embryonic developmental variant of the nematode *Caenorhabditis elegans*. *Dev. Biol.* 46, 326–342. [https://doi.org/10.1016/0012-1606\(75\)90109-8](https://doi.org/10.1016/0012-1606(75)90109-8)

Castro, G.A., 1996. *Helminths: Structure, Classification, Growth, and Development*,

in: Baron, S. (Ed.), *Medical Microbiology*. University of Texas Medical Branch at Galveston, Galveston (TX), p. 86. <https://doi.org/NBK8282> [bookaccession]

Cheng, G., Zielonka, J., McAllister, D., Hardy, M., Ouari, O., Joseph, J., Dwinell, M.B., Kalyanaraman, B., 2015. Antiproliferative effects of mitochondria-targeted cationic antioxidants and analogs: Role of mitochondrial bioenergetics and energy-sensing mechanism. *Cancer Lett.* 365, 96–106. <https://doi.org/10.1016/J.CANLET.2015.05.016>

Cocco, G., Chu, D.C.C., Pandolfi, S., 2010. Colchicine in clinical medicine. A guide for internists. *Eur. J. Intern. Med.* 21, 503–508. <https://doi.org/10.1016/J.EJIM.2010.09.010>

Coulter, C. V., Kelso, G.F., Lin, T.-K., Smith, R.A.J., Murphy, M.P., 2000. Mitochondrially targeted antioxidants and thiol reagents. *Free Radic. Biol. Med.* 28, 1547–1554. [https://doi.org/10.1016/S0891-5849\(00\)00255-0](https://doi.org/10.1016/S0891-5849(00)00255-0)

Culetto, E., 2000. A role for *Caenorhabditis elegans* in understanding the function and interactions of human disease genes. *Hum. Mol. Genet.* 9, 869–77. <https://doi.org/10.1093/hmg/9.6.869>

Curcio, M., Bradke, F., 2015. Microtubule Organization in the Axon: TRIM46 Determines the Orientation. *Neuron* 88, 1072–1074. <https://doi.org/10.1016/j.neuron.2015.12.006>

Dalbeth, N., Lauterio, T.J., Wolfe, H.R., 2014. Mechanism of action of colchicine in the treatment of gout. *Clin. Ther.* 36, 1465–79. <https://doi.org/10.1016/j.clinthera.2014.07.017>

De Nollin, S., Borgers, M., 1975. Scanning electron microscopy of *Candida albicans* after in vitro treatment with miconazole. *Antimicrob. Agents Chemother.* 7, 705–711. <https://doi.org/10.1128/AAC.7.5.704>

Demeler, J., Krüger, N., Krücken, J., von der Heyden, V.C., Ramünke, S., Küttler, U., Miltsch, S., López Cepeda, M., Knox, M., Vercruyssen, J., Geldhof, P., Harder, A., von Samson-Himmelstjerna, G., 2013. Phylogenetic Characterization of β -Tubulins and Development of Pyrosequencing Assays for Benzimidazole Resistance in Cattle Nematodes. *PLoS One* 8, e70212.

<https://doi.org/10.1371/journal.pone.0070212>

Diawara, L., Traoré, M.O., Badji, A., Bissan, Y., Doumbia, K., Goita, S.F., Konaté, L., Mounkoro, K., Sarr, M.D., Seck, A.F., Toé, L., Tourée, S., Remme, J.H.F., 2009. Feasibility of onchocerciasis elimination with ivermectin treatment in endemic foci in Africa: First evidence from studies in Mali and Senegal. *PLoS Negl. Trop. Dis.* 3, e497. <https://doi.org/10.1371/journal.pntd.0000497>

Donald L Riddle, 1997. *C. elegans* II. 2nd edition, 2nd ed, Cold Spring Harbor Laboratory Press. <https://doi.org/10.1186/1743-422X-2-34>

Dong, M., Liu, F., Zhou, H., Zhai, S., Yan, B., 2016. Novel natural product-and privileged scaffold-based tubulin inhibitors targeting the colchicine binding site. *Molecules* 21, pii: E1375. <https://doi.org/10.3390/molecules21101375>

Driscoll, M., Dean, E., Reilly, E., Bergholz, E., Chalfie, M., 1989. Genetic and molecular analysis of a *Caenorhabditis elegans* ??-Tubulin that conveys benzimidazole sensitivity. *J. Cell Biol.* 109, 2993–3003. <https://doi.org/10.1083/jcb.109.6.2993>

El-Kamel, A.H., Abdel-Aziz, A.A.-M., Fatani, A.J., El-Subbagh, H.I., 2008. Oral colon targeted delivery systems for treatment of inflammatory bowel diseases: synthesis, in vitro and in vivo assessment. *Int. J. Pharm.* 358, 248–55. <https://doi.org/10.1016/j.ijpharm.2008.04.021>

Epe, C., Kaminsky, R., 2013. New advancement in anthelmintic drugs in veterinary medicine. *Trends Parasitol.* 29, 129–134. <https://doi.org/10.1016/J.PT.2013.01.001>

Fairweather, I., Fairweather, I., 2005. Triclabendazole: new skills to unravel an old(ish) enigma. *J. Helminthol.* 79, 227–234. <https://doi.org/10.1079/JOH2005298>

Fennell, B., Naughton, J., Barlow, J., Brennan, G., Fairweather, I., Hoey, E., McFerran, N., Trudgett, A., Bell, A., 2008. Microtubules as antiparasitic drug targets. *Expert Opin. Drug Discov.* 3, 501–518. <https://doi.org/10.1517/17460441.3.5.501>

Ferreira, L.G., Dos Santos, R.N., Oliva, G., Andricopulo, A.D., 2015. Molecular docking and structure-based drug design strategies. *Molecules* 20, 13384–13421. <https://doi.org/10.3390/molecules200713384>

- Finichiu, P.G., James, A.M., Larsen, L., Smith, R.A.J., Murphy, M.P., 2013. Mitochondrial accumulation of a lipophilic cation conjugated to an ionisable group depends on membrane potential, pH gradient and pK_a: Implications for the design of mitochondrial probes and therapies. *J. Bioenerg. Biomembr.* 45, 165–173. <https://doi.org/10.1007/s10863-012-9493-5>
- Fournier-Dit-Chabert, J., Vinader, V., Santos, A.R., Redondo-Horcajo, M., Dreneau, A., Basak, R., Cosentino, L., Marston, G., Abdel-Rahman, H., Loadman, P.M., Shnyder, S.D., Díaz, J.F., Barasoain, I., Falconer, R.A., Pors, K., 2012. Synthesis and biological evaluation of colchicine C-ring analogues tethered with aliphatic linkers suitable for prodrug derivatisation. *Bioorganic Med. Chem. Lett.* 22, 7693–7696. <https://doi.org/10.1016/j.bmcl.2012.09.104>
- Gardner, M.K., Zanic, M., Howard, J., 2013. Microtubule catastrophe and rescue. *Curr. Opin. Cell Biol.* 25, 14–22. <https://doi.org/10.1016/j.ceb.2012.09.006>
- Gasser, R.B., Schwarz, E.M., Korhonen, P.K., Young, N.D., 2016. Understanding *Haemonchus contortus* Better Through Genomics and Transcriptomics. *Adv. Parasitol.* 93, 519–567. <https://doi.org/10.1016/bs.apar.2016.02.015>
- Getachew T, Dorchies P, Jacquiet P, 2007. Mise au point trend and challenges in the effective and sustainable control of *haemonchus contortus* infection in sheep. *Parasite* 14, 3–14. <https://doi.org/10.1051/parasite/2007141003>
- Guedes, I.A., de Magalhães, C.S., Dardenne, L.E., 2014. Receptor-ligand molecular docking. *Biophys. Rev.* 6, 75–87. <https://doi.org/10.1007/s12551-013-0130-2>
- Guggisberg, A.M., Amthor, R.E., Odom, A.R., 2014. Isoprenoid biosynthesis in *Plasmodium falciparum*. *Eukaryot. Cell* 13, 1348–59. <https://doi.org/10.1128/EC.00160-14>
- Halton, D.W., 2004. Microscopy and the helminth parasite. *Micron* 35, 361–390. <https://doi.org/10.1016/j.micron.2003.12.001>
- Hamada, Y., 2017. Recent progress in prodrug design strategies based on generally applicable modifications. *Bioorg. Med. Chem. Lett.* 27, 1627–1632. <https://doi.org/10.1016/j.bmcl.2017.02.075>
- Hamada, Y., 2016. Novel prodrugs with a spontaneous cleavable guanidine moiety.

- Hardy, M., Poulh s, F., Rizzato, E., Rockenbauer, A., Banaszak, K., Karoui, H., Lopez, M., Zielonka, J., Vasquez-Vivar, J., Sethumadhavan, S., Kalyanaraman, B., Tordo, P., Ouari, O., 2014. Mitochondria-targeted spin traps: Synthesis, superoxide spin trapping, and mitochondrial uptake. *Chem. Res. Toxicol.* 27, 1155–1165. <https://doi.org/10.1021/tx500032e>
- Hausen, M.A., Menna-Barreto, R.F.S., Lira, D.C., de Carvalho, L., Barbosa, H.S., 2011. Synergic effect of metronidazole and pyrantel pamoate on *Giardia lamblia*. *Parasitol. Int.* 60, 54–58. <https://doi.org/10.1016/j.parint.2010.10.003>
- Hinderliter, P., Saghir, S.A., 2014. Pharmacokinetics, in: *Encyclopedia of Toxicology: Third Edition*. pp. 849–855. <https://doi.org/10.1016/B978-0-12-386454-3.00419-X>
- Horio, T., Murata, T., Murata, T., 2014. The role of dynamic instability in microtubule organization. *Front. Plant Sci.* 5, 511. <https://doi.org/10.3389/fpls.2014.00511>
- Horton, J., 2003. Global anthelmintic chemotherapy programs: Learning from history. *Trends Parasitol.* 19, 405–409. [https://doi.org/10.1016/S1471-4922\(03\)00171-5](https://doi.org/10.1016/S1471-4922(03)00171-5)
- Hotez, P.J., Brindley, P.J., Bethony, J.M., King, C.H., Pearce, E.J., Jacobson, J., 2008. Helminth infections: the great neglected tropical diseases. *J. Clin. Invest.* 118, 1311–1321. <https://doi.org/10.1172/JCI34261>
- Hotez, P.J., Molyneux, D.H., Fenwick, A., Ottesen, E., Ehrlich Sachs, S., Sachs, J.D., 2006. Incorporating a rapid-impact package for neglected tropical diseases with programs for HIV/AIDS, tuberculosis, and malaria. *PLoS Med.* 3, e102. <https://doi.org/10.1371/journal.pmed.0030102>
- Howard, B., 2011. Ivermectin, in: *XPharm: The Comprehensive Pharmacology Reference*. pp. 1–5. <https://doi.org/10.1016/B978-008055232-3.61972-5>
- Jameson, V.J.A., Cochem , H.M., Logan, A., Hanton, L.R., Smith, R.A.J., Murphy, M.P., 2015. Synthesis of triphenylphosphonium vitamin E derivatives as mitochondria-targeted antioxidants. *Tetrahedron* 71, 8444–8453. <https://doi.org/10.1016/j.tet.2015.09.014>
- Janke, C., 2014. The tubulin code: Molecular components, readout mechanisms,

- functions. *J. Cell Biol.* 206, 461–472. <https://doi.org/10.1083/jcb.201406055>
- Jordan, M.A., Wilson, L., 2004. Microtubules as a target for anticancer drugs. *Nat. Rev. Cancer* 4, 253–265. <https://doi.org/10.1038/nrc1317>
- Kaletta, T., Hengartner, M.O., 2006a. Finding function in novel targets: *C. elegans* as a model organism. *Nat. Rev. Drug Discov.* 5, 387–98. <https://doi.org/10.1038/nrd2031>
- Kaletta, T., Hengartner, M.O., 2006b. Finding function in novel targets: *C. elegans* as a model organism. *Nat. Rev. Drug Discov.* 5, 387–399. <https://doi.org/10.1038/nrd2031>
- Kaplan, R.M., 2014. SHEEP Dewormer Chart [WWW Document]. URL www.acsrpc.org (accessed 1.30.19).
- Kaplan, R.M., 2004. Drug resistance in nematodes of veterinary importance: A status report. *Trends Parasitol.* 20, 477–481. <https://doi.org/10.1016/j.pt.2004.08.001>
- Kaplan, R.M., 2004. Drug resistance in nematodes of veterinary importance: A status report. *Trends Parasitol.* 20, 477–481. <https://doi.org/10.1016/j.pt.2004.08.001>
- Karbowski, J., Cronin, C.J., Seah, A., Mendel, J.E., Cleary, D., Sternberg, P.W., 2006. Conservation rules, their breakdown, and optimality in *Caenorhabditis sinusoidal* locomotion. *J. Theor. Biol.* 242, 652–669. <https://doi.org/10.1016/j.jtbi.2006.04.012>
- Kaufman, E.J., Miska, E.A., 2010. The microRNAs of *Caenorhabditis elegans*. *Semin. Cell Dev. Biol.* 21, 728–737. <https://doi.org/10.1016/j.semcdb.2010.07.001>
- Kenyon, C., 1988. The nematode *Caenorhabditis elegans*. *Science* (80-.). 240, 1448–1453. <https://doi.org/10.1126/science.3287621>
- Kezic, A., Spasojevic, I., Lezaic, V., Bajcetic, M., 2016. Mitochondria-Targeted Antioxidants: Future Perspectives in Kidney Ischemia Reperfusion Injury. *Oxid. Med. Cell. Longev.* 2016, 1–12. <https://doi.org/10.1155/2016/2950503>
- Kholod, Y., Hoag, E., Muratore, K., Kosenkov, D., 2018. Computer-Aided Drug Discovery: Molecular Docking of Diminazene Ligands to DNA Minor Groove. *J. Chem. Educ.* 95, 882–887. <https://doi.org/10.1021/acs.jchemed.7b00989>

- Kim, Y.E., Remme, J.H.F., Steinmann, P., Stolk, W.A., ROUNGOU, J.B., Tediosi, F., 2015. Control, Elimination, and Eradication of River Blindness: Scenarios, Timelines, and Ivermectin Treatment Needs in Africa. *PLoS Negl. Trop. Dis.* 9, e0003777. <https://doi.org/10.1371/journal.pntd.0003664>
- Kreston, R., 2014. The Fluke That Thwarted an Invasion - Body Horrors [WWW Document]. Discover. URL <http://blogs.discovermagazine.com/bodyhorrors/2014/09/30/fluke-china-schistosoma/#.XDHXN1X7TIU> (accessed 1.6.19).
- Kyelem, D., Fischer, P.U., Brattig, N.W., 2011. The diagnostics and control of neglected tropical helminth diseases. *Acta Trop.* 120, 3–5. <https://doi.org/10.1016/j.actatropica.2011.04.001>
- Labouesse, M., 2003. *Caenorhabditis elegans*. *Medecine/Sciences* 341–354. <https://doi.org/10.1016/B978-0-12-802147-7.00026-7>
- Lacey, E., 1988. The role of the cytoskeletal protein, tubulin, in the mode of action and mechanism of drug resistance to benzimidazoles. *Int. J. Parasitol.* 18, 885–936. [https://doi.org/10.1016/0020-7519\(88\)90175-0](https://doi.org/10.1016/0020-7519(88)90175-0)
- Lalchandama, K., Lalchandama, K., 2010. Anthelmintic resistance: the song remains the same 10, 111–122.
- Lamitina, S.T., 2004. Adaptation of the nematode *Caenorhabditis elegans* to extreme osmotic stress. *AJP Cell Physiol.* 286, C785-791. <https://doi.org/10.1152/ajpcell.00381.2003>
- Levine, N.D., 1980. Nematode parasites of domestic animals and man. *Nematode parasites Domest. Anim. man.* 59, 1772.
- Levy, B., Perez, P., Perny, J., Thivillier, C., Gerard, A., 2011. Comparison of norepinephrine-dobutamine to epinephrine for hemodynamics, lactate metabolism, and organ function variables in cardiogenic shock. A prospective, randomized pilot study. *Crit. Care Med.* 39, 450–455. <https://doi.org/10.1097/CCM.0b013e3181ffe0eb>
- Lindquist, H.D.A., Cross, J.H., 2017. 195 - Helminths, in: *Infectious Diseases*. Elsevier, p. 1763–1779.e1. <https://doi.org/10.1016/B978-0-7020-6285-8.00195-7>

- Lipinski, C.A., 2000. Drug-like properties and the causes of poor solubility and poor permeability. *J. Pharmacol. Toxicol. Methods* 44, 235–249. [https://doi.org/10.1016/S1056-8719\(00\)00107-6](https://doi.org/10.1016/S1056-8719(00)00107-6)
- Lu, P., Bruno, B.J., Rabenau, M., Lim, C.S., 2016. Delivery of drugs and macromolecules to the mitochondria for cancer therapy. *J. Control. Release* 240, 38–51. <https://doi.org/10.1016/J.JCONREL.2015.10.023>
- Lu, Y., Chen, J., Xiao, M., Li, W., Miller, D.D., 2012. An overview of tubulin inhibitors that interact with the colchicine binding site. *Pharm. Res.* 29, 2943–2971. <https://doi.org/10.1007/s11095-012-0828-z>
- Lüders, J., 2016. The microtubule cytoskeleton: Organisation, function and role in disease. *Microtubule Cytoskelet. Organ. Funct. Role Dis.* 1–189. <https://doi.org/10.1007/978-3-7091-1903-7>
- Maddison, J., Page, S., Church, D.B., 2008. *Small Animal Clinical Pharmacology*, 2nd ed, *Small Animal Clinical Pharmacology*. <https://doi.org/10.1016/B978-0-7020-2858-8.X5001-5>
- Markovsky, E., Baabur-Cohen, H., Eldar-Boock, A., Omer, L., Tiram, G., Ferber, S., Ofek, P., Polyak, D., Scomparin, A., Satchi-Fainaro, R., 2012. Administration, distribution, metabolism and elimination of polymer therapeutics. *J. Control. Release* 161, 446–460. <https://doi.org/10.1016/j.jconrel.2011.12.021>
- Martin, R.J., 1997. Modes of action of anthelmintic drugs. *Vet. J.* 154, 11–34. [https://doi.org/10.1016/S1090-0233\(05\)80005-X](https://doi.org/10.1016/S1090-0233(05)80005-X)
- Martin, R.J., Verma, S., Choudhary, S., Kashyap, S., Abongwa, M., Zheng, F., Robertson, A.P., 2015. Anthelmintics: The best way to predict the future is to create it. *Vet. Parasitol.* 212, 18–24. <https://doi.org/10.1016/j.vetpar.2015.05.016>
- Matoušková, P., Vokřál, I., Lamka, J., Skálová, L., 2016. The Role of Xenobiotic-Metabolizing Enzymes in Anthelmintic Deactivation and Resistance in Helminths. *Trends Parasitol.* 32, 481–491. <https://doi.org/10.1016/j.pt.2016.02.004>
- McCarty, T.R., Turkeltaub, J.A., Hotez, P.J., 2014. Global progress towards eliminating gastrointestinal helminth infections. *Curr. Opin. Gastroenterol.* 30, 18–24. <https://doi.org/10.1097/MOG.0000000000000025>

- Milane, L., Trivedi, M., Singh, A., Talekar, M., Amiji, M., 2015. Mitochondrial biology, targets, and drug delivery. *J. Control. Release* 207, 40–58. <https://doi.org/10.1016/J.JCONREL.2015.03.036>
- Millard, M., Gallagher, J.D., Olenyuk, B.Z., Neamati, N., 2013. A selective mitochondrial-targeted chlorambucil with remarkable cytotoxicity in breast and pancreatic cancers. *J. Med. Chem.* 56, 9170–9179. <https://doi.org/10.1021/jm4012438>
- Millard, M., Pathania, D., Shabaik, Y., Taheri, L., Deng, J., Neamati, N., 2010. Preclinical evaluation of novel triphenylphosphonium salts with broad-spectrum activity. *PLoS One* 5, e13131. <https://doi.org/10.1371/journal.pone.0013131>
- Modica-Napolitano, J.S., Weiss, M.J., Chen, L.B., Aprille, J.R., 1984. Rhodamine 123 inhibits bioenergetic function in isolated rat liver mitochondria. *Biochem. Biophys. Res. Commun.* 118, 717–723. [https://doi.org/10.1016/0006-291X\(84\)91453-0](https://doi.org/10.1016/0006-291X(84)91453-0)
- Moudi, M., Go, R., Yien, C.Y.S., Nazre, M., 2013. Vinca alkaloids. *Int. J. Prev. Med.* 4, 1131–1135. <https://doi.org/10.1007/BF00569574>
- Murphy, M.P., 1997. Selective targeting of bioactive compounds to mitochondria. *Trends Biotechnol.* 15, 326–30. [https://doi.org/10.1016/S0167-7799\(97\)01068-8](https://doi.org/10.1016/S0167-7799(97)01068-8)
- Nepali, K., Ojha, R., Lee, H.-Y., Liou, J.-P., 2016. Early investigational tubulin inhibitors as novel cancer therapeutics. *Expert Opin. Investig. Drugs* 25, 917–936. <https://doi.org/10.1080/13543784.2016.1189901>
- Nicol, J.M., Turner, S.J., Coyne, D.L., Nijs, L. Den, Hockland, S., 2011. Current Nematode Threats to World Agriculture, in: Jones J., Gheysen G., F.C. (Ed.), *Genomics and Molecular Genetics of Plant-Nematode Interactions*. Springer, Dordrecht, pp. 21–43. <https://doi.org/10.1007/978-94-007-0434-3>
- Nielsen, M.K., Pfister, K., Von Samson-Himmelstjerna, G., Gluck, M.H., 2014. Selective therapy in equine parasite control—Application and limitations. *Vet. Parasitol.* 202, 95–103. <https://doi.org/10.1016/j.vetpar.2014.03.020>
- O’Connell, E.M., Nutman, T.B., 2016. Review article: Molecular diagnostics for soil-transmitted helminths. *Am. J. Trop. Med. Hyg.* 95, 508–514. <https://doi.org/10.4269/ajtmh.16-0266>

- Ortiz de Montellano, P.R., 2013. Cytochrome P450-activated prodrugs. *Future Med. Chem.* 5, 213–228. <https://doi.org/10.4155/fmc.12.197>
- Pajouhesh, H., Lenz, G.R., 2005. Medicinal chemical properties of successful central nervous system drugs. *NeuroRx* 2, 541–553. <https://doi.org/10.1602/neurorx.2.4.541>
- Paleos, C.M., Tsiourvas, D., Sideratou, Z., 2016. Triphenylphosphonium decorated liposomes and dendritic polymers: Prospective second generation drug delivery systems for targeting mitochondria. *Mol. Pharm.* 13, 2233–2241. <https://doi.org/10.1021/acs.molpharmaceut.6b00237>
- Papadopoulos, E., Gallidis, E., Ptochos, S., 2012. Anthelmintic resistance in sheep in Europe: A selected review. *Vet. Parasitol.* 189, 85–88. <https://doi.org/10.1016/j.vetpar.2012.03.036>
- Parker, A.L., Kavallaris, M., McCarroll, J.A., 2014. Microtubules and Their Role in Cellular Stress in Cancer. *Front. Oncol.* 4, 153. <https://doi.org/10.3389/fonc.2014.00153>
- Passarella, D., Comi, D., Vanossi, A., Paganini, G., Colombo, F., Ferrante, L., Zuco, V., Danieli, B., Zunino, F., 2009. Histone deacetylase and microtubules as targets for the synthesis of releasable conjugate compounds. *Bioorganic Med. Chem. Lett.* 19, 6358–6363. <https://doi.org/10.1016/j.bmcl.2009.09.075>
- Payne, B.A.I., Chinnery, P.F., 2015. Mitochondrial dysfunction in aging: Much progress but many unresolved questions. *Biochim. Biophys. Acta - Bioenerg.* 1847, 1347–1353. <https://doi.org/10.1016/j.bbabi.2015.05.022>
- Peebles, K., 2007. Understanding the life cycle of ruminant parasites [WWW Document]. <https://doi.org/10.1063/1.1726787>
- Pemberton, D.J., Franks, C.J., Walker, R.J., Holden-Dye, L., 2001. Characterization of glutamate-gated chloride channels in the pharynx of wild-type and mutant *Caenorhabditis elegans* delineates the role of the subunit GluCl- α 2 in the function of the native receptor. *Mol. Pharmacol.* 59, 1037–1043. <https://doi.org/10.1124/mol.59.5.1037>
- Picard, M., Wallace, D.C., Burelle, Y., 2016. The rise of mitochondria in medicine.

Mitochondrion 30, 105–116. <https://doi.org/10.1016/j.mito.2016.07.003>

Prichard, R.K., Basáñez, M.G., Boatman, B.A., McCarthy, J.S., García, H.H., Yang, G.J., Sripa, B., Lustigman, S., 2012. A research agenda for helminth diseases of humans: Intervention for control and elimination. *PLoS Negl. Trop. Dis.* 6, e1549. <https://doi.org/10.1371/journal.pntd.0001549>

Prota, A.E., Danel, F., Bachmann, F., Bargsten, K., Buey, R.M., Pohlmann, J., Reinelt, S., Lane, H., Steinmetz, M.O., 2014. The novel microtubule-destabilizing drug BAL27862 binds to the colchicine site of tubulin with distinct effects on microtubule organization. *J. Mol. Biol.* 426, 1848–1860. <https://doi.org/10.1016/j.jmb.2014.02.005>

Ramos, F., Portella, L.P., Rodrigues, F. de S., Reginato, C.Z., Cezar, A.S., Sangioni, L.A., Vogel, F.S.F., 2018. Anthelmintic resistance of gastrointestinal nematodes in sheep to monepantel treatment in central region of Rio Grande do Sul, Brazil. *Pesqui. Vet. Bras.* 38, 48–52. <https://doi.org/10.1590/1678-5150-pvb-5188>

Ravelli, R.B.G., Gigant, B., Curmi, P.A., Jourdain, I., Lachkar, S., Sobel, A., Knossow, M., 2004. Insight into tubulin regulation from a complex with colchicine and a stathmin-like domain. *Nature* 428, 198–202. <https://doi.org/10.1038/nature02393>

Raza, A., Lamb, J., Chambers, M., Hunt, P.W., Kotze, A.C., 2016. Larval development assays reveal the presence of sub-populations showing high- and low-level resistance in a monepantel (Zolvix®)-resistant isolate of *Haemonchus contortus*. *Vet. Parasitol.* 220, 77–82. <https://doi.org/10.1016/j.vetpar.2016.02.031>

Richardson, H., Smaill, F., 1998. Medical microbiology. *BMJ* 317, 1060. <https://doi.org/10.1136/bmj.317.7165.1060>

Riva, E., Mattarella, M., Borrelli, S., Christodoulou, M.S., Cartelli, D., Main, M., Faulkner, S., Sykes, D., Cappelletti, G., Snaith, J.S., Passarella, D., 2013. Preparation of fluorescent tubulin binders. *Chempluschem* 78, 222–226. <https://doi.org/10.1002/cplu.201200260>

Rodriguez-Garcia, A., Hosseini, S., Martinez-Chapa, S.O., Cordell, G.A., 2017. Multi-target Activities of Selected Alkaloids and Terpenoids. *Mini. Rev. Org. Chem.* 14, 272–279. <https://doi.org/10.2174/1570193X14666170518151027>

- Roeber, F., Jex, A.R., Gasser, R.B., 2013. Impact of gastrointestinal parasitic nematodes of sheep, and the role of advanced molecular tools for exploring epidemiology and drug resistance - An Australian perspective. *Parasites and Vectors* 6, 153. <https://doi.org/10.1186/1756-3305-6-153>
- Román Luque-Ortega, J., Reuther, P., Rivas, L., Dardonville, C., 2010. New Benzophenone-derived bisphosphonium salts as leishmanicidal leads targeting mitochondria through inhibition of respiratory complex II. *J. Med. Chem.* 53, 1788–1798. <https://doi.org/10.1021/jm901677h>
- Römbke, J., Coors, A., Fernández, Á.A., Förster, B., Fernández, C., Jensen, J., Lumaret, J.P., Cots, M.Á.P., Liebig, M., 2010. Effects of the parasiticide ivermectin on the structure and function of dung and soil invertebrate communities in the field (Madrid, Spain). *Appl. Soil Ecol.* 45, 284–292. <https://doi.org/10.1016/j.apsoil.2010.05.004>
- Ross, M.F., Kelso, G.F., Blaikie, F.H., James, A.M., Cochemé, H.M., Filipovska, A., Da Ros, T., Hurd, T.R., Smith, R.A.J., Murphy, M.P., 2005. Lipophilic triphenylphosphonium cations as tools in mitochondrial bioenergetics and free radical biology. *Biochem.* 70, 222–230. <https://doi.org/10.1007/s10541-005-0104-5>
- Schindler, A.J., Baugh, L.R., Sherwood, D.R., 2014. Identification of Late Larval Stage Developmental Checkpoints in *Caenorhabditis elegans* Regulated by Insulin/IGF and Steroid Hormone Signaling Pathways. *PLoS Genet.* 10, e1004426. <https://doi.org/10.1371/journal.pgen.1004426>
- Scorza, A. V., Radecki, S. V., Lappin, M.R., 2006. Efficacy of a combination of febantel, pyrantel, and praziquantel for the treatment of kittens experimentally infected with *Giardia* species. *J. Feline Med. Surg.* 8, 7–13. <https://doi.org/10.1016/j.jfms.2005.04.004>
- Scott, I., Pomroy, W.E., Kenyon, P.R., Smith, G., Adlington, B., Moss, A., 2013. Lack of efficacy of monepantel against *Teladorsagia circumcincta* and *Trichostrongylus colubriformis*. *Vet. Parasitol.* 198, 166–171. <https://doi.org/10.1016/j.vetpar.2013.07.037>
- Singh, B., Kumar, A., Joshi, P., Guru, S.K., Kumar, S., Wani, Z.A., Mahajan, G.,

- Hussain, A., Qazi, A.K., Kumar, A., Bharate, S.S., Gupta, B.D., Sharma, P.R., Hamid, A., Saxena, A.K., Mondhe, D.M., Bhushan, S., Bharate, S.B., Vishwakarma, R.A., 2015. Colchicine derivatives with potent anticancer activity and reduced P-glycoprotein induction liability. *Org. Biomol. Chem.* 13, 5674–5689. <https://doi.org/10.1039/c5ob00406c>
- Stoll, N.R., 1999. This Wormy World. *J. Parasitol.* 85, 392. <https://doi.org/10.2307/3285767>
- Strobykina, I.Y., Belenok, M.G., Semenova, M.N., Semenov, V. V., Babaev, V.M., Rizvanov, I.K., Mironov, V.F., Kataev, V.E., 2015. Triphenylphosphonium Cations of the Diterpenoid Isosteviol: Synthesis and Antimitotic Activity in a Sea Urchin Embryo Model. *J. Nat. Prod.* 78, 1300–1308. <https://doi.org/10.1021/acs.jnatprod.5b00124>
- Swissadme.ch. (2019). SwissADME. [online] Available at: <http://www.swissadme.ch/index.php#> [Accessed 23 Sep. 2019].
- Tansatit, T., Sahaphong, S., Riengrojpitak, S., Viyanant, V., Sobhon, P., 2006. Immunolocalization of cytoskeletal components in the tegument of the 3-week-old juvenile and adult *Fasciola gigantica*. *Vet. Parasitol.* 135, 269–278. <https://doi.org/10.1016/j.vetpar.2005.10.018>
- Tchuem Tchuente, L.A., 2011. Control of soil-transmitted helminths in sub-Saharan Africa: Diagnosis, drug efficacy concerns and challenges. *Acta Trop.* 120, S4–S11. <https://doi.org/10.1016/J.ACTATROPICA.2010.07.001>
- Vásquez-Trincado, C., García-Carvajal, I., Pennanen, C., Parra, V., Hill, J.A., Rothmel, B.A., Lavandero, S., 2016. Mitochondrial dynamics, mitophagy and cardiovascular disease. *J. Physiol.* 594, 509–525. <https://doi.org/10.1113/JP271301>
- Vinaud, M.C., Ferreira, C.S., de Souza Lino Junior, R., Bezerra, J.C.B., 2008. *Taenia crassiceps*: Energetic and respiratory metabolism from cysticerci exposed to praziquantel and albendazole in vitro. *Exp. Parasitol.* 120, 221–226. <https://doi.org/10.1016/j.exppara.2008.07.008>
- Vokřál, I., Jirásko, R., Stuchlíková, L., Bártíková, H., Szotáková, B., Lamka, J., Várady,

- M., Skálová, L., 2013. Biotransformation of albendazole and activities of selected detoxification enzymes in *Haemonchus contortus* strains susceptible and resistant to anthelmintics. *Vet. Parasitol.* 196, 373–381. <https://doi.org/10.1016/j.vetpar.2013.03.018>
- Waight, A.B., Bargsten, K., Doronina, S., Steinmetz, M.O., Sussman, D., Prota, A.E., 2016. Structural basis of microtubule destabilization by potent auristatin anti-mitotics. *PLoS One* 11, 1–14. <https://doi.org/10.1371/journal.pone.0160890>
- Watson, T.G., Hosking, B.C., 1990. Evidence for multiple anthelmintic resistance in two nematode parasite genera on a Saanen goat dairy. *N. Z. Vet. J.* 38, 50–3. <https://doi.org/10.1080/00480169.1990.35615>
- Wilson, D.J., Sargison, N.D., Scott, P.R., Penny, C.D., 2008. Epidemiology of gastrointestinal nematode parasitism in a commercial sheep flock and its implications for control programmes. *Vet. Rec.* 162, 546–550. <https://doi.org/10.1136/vr.162.17.546>
- Wolstenholme, A.J., Fairweather, I., Prichard, R., Von Samson-Himmelstjerna, G., Sangster, N.C., 2004. Drug resistance in veterinary helminths. *Trends Parasitol.* 20, 469–476. <https://doi.org/10.1016/j.pt.2004.07.010>
- Woods, D.J., Vaillancourt, V.A., Wendt, J.A., Meeus, P.F., 2011. Discovery and development of veterinary antiparasitic drugs: past, present and future. *Future Med. Chem.* 3, 887–96. <https://doi.org/10.4155/fmc.11.39>
- Yang, L.P.H., 2010. Oral Colchicine (Colcris®) in the Treatment and Prophylaxis of Gout†. *Drugs Aging* 27, 855–857. <https://doi.org/10.2165/11206330-000000000-00000>
- Ye, Y., Zhang, T., Yuan, H., Li, D., Lou, H., Fan, P., 2017. Mitochondria-Targeted Lupane Triterpenoid Derivatives and Their Selective Apoptosis-Inducing Anticancer Mechanisms. *J. Med. Chem.* 60, 6353–6363. <https://doi.org/10.1021/acs.jmedchem.7b00679>
- Zahreddine, H., Borden, K.L.B., 2013. Mechanisms and insights into drug resistance in cancer. *Front. Pharmacol.* 4, 28. <https://doi.org/10.3389/fphar.2013.00028>
- Zawilska, J.B., Wojcieszak, J., Olejniczak, A.B., 2013. Prodrugs: a challenge for the

drug development. *Pharmacol. Rep.* 65, 1–14.

Zhang, X., Kong, Y., Zhang, J., Su, M., Zhou, Y., Zang, Y., Li, J., Chen, Y., Fang, Y., Zhang, X., Lu, W., 2015. Design, synthesis and biological evaluation of colchicine derivatives as novel tubulin and histone deacetylase dual inhibitors. *Eur. J. Med. Chem.* 95, 127–135. <https://doi.org/10.1016/j.ejmech.2015.03.035>

Zielonka, J., Joseph, J., Sikora, A., Hardy, M., Ouari, O., Vasquez-Vivar, J., Cheng, G., Lopez, M., Kalyanaraman, B., 2017a. Mitochondria-Targeted Triphenylphosphonium-Based Compounds: Syntheses, Mechanisms of Action, and Therapeutic and Diagnostic Applications. *Chem. Rev.* 117, 10043–10120. <https://doi.org/10.1021/acs.chemrev.7b00042>

Zielonka, J., Joseph, J., Sikora, A., Hardy, M., Ouari, O., Vasquez-Vivar, J., Cheng, G., Lopez, M., Kalyanaraman, B., 2017b. Mitochondria-Targeted Triphenylphosphonium-Based Compounds: Syntheses, Mechanisms of Action, and Therapeutic and Diagnostic Applications. *Chem. Rev.* 117, 10043–10120. <https://doi.org/10.1021/acs.chemrev.7b00042>

Appendices

Appendix A:

Calibration curves of AM1 (Col-Pro), AM2 (Col-Pro-TPP), AM3 (Col-4-hydroxypiperidine), AM4 (Col-(*R*)-3-pyrrolidinol), AM5 (Col-Boc-aminopyrrolidine) and AM6 (Col-aminopyrrolidine), AM7 (Col-aminopyrrolidine-TPP), AM8 (Col-4-hydroxypiperidine-TPP) and AM9 (Col-(*R*)-3-pyrrolidinol-TPP) plotted by octanol/water partition method.

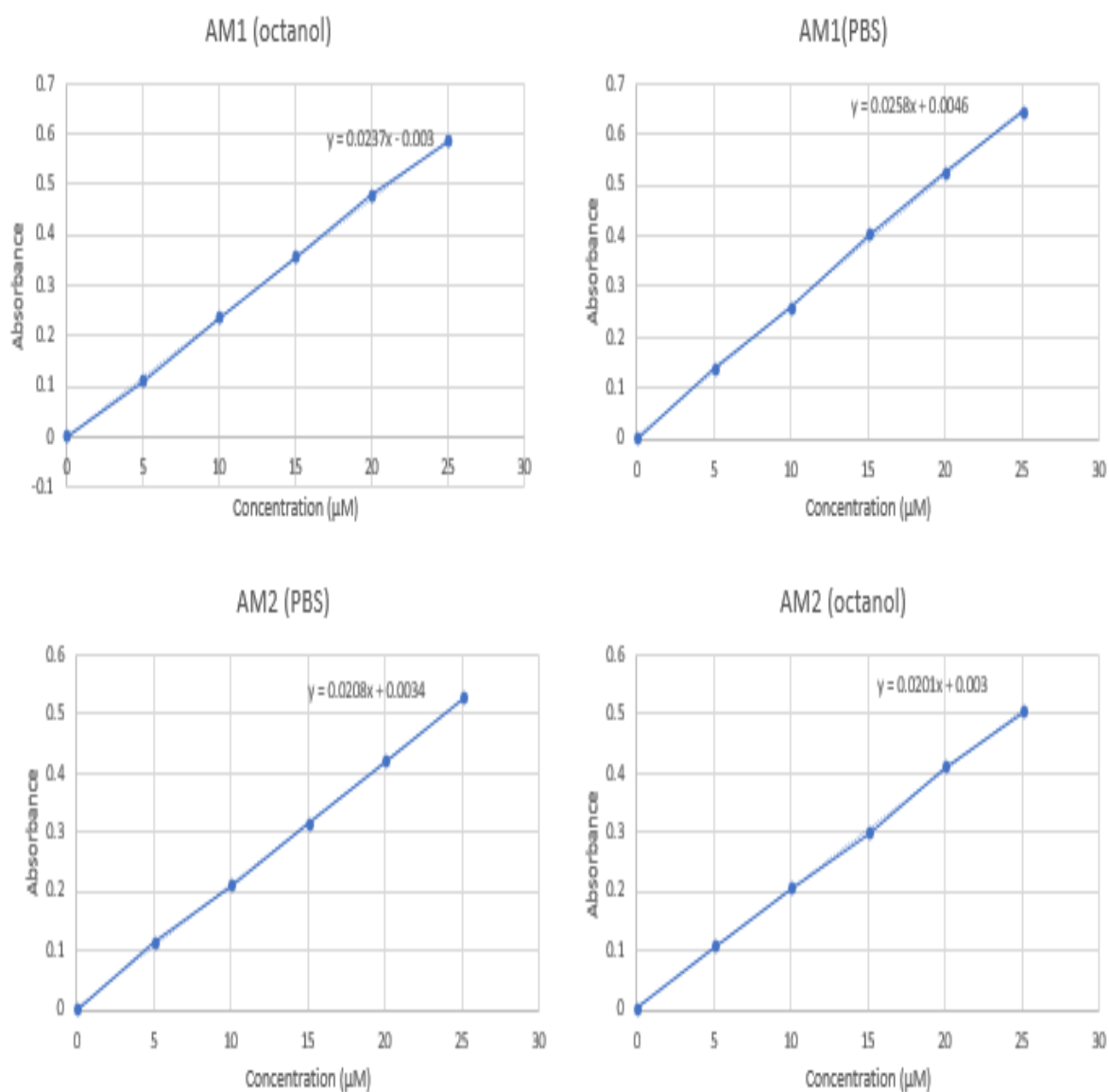


Figure A. 1.1 Calibration curves of AM1 and AM2 in PBS and octanol.

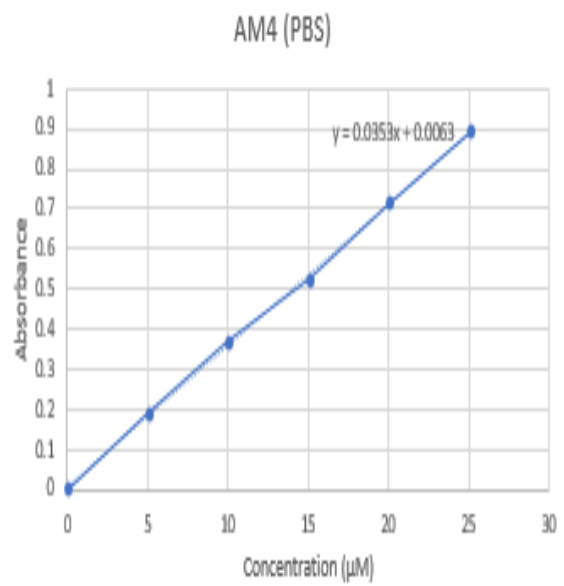
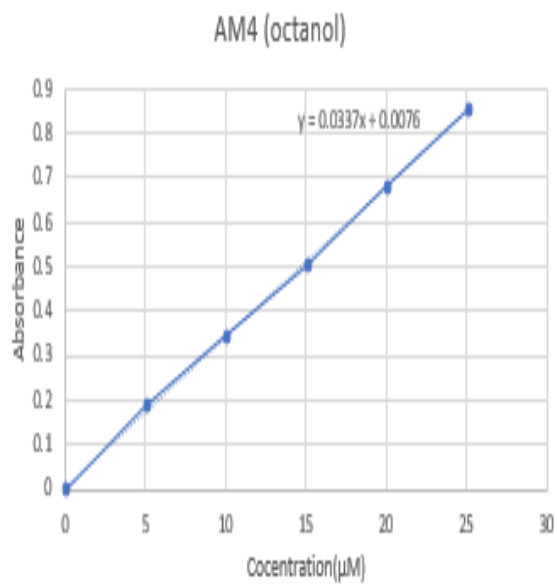
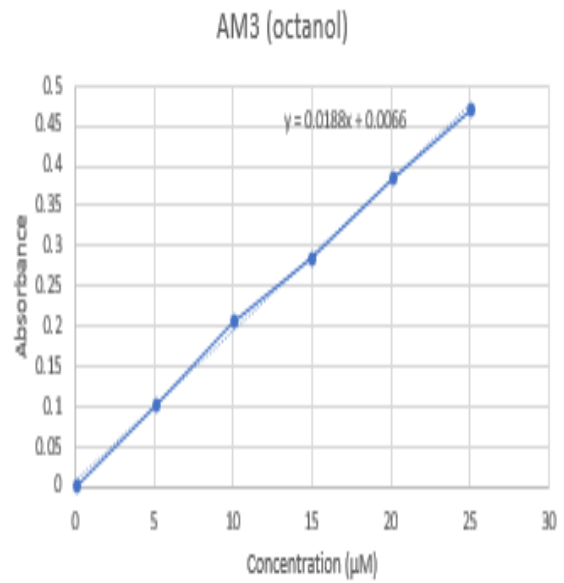
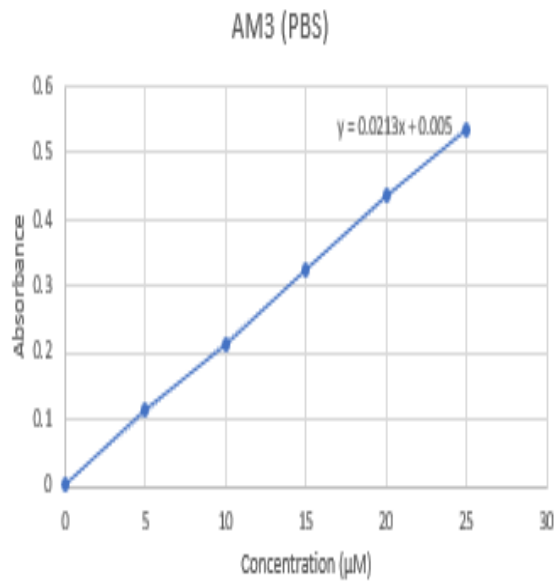


Figure A. 1.2 Calibration curves of AM3 and AM4 in PBS and octanol.

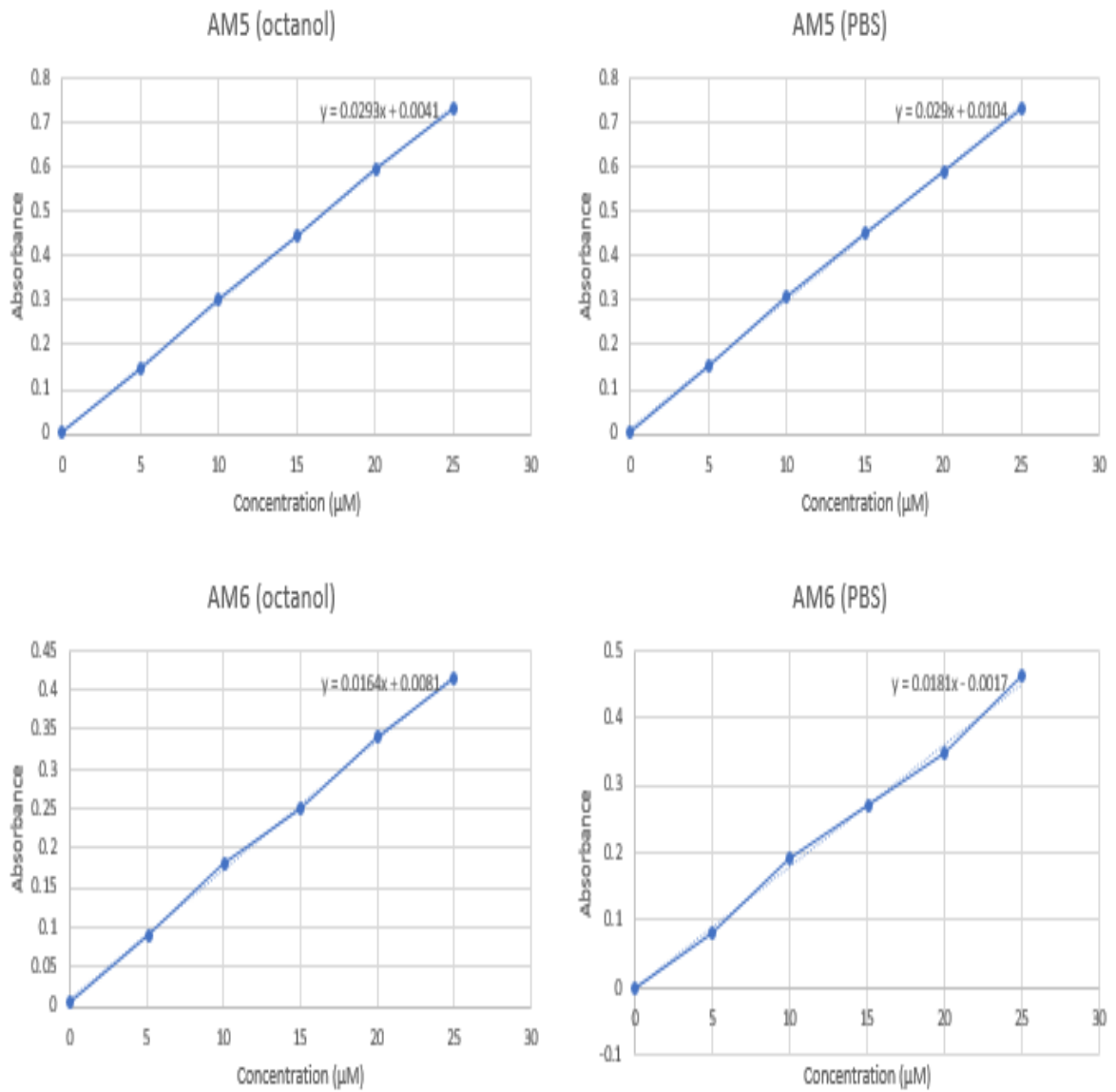


Figure A. 1.3 Calibration curves of AM5 and AM6 in PBS and octanol.

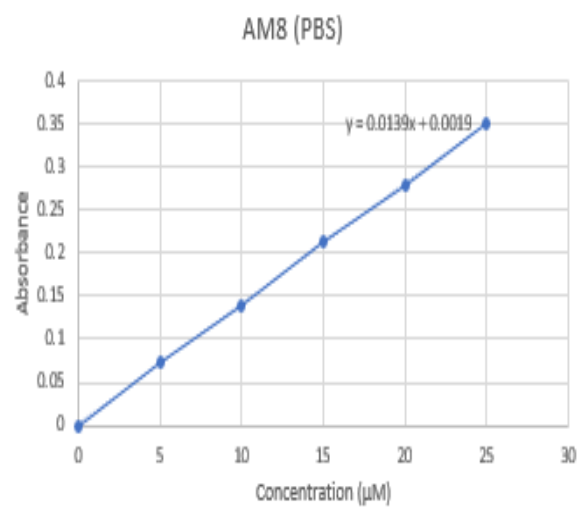
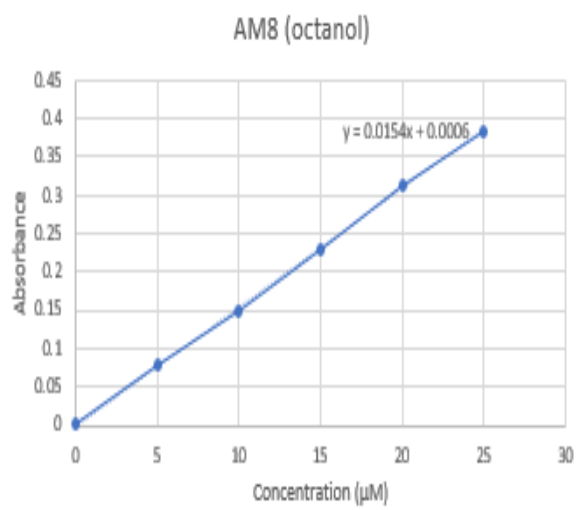
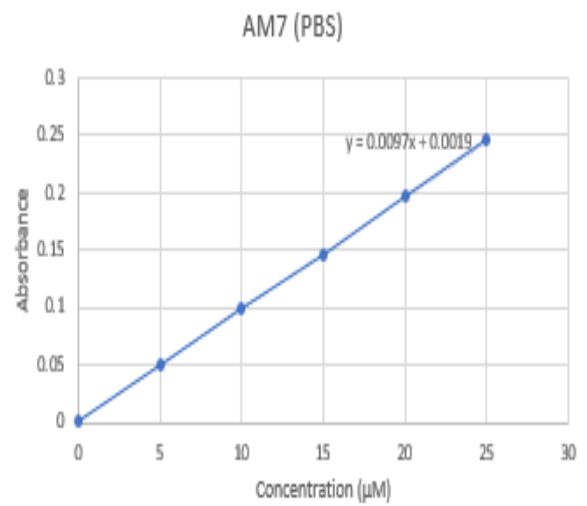
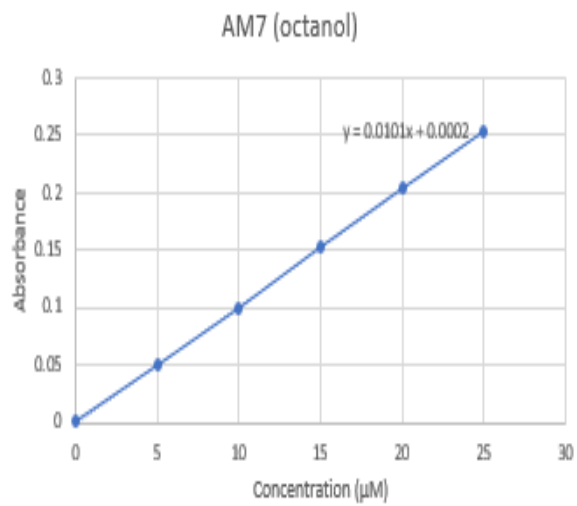


Figure A. 1.4 Calibration curves of AM7 and AM8 in PBS and octanol.

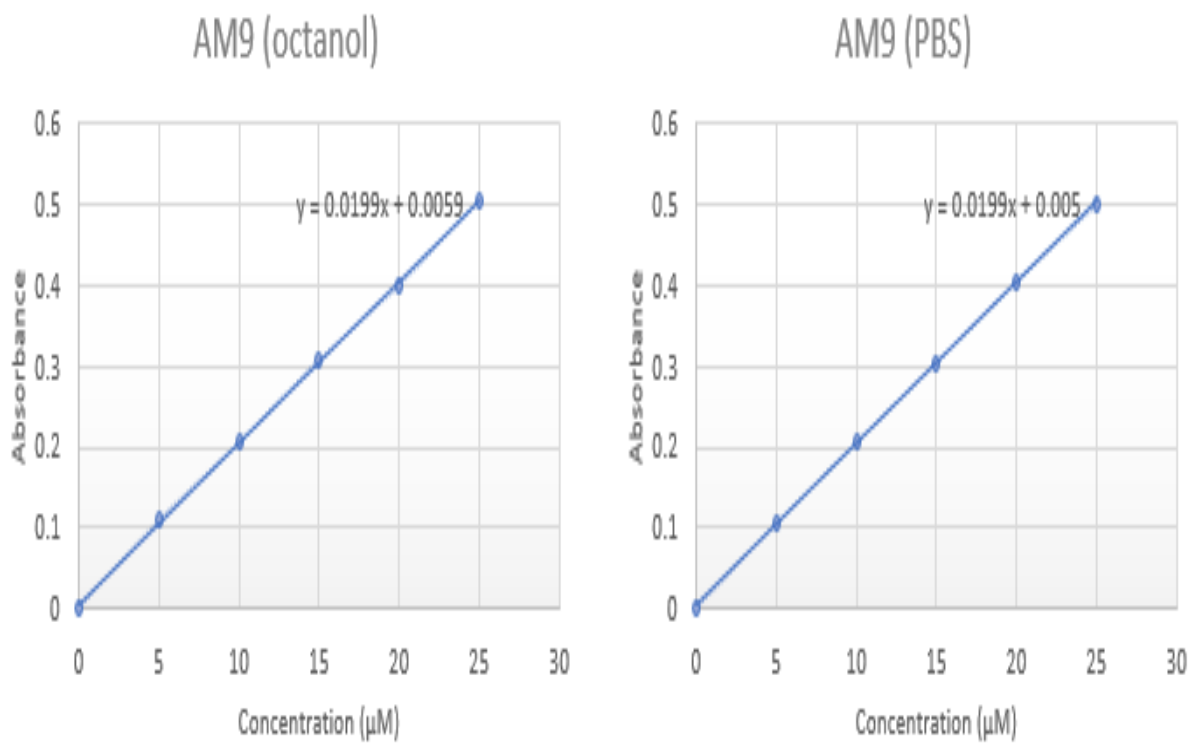


Figure A. 1.5 Calibration curves AM9 in PBS and octanol.

Appendix B:

Log D calculations for AM1 (Col-Pro), AM2 (Col-Pro-TPP), AM3 (Col-4-hydroxypiperidine), AM4 (Col-(*R*)-3-pyrrolidinol), AM5 (Col-Boc-aminopyrrolidine) and AM6 (Col-aminopyrrolidine), AM7 (Col-aminopyrrolidine-TPP), AM8 (Col-4-hydroxypiperidine-TPP) and AM9 (Col-(*R*)-3-pyrrolidinol-TPP).

Table A. 2.1 Log D values for AM1, calculated from concentration of AM1 in octanol and PBS considering dilution factor and absorbance intensities in triplicate.

Run No.	Solvent	Absorbance in cuvette	y=mx+c	Conc. in cuvette (μM)	Dilution Factor	Original conc in eppendorf (μM).	Log D	Log D Mean±
1	Octanol	0.217	$0.217=0.0201x+0.003$	10.64	99	1064	1.42	1.34± 0.06
1	PBS (pH7.4)	0.6209	$0.6209=0.0213x+0.005$	28.91	1.5	72.27		
2	Octanol	0.1837	$0.1837=0.0201x+0.003$	8.95	99	895.52	1.30	
2	PBS (pH7.4)	0.75	$0.75=0.0213x+0.005$	34.97	1.25	78.69		
3	Octanol	0.2165	$0.2165=0.0201x+0.003$	10.62	99	1062	1.32	
3	PBS (pH7.4)	0.845	$0.845=0.0213x+0.005$	39.43	1.75	108.45		

Table A. 2.2 Log D values for AM2, calculated from concentration of AM2 in octanol and PBS considering dilution factor and absorbance intensities in triplicate.

Run No.	Solvent	Absorbance in cuvette	y=mx+c	Conc. in cuvette (μM)	Dilution Factor	Original conc in eppendorf (μM).	Log D	Log D Mean \pm S.D
1	Octanol	0.7324	$0.7324=0.0237x-0.003$	30.77	99	3077.63	1.67	1.69 \pm 0.26
1	PBS (pH7.4)	0.898	$0.898=0.0258x+0.0046$	34.62	0.25	43.27		
2	Octanol	0.461	$0.461=0.0237x-0.003$	19.32 μM	99	1930 μM	1.97	
2	PBS (pH7.4)	0.6658	$0.6658=0.0258x+0.0046$	1.357	0.4	1.89		
3	Octanol	0.3158	$0.3158=0.0237x-0.003$	13.19	99	1319	1.44	
3	PBS (pH7.4)	0.877	$0.877=0.0258x+0.0046$	33.81	0.16	39.44		

Table A. 2.3 Log D values for AM3, calculated from concentration of AM3 in octanol and PBS considering dilution factor and absorbance intensities in triplicate.

Run No.	Solvent	Absorbance in cuvette	y=mx+c	Conc. in cuvette (μM)	Dilution Factor	Original conc in eppendorf (μM).	Log D	Log D Mean \pm
1	Octanol	0.420	$0.420=0.0188x+0.0066$	21.98	99	2199	1.62	1.64 \pm 0.02
1	PBS (pH7.4)	0.6424	$0.6424=0.0213x+0.005$	29.92	2.33	99.74		
2	Octanol	0.4447	$0.4447=0.0188x+0.0066$	23.30	99	2330	1.66	
2	PBS (pH7.4)	0.5703	$0.5703=0.0213x+0.005$	26.53	2.33	88.46		
3	Octanol	0.42	$0.42=0.0188x+0.0066$	22	99	2201	1.66	
3	PBS (pH7.4)	0.5468	$0.5468=0.0213x+0.005$	25.43	2.33	84.78		

Table A. 2.4 Log D values for AM4, calculated from concentration of AM4 in octanol and PBS considering dilution factor and absorbance intensities in triplicate.

Run No.	Solvent	Absorbance in cuvette	$y=mx+c$	Conc. in cuvette (μM)	Dilution Factor	Original conc in eppendorf (μM).	Log D	Log D Mean \pm
1	Octanol	0.4943	$0.4943=0.0337x+0.0076$	14.44	99	1444	1.60	1.65 \pm 0.04
1	PBS (pH7.4)	0.7598	$0.7598=0.0353x+0.0076$	21.34	2.66	78.24		
2	Octanol	0.5857	$0.5857=0.0337x+0.0076$	17.15	99	1715	1.68	
2	PBS (pH7.4)	0.6523	$0.6523=0.0353x+0.0076$	18.30	4	91.50		
3	Octanol	0.4487	$0.4487=0.0337x+0.0076$	13.09	99	1309	1.68	
3	PBS (pH7.4)	0.4941	$0.4941=0.0353x+0.0076$	13.81	4	69.09		

Table A. 2.5 Log D values for AM5, calculated from concentration of AM5 in octanol and PBS considering dilution factor and absorbance intensities in triplicate.

Run No.	Solvent	Absorbance in cuvette	y=mx+c	Conc. in cuvette (μM)	Dilution Factor	Original conc in eppendorf (μM).	Log D	Log D (Mean \pm)
1	Octanol	0.2723	$0.2723=0.0293x+0.0041$	9.15	99	915.35	1.63	1.63 \pm 0.005
1	PBS (pH7.4)	0.3645	$0.3645=0.029x+0.0104$	12.21	0	12.21		
2	Octanol	0.64	$0.64=0.0293x+0.0041$	21.70	74	1627.73	1.63	
2	PBS (pH7.4)	0.482	$0.482=0.029x+0.0104$	16.26	0	16.26		
3	Octanol	0.6354	$0.6354=0.0293x+0.0041$	21.54	74	1616	1.64	
3	PBS (pH7.4)	0.4416	$0.4416=0.029x+0.0104$	14.86	0	14.86		

Table A. 2.6 Log D values for AM6, calculated from concentration of AM6 in octanol and PBS considering dilution factor and absorbance intensities in triplicate.

Run No.	Solvent	Absorbance in cuvette	y=mx+c	Conc. in cuvette (μ M)	Dilution Factor	Original conc in eppendorf (μ M).	Log D	Log D (Mean \pm)
1	Octanol	0.2176	$0.2176=0.0164x+0.0081$	12.77	59	766.46	1.25	1.28 \pm 0.03
1	PBS (pH7.4)	0.5492	$0.5492=0.0181x+0.0017$	30.24	59	1815		
2	Octanol	0.2153	$0.2153=0.0164x+0.0081$	12.63	59	758.04	1.31	
2	PBS (pH7.4)	0.444	$0.444=0.0181x+0.0017$	24.43	59	1466.18		
3	Octanol	0.2199	$0.2199=0.0164x+0.0081$	12.91	59	774.87	1.28	
3	PBS (pH7.4)	0.4933	$0.4933=0.0181x+0.0017$	26.16	59	1630		

Table A. 2.7 Log D values for AM7, calculated from concentration of AM7 in octanol and PBS considering dilution factor and absorbance intensities in triplicate.

Run No.	Solvent	Absorbance in cuvette	$y=mx+c$	Conc. in cuvette (μM)	Dilution Factor	Original conc in eppendorf (μM).	Log D	Log D (Mean \pm)
1	Octanol	0.1672	$0.1672=0.0101x+0.0002$	16.53	20.42	354.31	0.6	0.72 ± 0.11
1	PBS (pH7.4)	0.6048	$0.6048=0.0097x+0.0019$	62.15	0	62.15		
2	Octanol	0.375	$0.375=0.0101x+0.0002$	37.10	17.75	695.79	0.73	
2	PBS (pH7.4)	0.888	$0.888=0.0097x+0.0019$	91.35	0.28	117.45		
3	Octanol	0.2287	$0.2287=0.0101x+0.0002$	22.62	17.75	424.19	0.83	
3	PBS (pH7.4)	0.388	$0.388=0.0097x+0.0019$	39.80	0.38	54.73		

Table A. 2.8 Log D values for AM8, calculated from concentration of AM8 in octanol and PBS considering dilution factor and absorbance intensities in triplicate.

Run No.	Solvent	Absorbance in cuvette	y=mx+c	Conc. in cuvette (μM)	Dilution Factor	Original conc in eppendorf (μM).	Log D	Log D (Mean \pm)
1	Octanol	0.178	$0.178=0.0154x+0.0006$	11.51	99	1152	1.34	1.28 ± 0.05
1	PBS (pH7.4)	0.5641	$0.5641=0.0139x+0.0019$	40.44	0.42	57.78		
2	Octanol	0.2838	$0.2838=0.0154x+0.0006$	18.38	59	1103.37	1.28	
2	PBS (pH7.4)	0.5447	$0.5447=0.0139x+0.0019$	39.05	0.42	55.78		
3	Octanol	0.523	$0.523=0.0154x+0.0006$	33.96	41.85	1455.47	1.24	
3	PBS (pH7.4)	0.6701	$0.6701=0.0139x+0.0019$	48.07	0.42	68.67		

Table A. 2.9 Log D values for AM9, calculated from concentration of AM9 in octanol and PBS considering dilution factor and absorbance intensities in triplicate.

Run No.	Solvent	Absorbance in cuvette	$y=mx+c$	Conc. in cuvette (μM)	Dilution Factor	Original conc in eppendorf (μM).	Log D	Log D (Mean \pm)
1	Octanol	0.2851	$0.2851=0.0199x+0.0059$	14.03	99	1403	1.43	1.37 ± 0.04
1	PBS (pH7.4)	0.7439	$0.7439=0.0199x+0.005$	37.13	1.5	92.82		
2	Octanol	0.1954	$0.1954=0.0199x+0.0059$	9.52	99	952.26	1.34	
2	PBS (pH7.4)	0.6729	$0.6729=0.0199x+0.005$	33.56	1.5	83.90		
3	Octanol	0.2162	$0.2162=0.0199x+0.0059$	10.56	99	1056.78	1.36	
3	PBS (pH7.4)	0.7053	$0.7053=0.0199x+0.005$	35.19	1.5	87.97		